The Impact of Global Climate Change on the Runoff and Ecological Sustainability of the Breede River

Anna C Steynor

Submitted in fulfilment of the requirements for the degree of Master of Science
University of Cape Town
2004

ABSTRACT

The Breede River catchment in the South Western Cape is already under pressure for its water resources due to its supporting a variety of different land uses. The predominant land use in this catchment is agriculture, which demands the majority of river water for irrigation. The Department of Water Affairs and Forestry are currently investigating the future demand for water from the river, in this respect it is important to know what effect climate change will have on the change in river flow. Self Organising Maps (SOMs) are used to identify changes in the circulation systems contributing to the rainfall of the region and from this the potential change is assessed for the Breede River flow under future climate change.

It is assessed that the runoff in the Breede River is expected to change under all the models of ECHAM4, CSIRO and HadAM. The magnitude of this alteration is calculated by using the change in the SOM node frequencies between the present and the future data. This is then subtracted from the present runoff data supplied by DWAF.

A source of runoff decrease in the future is agricultural irrigation. The increase in irrigation under climate change is determined by inserting future climate data into an agricultural model. Once the increased amount of water used in irrigation is determined, it is subtracted from the projected future runoff. From this it is determined whether the river will be ecologically sustainable under climate change.

ACKNOWLEDGMENTS

- Bruce Hewitson (Supervisor)
- Emma Archer (Co-supervisor)
- Herman Keuris (DWAF)
- Frans Stoffberg (DWAF)
- Elias Nel (DWAF)
- Hans Beuster (Ninham Shand)
- Johan van Rensburg (Ninham Shand)
- Peter Dall (Independent consultant)
- Briaan Stipp (Vinpro)
- Daan Louw (Deciduous Fruit Producers Trust)
- Grant Smuts (Smuts Bros)
- Wilhelm Naude (Oudewagensdrift)
- Eben van Niekerk (Spes Bona)
- Chris Jack (CSAG, UCT)
- Karen Alston (Conservation Biology Department, UCT)

INDEX

LIST OF FIGURES

LIST OF TABLES

LIST OF EQUATIONS

A prominent hydrologists response to climate change predictions:

The Risk is too large not to look for possible alternatives and means of mitigation, even if the search is based on predictions with a large margin of error. Forecasting is a dangerous game. Blind and passive waiting for disaster is even more dangerous.

~ Nemec (1988)

PART ONE

SOM analysis: projected change in future runoff

CHAPTER ONE 1 :INTRODUCTION AND LITERATURE REVIEW

The impact of climate change on the Western Cape warrants research because it is vulnerable to climate changes, and the wealth of scientific understanding indicates that global climate change is probable (Intergovernmental Panel on Climate Change, 2001). There is a projected drying in the Western Cape along with a temperature increase. This may have impacts on every aspect of society, however, it is expected that the impact on water resources will be strongly felt. This projection prompted an investigation into the climate change impacts on one of the major rivers of the Western Cape.

The Breede River valley is a key agricultural region of the Western Cape in South Africa. The river lies on the East coast of the Western Cape, approximately 250 kilometres from Cape Town, and extends from Cape Infanta up into the Hex River Mountains. Past studies of the Breede River catchment have explored the projected future water demand and consumption from each land use in the basin and have considered the possibility of additional water transfer schemes out of the Breede River valley. This work, however, failed to take into account the possibility of global climate change. This omission could have far reaching effects once decisions have been made to put transfer schemes in place.

This thesis attempts to address this omission by asking the question, "How will the runoff in the Breede River change under the future climate?" In this case runoff is defined as the amount of water flowing in the river at different points throughout the catchment.

In addition to simply projecting future runoff under a changing climate, additional non-climatic processes that affect runoff are also considered, to a limited extent, as well as feedbacks such as increased reliance on irrigation under the future climate. Considering that 66% of the water usage in the catchment is used by the agricultural sector (Department of Water Affairs, 2003), the complex interdependencies could have a significant impact on the catchment ecosystem and societal activities.

For example, runoff should not only be considered in terms of water availability for extraction purposes but also in terms of water levels required to sustain ecological functioning. In this respect, there is a need for an exploration into ecological sustainability using future projected runoff levels. Thus the question is also posed, "Are there areas that are ecologically sustainable at present but will cease to be so under future climate change?" The answer to this question of ecological sustainability will have a significant impact on tourism and industry, among other key sectors. If areas of the river cease to be ecologically sustainable this may prove to have a more serious impact than water availability alone.

Keeping these research objectives in mind, the thesis is divided into three parts. The first part assesses the first order consequences of possible climate change, and the impact these

consequences may have on the Breede River runoff. To realise this objective, Global Climate Model (GCM) projections for the catchment are first assessed in terms of the ability of GCMs to capture current synoptic-scale atmospheric circulation and, following this, the GCM simulated changes in circulation. These changes in synoptic circulation are then translated into a runoff associated with the new circulation patterns.

After this first level of assessment, the second part of the project focuses on hydrological consequences. In this section, the agricultural impact on future runoff is investigated with the use of a relatively simple biophysical crop simulation model.

The third and final part characterises the impacts of climate change and its associated change in runoff on the ecological sustainability of the river, at each station. The addition of this section allows for the linking of land use impacts due to a change in runoff with the ecological impact.

1.1 Study Area

The Breede River, situated in the Western Cape, is the largest river in the province with a total catchment area of 12600 km^2 (DWAFa, 2002). The catchment area comprises seven drainage basins (Figure 1) divided into the following areas; Ceres basin, the Upper Breede River, the Hex River, the Middle Breede River, the Riviersonderend valley and the Lower Breede River (DWAFa, 2002). Originating in the Ceres Valley, it drains in a South Easterly direction meeting the Indian Ocean at Witsand/Cape Infanta (Sebastian Bay).

The Breede River falls within the winter rainfall region of the Western Cape. Roughly 80% of precipitation falls within the months of April to September, brought by mid-latitude cyclones dominant over the region in these months. The rainfall in the area varies considerably. In the Western mountainous areas the rainfall can be as high as 2300 mm/year whereas in the middle reaches and the area North of Langeberg, rainfall decreases to as low as 400 mm/yr (DWAFa, 2002). Water is collected during the winter period in municipal storage dams for subsequent dispersal during summer.

Incorporated into the river's drainage basin are the major municipal storage dams of Brandvlei and Theewaterskloof. A unique feature in the operation of the Theewaterskloof dam is the transference of water into the dam from the Berg water management area for seasonal storage, as the Berg river does not have significant storage capacity. During the dry season, the water is then transferred back into the Berg River together with a large quantity of additional water from the Breede River (DWAFc, 2002). This process may cease in the future post the completion of the Berg river storage dam, which is presently under construction.

The Breede River supplies water for several land use practices. The most prominent land use, however, is that of cultivated land (DWAFb, 2002). Currently 105 000 hectares (8.3% of the total area) of the basin is used for agriculture and many of the farmers rely on a transfer scheme of water piped directly from Brandvlei dam. The majority of the cultivated land in the Northern portion of the basin is used in the production of fruit and wine and is situated along river courses in valley regions. The Southern portion of the basin is dominated by wheat production. Other land use practices supported by the river basin include urban and rural settlement, afforestation and tourism. Interspersed between these areas is a high density of alien vegetation with the greatest infestation found in the Riviersonderend valley (DWAFa, 2002).

Due to the poor performance of this regions agricultural sector in the past ten years, there has been no significant growth in population (DWAFa, 2002). Both agricultural productivity and population numbers may change in the future as agricultural sectors shift their focus from quantity to quality of fruit, as demanded by the export market (Kriel, 2004). Demographic projections show a growth in population in the coastal areas but a decline inland.

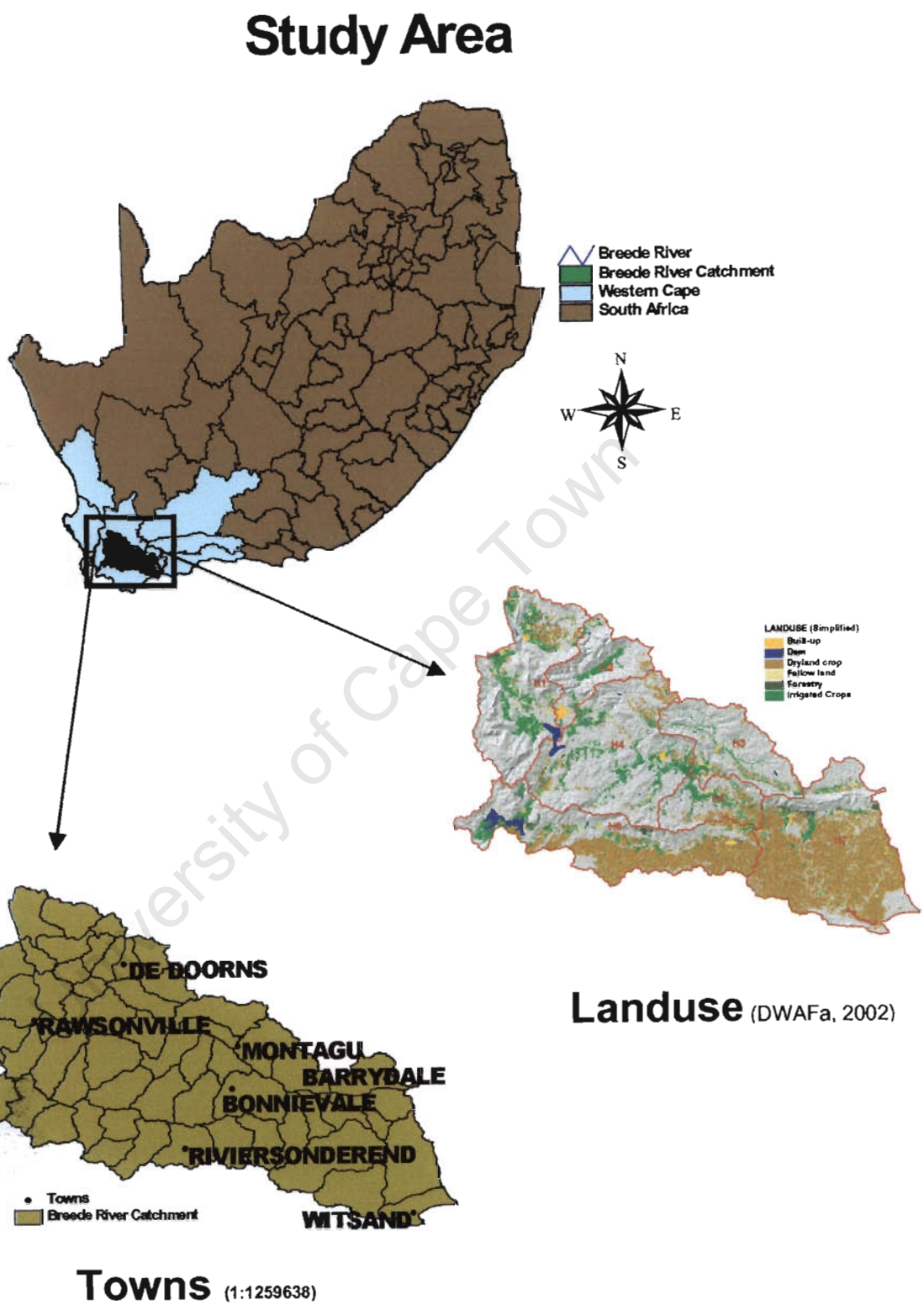

FIGURE 1: The Breede River study area

1.2 Introduction to Water Management

The concept of water management is described here as part of this project's objective of assessing climate change impacts on a major South African water resource. Water is a scarce resource and needs to be managed worldwide as reliance on market forces alone will not maintain a satisfactory yield (Easter, 1993). The National Water Act of South Africa recognises that 'the ultimate aim of water resource management is to achieve the sustainable use of water for the benefit of all users' (National Water Act, 1998). Under conditions of climate change, water management becomes more crucial as population growth rates and water demand increase and water yields change. The costs of tapping new water resources are also rising, making water a very important economic resource (Easter, 1993).

Water management is particularly important in South Africa as the average water supply falls below $1700m^3$ per capita per annum which is officially accepted as within the definition of water scarcity (Pretorius and DuToit De Viliiers, 2001). The high pollution levels in South Africa, in comparison to first world countries, contribute to the limited water supply as some viable water resources are found to be polluted. In addition, rapid urbanisation, typical of most South African cities, is creating a backlog in many of the water services (Pretorius and DuToit De Viliiers, 2001) and is causing a significant increase in surface runoff (Braune and Wood, 1999). This problem is projected to increase in the future.

A goal of sustainable water resource management is to simultaneously satisfy environmental, social and economic demands (Feng, 2001). The South African National Water Act underpins this theory of sustainable water use in the set of guidelines for a catchment management strategy. These guidelines include taking into account 'any relevant national or regional plans' (Republic of South Africa National Water Act, 1998) and allowing for public participation while bearing in mind the needs of the 'existing and potential water users' (National Water Act, 1998).

Management measures can be technical, economic and institutional. Technical water management takes into account elements such as storage of water, desalination, pollution control, reuse and recycling. Economic water management takes into account pricing policies, tax exemptions and pollution control incentives. Institutional water management supervises existing administrative institutions, delivery of services and future requirement of systems (Chenje and Johnson, 1996). All these management measures need to take into careful consideration the demand for water used in both a consumptive and a non-consumptive capacity. Consumption of water occurs when it is used in processes such as irrigation, industry, mining and domestic use, therefore not returning to the water body from which it was extracted. Non-consumptive use of water refers to water that is used without extracting it from the water body such as hydroelectric power (Chenje and Johnson, 1996).

Competition may arise between these different users as water shortages become more problematic.

1.2.1 Urban Water management

Water in urban areas needs to be dealt with differently from water in other areas because there is a high interference with the natural water flow process in built-up areas. This interference means that water management needs to be undertaken on a smaller space and scale than in other areas. In addition, an extensive paved surface causes infiltration to decrease and hence increases runoff (Niemczynowicz, 1999). Unlike other areas of water use, urban areas use water for many different activities. Water supply in an urban context is used in areas such as the supply of drinking water, sanitation and urban agriculture.

It has been hypothesised that an ideal urban management plan must satisfy certain conditions. Water must be supplied 24 hours a day with regular inspection of the whole system to allow for maintenance. Plumbing must be such as to avoid wastage so that water can be supplied at an adequate price while still conveying the value of water. Lastly, it must be ensured that wastage by the consumers does not occur and the lines of communication remain open between the supplier and the consumers to educate them about waste, maintenance and hygiene (Chenje and Johnson, 1996).

It has been found, from studies of urban hydrology, that in order for comprehensive water management to take place in the urban area the whole river basin must be considered in the management plan (Niemczynowicz, 1999). This is because hydrological conditions such as the size of the river, its location and groundwater table can be determining or even limiting factors on the development and growth of the city.

1.2.2 Rural Water Management

The mean per capita water consumption in rural areas is generally less than the national average (Boonzaier, 2000). This fact decreases the priority of water management in rural areas when compared to other areas.

The management of water resources in rural areas is highly dependent on the community cooperation and involvement. The community must have a sound approach and knowledge of the water supply structure in their area. They must be willing to participate in the design and implementation of the infrastructure and be able to pay for the water either in reciprocal favours or in cash (Chenje and Johnson, 1996).

1.2.3 Agricultural Water Management

Although rainfall may be enough to supply crops with sufficient water in some areas of South Africa, it may be insufficient in other regions. Where rainfall is scarce, water management is necessary in order to irrigate all year round. In this case, the building of storage structures

such as dams is necessary, which have a major environmental impact (Chenje and Johnson, 1996).

Irrigated agriculture is the sector that has the potential to conserve the most water, not only due to the predominance of this sector in the South African economy but also because the irrigation methods can be improved significantly to reduce water use. Schemes such as flood irrigation use up to ten times more water than is necessary to irrigate the crop (Boonzaier, 2000). Commercial farmers, with on-farm dams, have an incentive to manage their water resources wisely because they control supply and demand themselves which means that they supply at their own cost for their own use.

1.2.4 Industrial Water Management

Finally, even though statistics show that industry uses less water than agriculture in South Africa, it is still a significant consumer of water. Many production processes are water based and, as a result, water is crucial to industry in South Africa. Due to the fact that most of the industrial sector is based within the urban area; water for industry must be budgeted for over and above domestic use (Chenje and Johnson, 1996).

1.3 Introduction to Water Management in the Breede River

At present, all water needs are being met in the Breede River water management area. The current situation has led to enquiries into whether water from the catchment could be used in transfer schemes into other catchments and whether this would be a viable long-term plan. Considering that, at present, the largest percentage of the water usage in the catchment is consumed by the agricultural sector, it would be prudent to pay specific attention to the potential expansion of this land use (DWAFc, 2002).

After communication with consultants at the Department of Water Affairs and Forestry who are involved in the investigation into future water transfer schemes it was discovered that the possibility of climate change had not been taken into account in the current Breede River Basin Study. This omission could have far reaching impacts on future water usage and management plans in the area because the preliminary decision of the study is to transfer water out of the Breede River for use in other catchments.

Currently, there is a list of priority activities with regard to water management in the Breede River. Improved management of salinity levels in the lower Breede River are of major concern, as water with high levels of salinity cannot be used for irrigation purposes. Salinity levels are increasing mainly due to irrigation return flows (DWAFc, 2002). Groundwater abstraction needs improved management, this would require better knowledge of the linkages between groundwater and surface water. Levels of afforestation need to be monitored in

order to keep a close check on groundwater recharge and salinity levels (DWAF (NWRS), 2002).

Up until now, management measures have been focused on the supply-side of water rather than the management of demand. For instance, supply from Brandvlei dam is carefully monitored and in times of drought release from the dam is limited (DWAF, 2003). It is this focus on supply and not on demand that is a concern in the development of new water transfer schemes from the Breede River, hence the recent study into future water demand.

1.3.1 Agricultural Water Management

The largest component of water use in the catchment is irrigation, accounting for 66% of total usage. This makes the agricultural sector the area that would require improvement if water supply is under stress. It is estimated that within the next ten years there will be a 30% decrease in water supply for agricultural use in the Western Cape due to population growth (Enright, 2004). An initial improvement that could increase the water supply in this sector would be to repair ageing water distribution infrastructure. At present, it is estimated that only 36% of water diverted into the dam actually reaches the farm boundary (DWAF, 2003). An increase in alien invasive vegetation could decrease this value even more because of their high water intake in comparison to indigenous species (Le Maitre et al., 1996). In this respect clearing of alien invasive vegetation is imperative.

Alien invasive vegetation accounts for 7% of the water usage at present, being higher than urban usage. Approximately 33 000 hectares of the Breede River catchment are invaded with alien species (DWAF, 2003). If this invasion goes unchecked it is expected to triple by the year 2020. Amongst other benefits of clearing alien vegetation it has been calculated that clearing aliens would provide the same amount of extra water to agriculture as building dams but at a much lower cost (DWAF, 2003). Other benefits of clearly alien vegetation include employment opportunities, a reduced fire hazard, conservation of endemic plants and restoration of low flows required for riverine ecology (DWAF, 2003).

Education about on-farm water management could improve water shortages significantly. At present only about 5% of the total farm expenditure is spent on water costs. This gives the farmer little incentive to reduce water usage (DWAF, 2003).

1.3.2 Urban Water Management

Urban water usage only accounts for 3% of the total water usage in the basin. However, it is thought that with proper management, significant water savings can be achieved in this area (Niemczynowicz, 1999). It is obvious that water management and usage have not been a priority in this sector in the past as there is no available data regarding water loss from this area (DWAF, 2003).

Other regions of water use in the catchment include water used in afforestation (3%) and in DWAF-controlled transfer schemes to other catchments (21%). These areas require less obvious management measures than urban or agricultural usage (DWAF, 2003). However, levels of afforestation must be monitored for both their water usage and impact on salinity levels in the river.

1.4 General Approaches to Studying Climate Change and Water Management

Different researchers have adopted a wide range of approaches to assessing water management issues under climate change. For example, Arnell (1999) found that there are many factors that will affect the growth of water demand in the future. The first of these factors is population growth since an increase in population will increase the demand for water. This is closely related to the population concentration, as there is an increasingly disproportionate concentration of people living in urban areas as opposed to rural. This will result in water supply being channelled into urban areas as a priority. The amount of extra water needed for an increase in population and concentration will clearly depend on the water use efficiency and management techniques. Industrial and agricultural change will also affect the future demand for water. These effects could either increase the demand as industry and agriculture expand or could decrease the demand as water is seen as a more valuable resource and is used more efficiently by both sectors.

To investigate the effect that climate change will have on the global water resources Arnell (1999) used two GCMs and simulated future river flows using a coarse resolution hydrological model. These projections were then combined with the future projections of water demand so that the impact could be estimated. From this coarse resolution, the study showed that by 2025 there may be an increase in the number of countries experiencing water stress. Some countries may experience less water stress, however. The projection for 2050 showed a discrepancy for the two GCMs. Under HadCM3 (a coupled atmosphere-ocean general circulation model developed at the Hadley Centre) there was an increase in populations experiencing water stress but under HadCM2 (an earlier version of the Hadley coupled atmosphere-ocean GCM) there was a decrease in water stress. This result was accentuated in the 2085 projection. Over both of the HadCM2 and HadCM3 scenarios, South Africa was shown to exhibit a decrease in annual runoff from its rivers therefore increasing its water scarcity.

The GCMs used in this type of research, ideally, need to be statistically downscaled in order to draw conclusions about the impacts for a particular area. Statistical downscaling, premised on the hypothesis that the synoptic scale is the dominant control of regional climate, uses the relationship between synoptic-scale variables and site-specific variables to infer a finer spatial

resolution (von Storch, 1995; Wilby and Wigley, 1997). There are, however, different ways of studying the climate change impacts on hydrology at a smaller scale.

In contrast to Arnell (1999), Werrity (2002) researched the impact of climate change on the management of water resources in Scotland using two strategies. The first strategy was a trend analysis of runoff and rainfall since 1960 for short-term planning. The second strategy fed results from statistically downscaled climate change scenarios of temperature and precipitation into a rainfall-runoff model. In the latter process, 38 river gauging stations widely distributed across Scotland were used. The results showed that between 2020 and 2080 there may be an annual increase in precipitation of 6 to16% and runoff was predicted to increase by between 5% to 15% by 2050. These predictions were found to be consistent with the trend analysis in precipitation and runoff for Scotland since the 1970's.

Werrity (2002) also suggested some impacts of this change in hydrology in Scotland due to climate change, which would be of interest to water managers. It was concluded that together with an increase in flood events higher water temperatures could accelerate the eutrophication of rivers by increasing algal blooms. Higher temperatures would also affect fish species by changing their breeding habitat and a change in water levels may cause damage to wetlands and river corridors (Gilvear et al., 2002). Together with these physical changes in the river system there was a projected increase in the human population, which is likely to cause a 5% enlargement in the demand for water by 2021. Overall, it was likely that the system would prove unsustainable in the future, without improved management (Werrity, 2002).

Menzel and Bürger (2002) took a slightly different approach in the investigation of runoff response to climate change in Southern Elbe, Germany. Firstly, the HBV-D hydrological model (Sælthun, 1996) was applied in order to simulate present runoff conditions. Statistically downscaled GCM scenario conditions were then used as input for the HBV-D model to simulate the future regional hydrology. Using 72 precipitation stations and four temperature stations distributed over the Mulde catchment, the result showed an increase in temperature with a trend towards decreased precipitation across the whole catchment. These conditions were projected to cause a decrease in the mean runoff currently experienced in the catchment (Menzel and Bürger, 2002).

Despite the slightly different approaches used in the investigation of hydrological response to climate change in Scotland and Germany, both sets of researchers warned of the uncertainties of basing results on a single GCM and advised that a range of GCMs be used in order to increase the certainty of the result.

1.5 Approaches to Studying Climate Change and Water Management in South Africa

Extensive research has been undertaken by Schulze (1990, 1995, 1997) of the University of Natal on the impact of climate change on the hydrology of South Africa. This research by Schulze used the ACRU hydrological model (Schulze, 1989). As seen in the previous section there is a suite of hydrological models from which to choose when undertaking hydrological studies. The choice of hydrological model is usually undertaken based on the area of study. Each hydrological model has a particular region of suitability. The ACRU model is suitable for simulation of river flow in many rivers throughout South Africa but does not simulate inter-basin transfer (New, pers. comm., 2003) so is not ideal for the Breede River, which has many tributaries extending into adjacent catchment basins.

The ACRU hydrological model was developed using the fundamental interactions between carbon dioxide levels, temperature and precipitation. These primary interactions showed that stream flow can be simply described by subtracting evaporation from precipitation and taking into account the storage of the surface, soil and groundwater (Schulze, 1989). However, when the carbon dioxide induced change in temperature due to climate change was taken into account it was seen that evaporation and precipitation are also affected. These types of interdependences showed that hydrologically related responses to climate change are complex and that there are still many uncertainties (Pittock, 1988).

The ACRU model takes into account the sensitivities of climate and land cover on the hydrological system. The model output consists of simulated stream flow, reservoir yield, sediment loss, irrigation and crop yield (Schulze, 1990). New (2002) used this model to investigate the climate change sensitivity of four Western Cape catchments. The four catchments were Langrivier, Bokke, Willemnels and Kleinsanddrif. Each catchment is supported by only one tributary of the Breede River instead of many inter-connecting tributaries. This allowed for the legitimate use of ACRU, which does not simulate inter-basin transfer. Results showed that, over all four catchments, there were sensitivities to a change in climate. It was found that stream flow decreased under decreased precipitation or increased potential evapotranspiration. Stream flow response was greater for a change in precipitation than potential evapotranspiration. However, catchments that received a lower precipitation under the current climate showed a more marked change in stream flow under a change in precipitation. This change was projected to exhibit an annual decrease of 14% in a humid catchment and 32% in an arid catchment as predicted by the GCMs, by 2050. This correlated to an average reduction in stream flow of 0.32% per year for the next fifty years (New, 2002).

The results from the study undertaken by New (2002) will be of significant use to water managers who must take these projections of water supply into account when planning for future demand. Hydrological responses are particularly vulnerable to climate change as the

impacts of the changing climate are exacerbated through regional interactions with water resources (Schulze 2000; Schulze et al., 2001). The ACRU model has proved suitable for use in this future hydrological projection process.

Little additional research has been undertaken within the Western Cape as to the impact that climate change will have on the hydrological resources of the area. This project will attempt to begin to rectify this by contributing towards a greater understanding of climate change impacts on one of the major rivers in the Western Cape system.

1.6 Introduction to Global Climate Change

This section presents an overview of past and projected future climate change at a global level. An introduction is also given to the use of GCMs in climate change research. Global Climate Change has become a well researched topic across the world, and while some uncertainty remains, this is largely around issues of regional manifestation.

The latest Intergovernmental Panel on Climate Change (IPCC) Third Assessment Report defines climate change as 'statistically significant variations that persist for an extended period, typically decades or longer. It includes shifts in the frequency and magnitude of sporadic weather events as well as the slow continuous rise in global mean surface temperature' (IPCC, 2001). IPCC (2001) propose that one of the foremost impacts of climate change will be the impact on the world's water resources. With the aims of this project in mind, it is therefore important not only to appreciate the concept of climate change but also to have an understanding of the tools used to project future climatic conditions.

Human industrial and agricultural activities have released greenhouse gases into the atmosphere at an increasing rate in the 20th century in comparison to previous centuries (IPCC, 2001). There is a current exponential growth in industrial emissions when compared to pre-industrial times. These gases enhance the natural greenhouse effect of the earth's atmosphere leading to a rise in average global temperature. Greenhouse gases are extremely efficient absorbers of infra-red radiation emitted by the earth and consequently the emission of these gases such as carbon dioxide, produced by human processes, is altering the radiative balance of the earth (Parry and Carter, 1998).

Evidence shows that the earth's climate has changed on a regional and global scale since the pre-industrial era, and the theory that most of these changes are due to human activities is now largely accepted based on a broad range of historical data (IPCC, 2001). Examining the decade of the 1990's alone, there is a definite correspondence between the decade being, not only the hottest year on record, but also exhibiting the highest recorded levels of greenhouse gases (IPCC, 2001). The correlation between the high levels of greenhouse gases and the high temperatures lead to the hypothesis that these records are not purely a result of natural variability.

The two most influential greenhouse gases emitted by humans since 1750 are carbon dioxide and methane. The amount of greenhouse gas emission is directly proportional to their corresponding concentration in the atmosphere. Historically, concentrations of these two gases have fluctuated between glacial and interglacial periods but even the largest of these values does not compare to the current atmospheric concentrations (IPCC, 2001). Since 1750 carbon dioxide has increased by 31% ± 4% and methane by 151% ± 25% as measured by studying gas trapped in ice cores and direct measurements over the past 40 years (Broecker, 1987). The increase in carbon dioxide is attributed to fossil fuel burning and land use changes such as deforestation, whereas the increase in methane is attributed to activities such as energy use, livestock, rice production, agriculture and landfills (IPCC, 2001). Additional greenhouse gases that have contributed to the changing climate are atmospheric nitrous oxide, which has increased by 17% ± 5% since 1750, tropospheric concentration of ozone, which has increased by 35% ± 15% since 1750 and stratospheric concentration of ozone, which has decreased since the 1970's (IPCC, 2001).

The biophysical effect of these changes in climate, driven by both natural variability and atmospheric gas concentration changes, is becoming evident, as seen in the following areas. The global mean surface temperature has increased by 0.6°C ± 0.2°C during the 20th century with a high possibility that the land has warmed more than the oceans (IPCC, 2001). Diurnal surface temperature ranges have decreased in the past 50 years due to minimum temperatures increasing at a rate twice that of the maximum temperatures (IPCC, 2001). Continental precipitation has increased, on average, by 5% to 10% in the 20th century throughout the Northern Hemisphere but has decreased in areas such as North and West Africa and parts of the Mediterranean. Heavy precipitation events have increased in the mid and high Northern latitudes by a magnitude of between 2% and 4%. Lastly, there has been an increase in the frequency and severity of droughts in areas such as Africa and Asia (IPCC, 2001).

Additional significant biophysical factors that have been affected include global mean sea level, which has risen, on average, 1mm to 2mm per year in the last century. El Niño events have also become more frequent and severe in the last 20 to 30 years (Andreae et al., 2001). The growing season of plants has been lengthened by 1 to 4 days per decade in the last 40 years, especially in the higher Northern latitudes and there has been earlier plant flowering, earlier breeding of insects and earlier bird migration (Andreae et al., 2001).

Unfortunately, most of the surface climatic data prior to 1860 is unavailable for the Southern Hemisphere, with significant regional gaps for much of the hemisphere for a lot of the 20th century. Atmospheric circulation data for the Southern Hemisphere is even more limited, and upper troposphere hemispheric-scale data is only robust subsequent to the advent of the

satellite era. Consequently, the conclusions drawn above are most valid for the Northern Hemisphere. Nonetheless, the available Southern Hemisphere record does concur with the broad conclusions.

1.7 Introduction to Global Climate Models

Global Climate Models (GCMs) were originally derived from weather forecast models. They were designed to be able to capture the three-dimensional aspects of the earth's system and climate processes (Thompson and Parry, 1997). It is recognised, however, that the atmosphere is coupled with the earths water balances and surface energy (Harrison and Foley, 1995). This recognition drove the development of coupled ocean-atmosphere models. The water circulation and heat of the oceans could have a significant effect on the outcome of climate change projections because of their derivation over a long time scale, this makes the oceans important to consider.

Radiation, which includes the input, absorption and emissions, is a central component of any GCM development. Dynamics, such as global movements caused by winds, ocean currents and vertical movements require consideration as well as surface processes such as sea, land and vegetation. The chemistry, constituency and dynamics of the earth and atmosphere such as carbon exchanges require measurement and the time and space resolution needs to be taken into account (Thompson and Parry, 1997). The inclusion of these and other external forcings in driving a GCM can result in a simulation of the full thermodynamics and kinetics of the earths system, from which several variables are commonly used in analysis (Harrison and Foley, 1995). From these basic variables, other variables can be derived, such as a moisture index and a mean temperature of the warmest month (Harrison and Foley, 1995).

GCMs fall into categories of either slab ocean models or coupled ocean-atmosphere models. The slab ocean model, that represents the ocean as one layer rather than a full system, is conceptually inferior to the coupled ocean-atmosphere model described below. However, it is not always necessary to use a coupled model. In the Northern Hemisphere, the results from the coupled and slab models are relatively similar, largely because there is a greater area of land in the Northern Hemisphere compared to oceans (Cracknell, 2001). In the Southern Hemisphere, it is more accurate to use a coupled model because there is greater ocean coverage than in the Northern Hemisphere. The greater ocean coverage results in a greater impact on the climate processes due to interaction with the ocean. For instance, in the Southern Hemisphere, the coupled model simulates a significant uptake of heat into the ocean, which greatly reduces the surface warming. There is also concern that the coupled model may be overestimating the amount of heat taken up by the ocean in the Southern Hemisphere.

A coupled ocean-atmosphere model takes into account that the oceans and atmosphere are linked through exchanges of heat, matter and momentum (Peixoto and Oort, 1992). The coupled ocean-atmosphere model also suggests that the change in maximum and minimum temperature will be of a similar magnitude, except when there are changes in precipitation and cloud cover. Wetter, cloudier climatic conditions will result in a greater increase in the minimum temperature whereas drier, less cloudy conditions will lead to a greater increase in maximum temperature (Chakraborty et al., 1998). Due to the fact that using a coupled atmospheric-ocean model is more complex and computationally demanding than an atmospheric model (as used in weather forecasting), the former is generally run at a coarser spatial resolution (Harrison and Foley, 1995). Generally, the spatial resolution of a current coupled GCM has grid cells of between 2° and 4° in latitude and longitude and the vertical structure of the atmosphere is typically represented by 9 to 25 levels. With such coarse grid spacing it is not possible to model small-scale atmospheric features such as microclimatic processes, even though they may be very important to the overall climatic process (Harrison and Foley, 1995).

In all GCMs it is not possible to take into account every anthropogenic as well as natural process for every model; and it is difficult, therefore, to reproduce regional features with good accuracy. Added to this, some GCMs do not replicate the effect of regional sulphate aerosols, which would have a significant cooling effect (Watterson et al., 1997). Another drawback in most current generation GCMs is that plant physiology is not included; this means that any change in vegetation cover, which could affect the climate processes, have not been included in the model.

Apart from these drawbacks of using GCMs, they are generally considered reasonable tools in assessing future climate. They are advantageous due to their robust modelling of large-scale atmospheric processes. Without GCMs, climate change projections would be impossible at a synoptic level. The accuracy of the models are constantly being improved and the projections refined.

Three GCMs are used for analysis in this project, namely, the Deutsches Klimarechenzentrum and Max Planck Institute model (ECHAM4), Australia's Commonwealth Scientific and Industrial Research Organisation model (CSIRO Mk2) and the Hadley Centre for Climate Prediction and Research model (HadAM). All the models are variants of the general GCM form.

There are strengths and weaknesses associated with each GCM for use in climate change impact studies and every model has a specific climatic region for which it has more skill. For instance, when examining the GCMs in this project, sulphate aerosols are modelled by HadAM, which CSIRO and ECHAM4 do not attempt to do. This could have a major effect on

the resultant climate prediction because sulphate aerosols have a cooling effect on the atmosphere whereas most greenhouse gases have the opposite effect. It is also known that the CSIRO model does not model precipitation in the Western Cape climatic region very well since it models a higher summer rainfall than winter rainfall (Steynor, 2002). This does not mean, however, that it is not accurate in modelling other climate variables in the Western Cape.

Due to the fact that each GCM has strengths and weaknesses in climate modelling it is thus important to use multiple models for the purposes of this project. In doing so, a more comprehensive view of the impact of climate change in the Western Cape is attained.

1.8 Uncertainty Incorporated into Climate Change Projections

By their nature, there is an inherent uncertainty associated with Climate Change projections because they are only projections of possible outcomes subject to a number of unknowns. A reasonably large envelope of possible scenarios could unfold in the future climate. These scenarios are predominantly based on the actions of mankind in terms of emission output and management of the earth's resources.

All climate change models use an emission scenario as a basis for representing the forcing leading to climate change. These emission scenarios include assumptions about different socio-economic conditions, projected concentrations of greenhouse gas emissions, radiative forcing projections and so on. These are all anthropogenically forced variables with a lot of possibilities and combinations, thus increasing the uncertainty of climate change projections (Morita and Robinson, 2001). In addition, it is known that if emissions are abruptly stopped the global warming process will not cease immediately since the earths system requires sufficient time to elapse for the emitted gas to be absorbed by the earth's natural sinks or absorbers.

In order to limit the infinite number of future emission scenarios for use in GCMs, Nakic´enovic et al., (2000) prepared the Special Report on Emission Scenarios (SRES). As described by Nakic´enovic et al. (2000) these scenarios "exclude only outlying surprise or disaster scenarios in the literature." For the purposes of this project the SRES A2 emission scenario is used to force the GCMs because of its preferential availability over other SRES scenarios[1]. The SRES A2 scenario focuses on a world where regional cultural identities are strengthened and stress is placed on family values and traditions relevant to a local community. There is a high population growth rate but fast economic growth is not a priority. Although this is one of a "family" of possible future scenarios in the Special Report on Emission Scenarios (Nakic´enovic et al., 2000), it is only one of many scenarios that could be used. The use of only one possible future scenario can cause an uncertainty in the study.

[1] http://ipcc-ddc.cru.uea.ac.uk/asres/sres_home.html

Other practical uncertainties arise out of unknown variables such as insufficient scientific knowledge and known variables such as the unpredictability of the earths system due to climate variability. The rest of this section deals specifically with uncertainties resulting from using different GCMs in modelling the future climate because the choice of GCM causes one of the greatest uncertainties in climate change projections.

All GCMs have limited capacity in fully simulating the earths system. These weaknesses are largely due to computational restraints and limited information or understanding around the topic of climate physics (New and Hulme, 2000). Each GCM uses different physical input parameters (Mearns et al., 2001), which result in a slightly different outcome being expressed in each future climate projection.

Added to this, every GCM has areas on the earth that are modelled more accurately than other areas and vice versa. This factor is also brought about due to the differing input physics in each GCM. For instance, in the Western Cape, HadAM and ECHAM4 are better at modelling winter rainfall than CSIRO (Steynor, 2002).

There are modelling uncertainties such as modelling the climate response to forcing and using model responses in impact studies (Mearns et al., 2001). There are also uncertainties in converting emissions to concentrations and converting concentrations to radiative forcing (Mearns et al., 2001). These factors limit skill in climate change model simulations. As computer complexity and knowledge increases these uncertainties may decrease and predictions may become more reliable.

Another issue to consider when using GCMs is that there is no probability value attached to predictions. As a result, model outputs, using various scenarios, are supposedly equally plausible (Jones, 2000). Even though, at a global level, all SRES emission scenarios result in an increase in atmospheric carbon dioxide concentrations, which, based on simple energy balance principles indicate an increase in global mean temperature, certain scenarios hold a greater probability, given the present trend in industrial emissions. If one uses multiple GCMs forced by several emission scenarios to represent the uncertainty, one can more easily determine the range of uncertainty associated with the projections. Knowing the sensitivity of each GCM and the associated uncertainty will allow for more robust climate impact strategies to be developed (Jones, 2000).

While acknowledging the uncertainty associated with GCMs, it is recognised that they generate projections of future climate that are to the best of our capability, using present scientific knowledge. These models are considered good scientific assessments of the future climate and it is reasonable to use them in analysis of future terrestrial systems. In recent

studies GCMs have been confirmed as appropriate tools in assessing climate change when US researchers compared the rise in ocean temperatures with predictions from climate models and found that they compared with a statistical confidence of 95%[1].

[1] http://news.bbc.co.uk/2/hi/science/nature/4275729.stm

CHAPTER TWO: SOM ANALYSIS

Classification of synoptic weather patterns has a long history and forms a distinct sub-discipline of synoptic climatology (Yarnal, 1984). The intent in classification is to extend data records by use of a transfer function between the environmental parameter, such as runoff, and the synoptic types. This circulation record can then be used to extend the local environmental data into the future.

The use of Self-Organising Maps in this project enabled classification of a user-specified amount of synoptic circulation patterns. Association of each synoptic circulation pattern with a range of runoff regimes allowed for the extension of predominant runoff patterns into the future.

2.1 Analysis Techniques

2.1.1 The Kohonen Self-Organising Map

Self-Organising Maps (SOMs), which are a type of Artificial Neural Network (ANN), are the principle technique used for the present analysis of atmospheric data. ANNs, initially thought to replicate the general connection structure of the brain, are a network of inter-connected simple computational 'neurons'. The design philosophy of ANNs has proved to be very successful with many applications including speech recognition, handwriting analysis and protein structure analysis (Risien, 2002). More recently, ANNs have been used in the analysis of synoptic circulation patterns, in the form of SOMs.

SOMs are a powerful technique for use in climatology because they allow for the visualisation of an array of synoptic states by facilitating the grouping of large amounts of synoptic data into a specified amount of synoptic patterns or nodes. This is achieved in the same way as cluster analysis, which identifies dominant modes within the data space (Tennant, 2003). For instance, if a 7x5 SOM is defined at the beginning of the training then the input data will be limited to mapping to 35 atmospheric states. Each node represents a state in the data space that is nominally the mean of all synoptic patterns mapping to the node after training. Frequently occurring synoptic patterns can easily be visualised in a SOM map which displays all the nodes simultaneously. Without this visualisation feature, analysis of synoptic circulation data with SOMs would not be as user-friendly.

The Self-Organising Map is particularly competent at pattern recognition (Kohonen et al., 1996). In contrast to other clustering algorithms, basic SOM methodology is not primarily concerned with grouping of data or identification of clusters, although data clustering can result from a SOM analysis. The first step in the SOM routine is to define a random distribution of nodes (otherwise known as arch-type patterns) within the data-space. For instance, if it were decided that all synoptic states should be classified into 35 arch-type patterns, this would be the same as classifying 35 "nodes".

Each node has an associated reference vector equal in dimension to the input data. The similarity between the input data and each of the node reference vectors is calculated while data is presented to the SOM. The reference vector of the "winning" node is then modified, during the user-defined learning period, to reduce the difference between itself and the input vector. The input vector is thus only used to adjust the location of the SOM node in the data-space (Hewitson and Crane, 2002).

The major advantage of a SOM in comparison to other clustering algorithms is that, for a SOM, not only is the "winning" node updated but all of the surrounding nodes are also adjusted in proportion to their distance from that particular node. This process continues until the changes in node location are negligible. The final result is a concentration of nodes in regions of the data-space with a higher data density. Reference vectors are adjusted to span the data-space, and each node represents a position that corresponds to the median of nearby data samples. This procedure effectively identifies "arch-type" points in the data-space that span the data set (Hewitson and Crane, 2002).

A 7x5 SOM was defined for the purposes of this project. This encompasses five nodes in the vertical and seven nodes in the horizontal on the SOM map, allowing 35 "arch-type" synoptic states after training. Each node/"arch-type" synoptic state (each individual picture) in the SOM map represents the mean of all the synoptic patterns mapping to that node. All data presented to the SOM are assigned to one of these nodes. Nodes represented as diagonally opposite in the SOM map indicate the opposite extremes in the data presented to the SOM, and neighbouring nodes are indicative of the most similar data. Therefore, synoptic states that are dissimilar are widely separated over the SOM space and transitional states are represented between the groups (Hewitson and Crane, 2002). Figure 2 is an example of the typical representation of a 7x5 SOM of specific humidity.

FIGURE 2: An example of a 7x5 SOM of specific humidity

There are three key aspects of SOM behaviour; first, the SOM always assumes the data to be continuous. If there is a break in the data, the SOM will attempt to interpolate data within the discontinuous region. Second, SOM nodes represent positions in the data space, with more nodes in regions of the data space where there are more data samples. Third, the SOM captures non-linear characteristics of the data, therefore accounting for non-linear data distributions (Hewitson and Crane, 2002).

SOMs have a number of advantages over traditional statistical methods of analysing spatial data. First, they are able to give insight into non-linear problems of great complexity, and second they are more robust in handling noisy and missing data than traditional methods of analysis (Dayhoff, 1990). For identifying groups in a data set, one particular advantage of SOMS over other multivariate techniques is that the relationship among the identified patterns can be visualised in the same form as the original data. For example, because the node reference vectors reflect the input format, the span generalised patterns identified by SOMS are more easily interpreted than outputs from conventional multivariate techniques.

2.1.2 Frequency Analysis Using SOMs

The use of frequency analysis in this project determined the difference between the frequency with which the control atmospheric data and the simulated future atmospheric data mapped to each node in the NCEP-trained SOM. A list of each time-step in the data series and SOM node to which it mapped was generated by the SOM program, from which frequency maps could be constructed showing the frequency of data mapping to each node. The SOM program also generated the quantization error of each time step (the degree to which the data of this time step is matched by the node reference vector), typically expressed as the mean absolute error.

The frequencies could be displayed in a number of ways; as a value assigned to each individual SOM node in a grid display format along with colour denoting the magnitude of the node frequency (Figure 3), as a contour map indicating the distribution density across the SOM surface (Figure 4) or as a line graph (Figure 5). Figures 3, 4 and 5 depict an example of the manner in which frequencies of synoptic patterns of specific humidity in each SOM node in a 35-node array can be displayed. The same input data was used to create all the frequency maps. In the example, the highest frequency of synoptic pattern is mapping to the central node (3;2) at a frequency of 3.614.

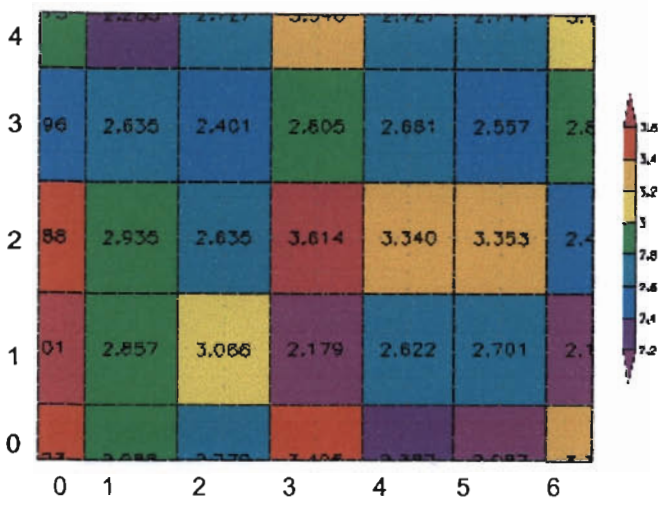

FIGURE 3: Example of a grid-map showing the frequency of specific humidity data at each SOM node

Figure 4 displays a user-friendlier pattern of frequency across the SOM space. Rather than just the frequency value assigned to each node, it shows the distribution density of data across the SOM space.

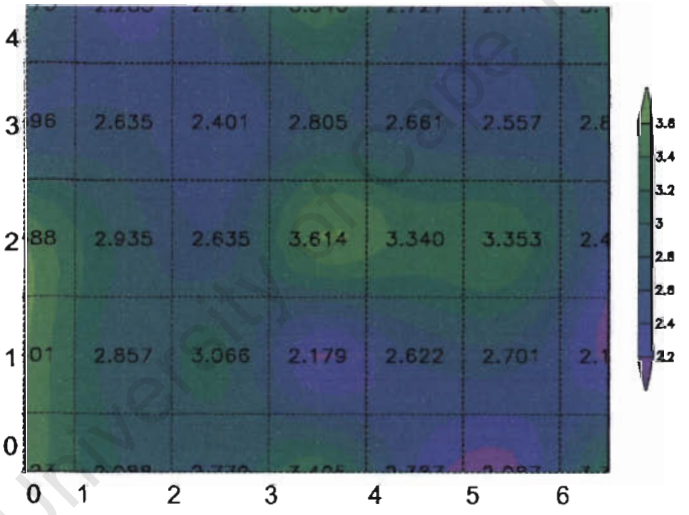

FIGURE 4: Example of contour map showing the frequency of specific humidity data across the SOM surface

A final method of displaying frequency is the use of a line graph (Figure 5). This method plots each SOM node frequency linearly across a graph. High points in the graph show areas of high frequency with regions of high data density. Low points in the graph depict nodes that have a low data frequency. This is not the best depiction of frequency pattern as SOM maps cannot be analysed in columns or rows, which is how the line graph depicts the SOM space.

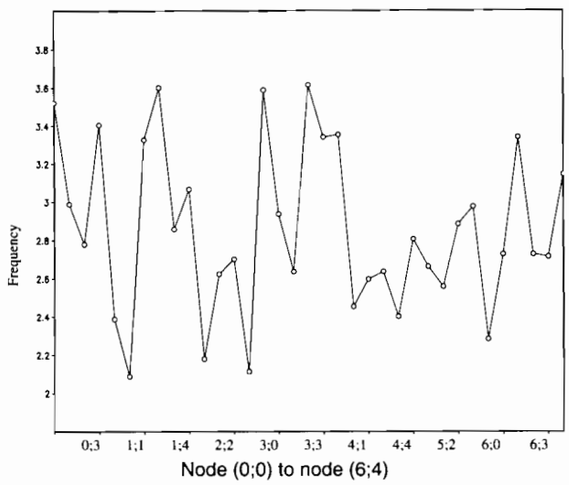

FIGURE 5: Example of a line graph showing frequency of specific humidity data at each node

2.2 Data Acquisition and SOM training

A methodology was developed in order to assess the accuracy of the GCM data in simulating the present day climate and to assess the changes between the control and projected future climate data. These initial steps ultimately led to a base from which an assessment of future runoff in the Breede River commenced.

Initially, the NCEP (National Centres for Environmental Prediction) reanalysis data for 1979 to 1999 was extracted using GrADS (Gridded Analysis Display System) for use as a baseline climate. Although this data was used as a representative of present day climate, it may not be strictly identical. The area used for extraction was an atmospheric window situated over the Western Cape. It must be noted that NCEP reanalysis data (resolution of 2.5° x 2.5° in latitude and longitude) is constrained by observations but is also a product of an atmospheric model. Owing to the difference in the horizontal resolution of the GCM's and the reanalysis data, interpolation function grid-box averages were used to convert all the data to a common 4° x 3° resolution. This resulted in an area of 12° to 28° in longitude and –39° to –27° in latitude comprising a 5x5 grid size. Completion of the regridding process resulted in a coarser resolution data set.

Variables extracted from the NCEP data included geopotential height and specific humidity at 700 hPa, and for two time steps per day. These two variables were chosen because they characterise the general atmospheric state related to rainfall. Specific humidity depicts the mass of water vapour contained in a unit mass of moist air (Tyson and Preston-Whyte, 2000) and geopotential heights depict height levels containing surfaces of constant potential energy (Tyson and Preston-Whyte, 2000). By using a combination of these two variables, an evaluation of rainfall potential could take place. Using a rainfall related synoptic state was more accurate than using model-derived precipitation data because there is a lot of uncertainty in the parameterisations used to derive precipitation data from atmospheric

models. In addition, the aim was to observe the large-scale atmospheric condition over the study area.

The standardised resultant NCEP data was used for input into the SOM for analysis purposes. The SOM was trained, with specific humidity and geopotential heights as part of the same SOM, in order to produce 35 archetypal patterns over a 7x5 SOM space. The daily input data was associated with the closest synoptic archetype and an error value was produced corresponding to each day's association with its closest synoptic state.

A SOM node distortion surface was produced after SOM training with the purpose of showing the Euclidean distance between nodes (Hewitson and Crane, 2002) and was computed by calculating the distance between each node and its adjacent nodes. Checking the SOM node distortion surface ensured that the SOM surface was not twisted; twisting would cause a distortion in the continuum of atmospheric conditions represented by SOM nodes. The distortion surface map output for this particular SOM is represented in Figure 6 below.

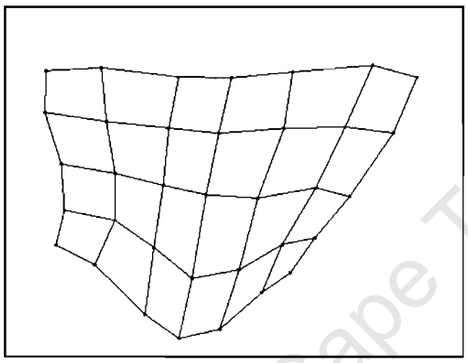

FIGURE 6: Map of the distortion surface from the NCEP SOM

ECHAM4, CSIRO and HadAM data was extracted once the SOM had been run with the NCEP reanalysis data. This data was extracted from each GCM climate simulation for a control climate ranging from 1979 to 1999 and a projected A2 scenario based future climate from 2079 to 2099 at two time-steps per day. The data encompassed the same variables and same area as NCEP. The extracted data from all the GCMs was regridded to the same resolution as the regridded NCEP data (4° x 3°) in order to form a 5 x 5 grid.

The only difference in this process in comparison to the NCEP data extraction was that each GCM's projected future data was standardised with its own control mean and standard deviation. In addition, ECHAM4 and HadAM have a 360-day modelled year, which caused a difficulty in analysis because each month has a standard 30 days. This 30-day month was noted and accounted for in the extraction of the data.

The extracted GCM data was then used to examine the correlation between the NCEP-modelled observed synoptic state and the GCM-modelled synoptic states. Both the control and projected future climate data for each model were mapped onto the NCEP-trained SOM

nodes producing six separate SOM maps. Three of these SOM maps showed the distribution of the GCM control data over the SOM space and a further three maps showed the distribution of the GCM-simulated future data over the SOM space. These results were used to assess the credibility of the GCM's in simulating the synoptic scale circulation of the region, which was accomplished by comparing the NCEP frequency map to each GCM control frequency map. The similarity of these maps indicated the similarities and differences between the data sets of NCEP and each GCM and hence whether all the models depicted the observed climate adequately. Following this, the projected changes in the frequency of synoptic events were determined under future climate by comparing the changes between each GCM-simulated future frequency map with their associated control frequency map.

2.3 NCEP SOM Results and frequency analysis:

Frequency analysis began using a SOM trained with NCEP reanalysis data. The use of this data created a baseline climate from which GCM data could be analysed. All the GCM data was mapped on to this initial NCEP-trained SOM therefore analysis of this SOM was necessary before any examination of GCM data could take place.

Specific humidity and geopotential height for two time steps per day from 1979 to 1999 were trained in the same SOM. The result is a 5x7 SOM of NCEP reanalysis data, initially displaying specific humidity at 700 hPa, and then geopotential height at 700 hPa. The 35 atmospheric conditions displayed indicate a range of conditions occurring throughout an annual cycle. The overall SOM used as a basis for analysis in this project represents a combination of specific humidity and geopotential heights ie a combination of figures 7 and 8.

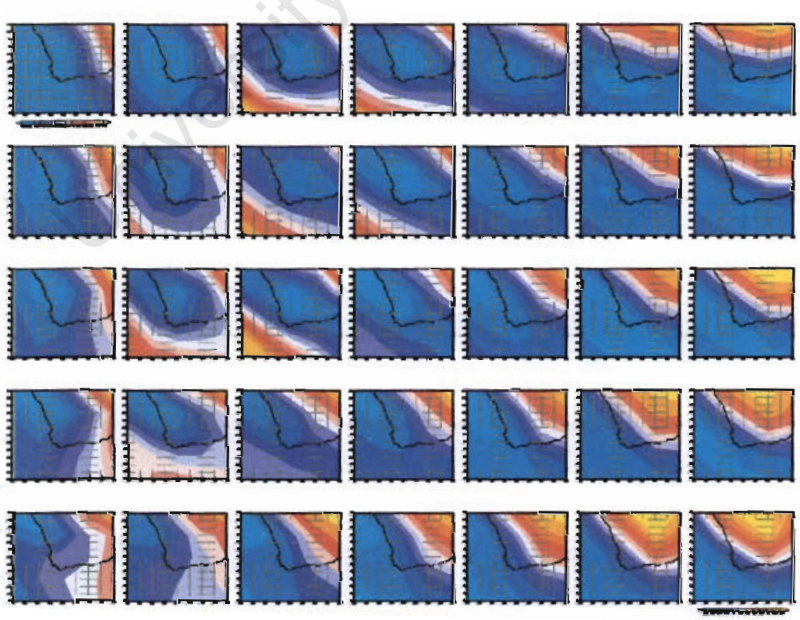

FIGURE 7: NCEP SOM of specific humidity at 700hPa

The light blue areas in Figure 7 are regions of low water vapour content and the areas of red, orange and yellow are regions of increasingly higher water vapour content. Intuitively, a high specific humidity is needed for precipitation. Therefore, as a very crude interpretation it can be said that areas of high specific humidity are areas where possible rain may fall whereas areas of low specific humidity are areas of dryness. This interpretation, together with the knowledge that the Western Cape is a winter rainfall region, allowed for analysis of the seasonality over the SOM space by inspecting synoptic patterns.

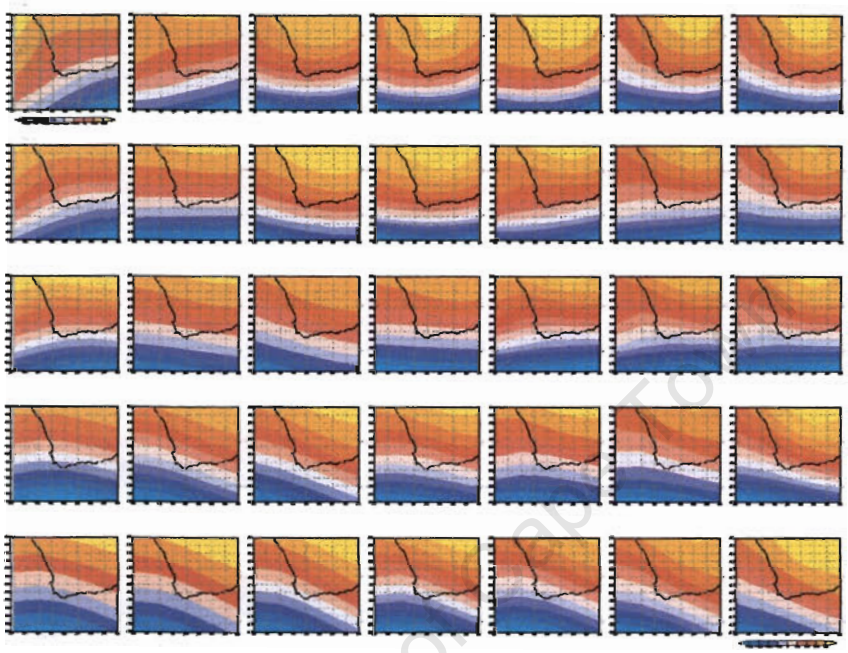

FIGURE 8: NCEP SOM of geopotential height at 700 hPa

In the SOM image in Figure 8 the red, orange and yellow areas illustrate areas with warmer air, while the blue to light blue areas illustrate colder air regions. This is known because warmer air corresponds with regions of greater geopotential height values whereas colder air corresponds with regions of lesser geopotential height values.

The SOM process created a file containing information as to which dates were associated with which node in the SOM space. By briefly examining this file, it was determined where in the SOM space each date in the daily data was mapping. From this, it was concluded that the majority of dates falling into the winter months were mapping to the left-hand side of the SOM surface. Conversely, the majority of days in the summer months were mapping to the right-hand side of the SOM surface. This conclusion is confirmed by examining the atmospheric patterns displayed across the SOM surface. When looking at the SOM of specific humidity (Figure 7) it is seen that the right-hand side of the SOM surface displays nodes representing days with a high specific humidity over central South Africa. This is a summer condition, as it is known that rain falls over the escarpment in summer due to the thermal low (Tyson and Preston-Whyte, 2000). The left-hand side of the SOM surface shows a predominance of days with the high specific humidity previously found in the interior of South Africa lying further to the east and some days displaying a high specific humidity

around the Western Cape. This indicates mid-latitude cyclones passing the Western Cape. Mid-latitude cyclones over Cape Town are a consequence of the migration of the sun Northwards. This means that they are predominant in the winter season.

The SOM of geopotential height in Figure 8 confirms the result that the right-hand side of the SOM space has nodes that encompass a large proportion of summer days whereas the majority of winter days in the daily data fall into nodes on the left-hand side of the SOM space. The cold, dense air conditions associated with a mid-latitude cyclone are more prominent over the Western Cape on the left-hand side of the SOM. This indicates a winter condition. The Westerly waves present to the South of South Africa that bring the mid-latitude cyclones are further South on the right-hand side of the SOM space, indicating a summer condition. This result shows a propensity that some archetypal synoptic patterns exhibit towards favouring certain seasons.

By looking at the frequency map generated with the NCEP data (Figure 9) an examination of high and low-density nodes could take place. Each grid-box in the frequency map represents the frequency of the archetypal pattern of both specific humidity and geopotential height in that same node in Figures 7 and 8. For the purposes of this project it is stated that only SOM nodes with a high data mapping frequency will be used for analysis, SOM nodes that display a low density of data mapping have not been analysed in this study due to time constraints, although these transitional states may have an effect on the length and timing of rainfall.

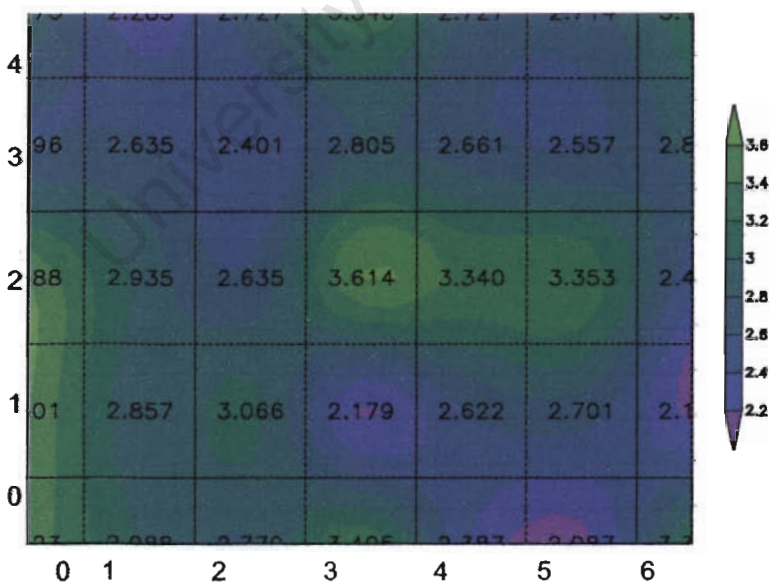

FIGURE 9: The frequency map of the NCEP SOM

Representing the bottom left-hand corner of the frequency plot as SOM node (0;0), The SOM of NCEP reanalysis data indicates that the highest frequencies of data (in percentages) are mapped to the nodes (0;0), (0;1), (0;2) and (3;2). However, overall, the data is distributed relatively evenly across the SOM space. These high frequency nodes do not display a strong seasonal signal although most of the high frequency nodes fall into the 'winter half' of the

SOM space. However, the highest frequency node (3;2) lies on the interface between the nodes representing predominantly winter days and those representing predominantly summer days. The lowest frequency of data mapping falls into nodes (4;0), (5;0), (3;1), (6;1) and (1;4). These nodes display a random seasonal signal and therefore warrant no further analysis.

The development of a line graph of frequency across the NCEP SOM space (Figure 10) confirms that the NCEP data maps relatively evenly across the SOM space. This is concluded since the line graph shows a small range of data-mapping frequencies across all the SOM nodes.

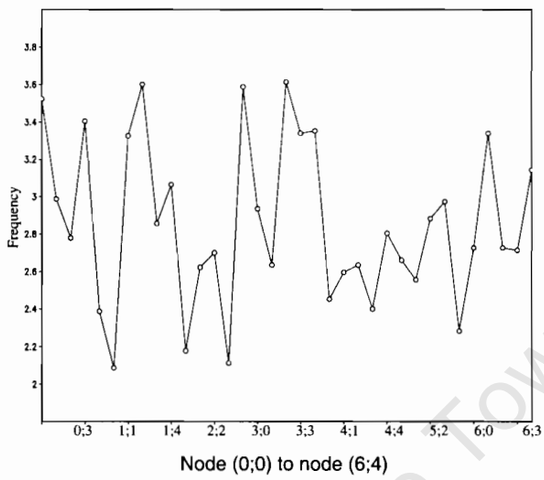

FIGURE 10: The frequency line graph of the NCEP SOM

Whenever a large amount of data, such as this, is clustered into 35 archetypes, there is a certain amount of error associated with the result. Figure 11 is represented in a similar format to that of a frequency map but shows areas of high and low error in data mapping. Due to the fact that the NCEP data was used to train this SOM, it was expected that the error would not be unduly large at any particular node. This assumption is confirmed in the error map, which shows a relatively uniform error across the SOM space.

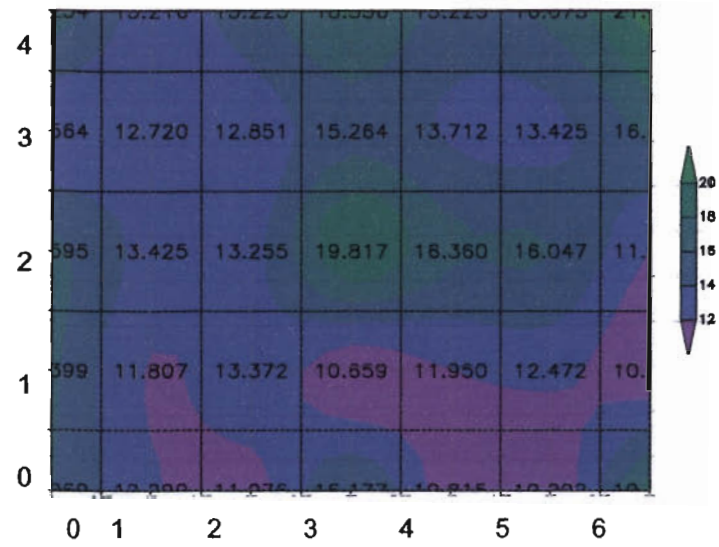

FIGURE 11: The error plot of The NCEP SOM

The results from the analysis of NCEP data in this section were now used to further assess the validity of GCM data and, hence, future climate projections. This was achieved by using the NCEP reanalysis data as an approximation of present climate.

2.4 Frequency Analysis using GCM data

In this section, each GCM was compared to the NCEP data as analysed in section 2.3. This comparison was firstly used to assess the GCMs ability to simulate present climate. Secondly, the departure from this baseline climate was assessed in order to begin to understand future changes in climate. Each GCM was taken in turn and underwent an analysis of the change in high frequency nodes in the SOM map, from present to future. This was a crucial step in the project as it provided a base from which to start analysis of the change in runoff from present to future, in the next chapter.

2.4.1 ECHAM4 Frequency Analysis

The Deutsches Klimarechenzentrum (DKRZ) in Hamburg, Germany and the Max Planck Institute for meteorology developed the GCM, ECHAM4. It was developed from the European Centre for Medium-range Weather Forecasts model (ECMWF), hence the first part of the acronym, and in Hamburg, hence the second part of the acronym. The parameterisation of ECMWF was adjusted for output of climate simulations[1]. ECHAM4 is coupled with OPYC3 (ocean and isopycnal co-ordinates model) and has 19 atmospheric layers and a resolution of 2.8° in latitude and longitude.

Terrain heights for the GCM are taken from a high resolution United States Navy data set (Roeckner, 1999). Data for temperature and sea-ice were transferred into the GCM from the COLA/CAC AMIP SST and sea-ice data set.[2] This enabled the coupling of the ocean and the

[1] http://cera-www.dkrz.de/IPCC_DDC/IS92a/Max-Planck-Institut/echam4opyc3.html
[2] http://ipcc-ddc.cru.uea.ac.uk/cru_data/examine/echam4_info.html

atmosphere components in order to create a coupled GCM. The area of each grid that is covered by vegetation is based on the Wilson and Henderson-Sellers (1985) data set.

Data from the ECHAM4 model was mapped on to the NCEP-trained SOM nodes in order to assess the credibility of the ECHAM4 control data (1979 to 1999) in representing the observed climate as shown by the NCEP reanalysis data. This also showed the ability of the GCM in simulating the synoptic scale circulation of the region. Following this, the changes in the frequency of synoptic patterns between the present and projected future climate were determined.

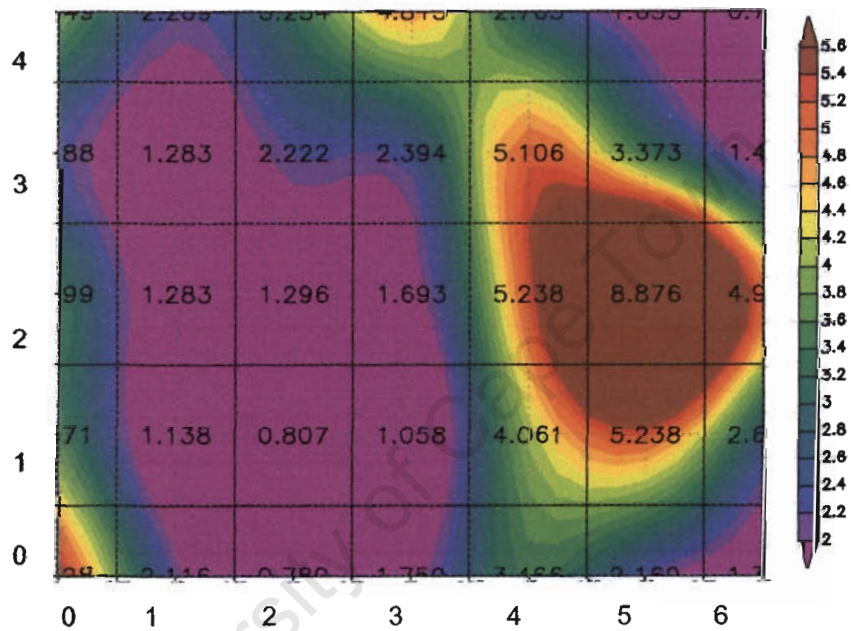

FIGURE 12: The frequency map of the ECHAM4 control SOM (1979 – 1999)

The frequency map of ECHAM4 GCM data in Figure 12 indicates that the greatest frequencies of data fall within node (5;2). For comparison purposes, the colour range was limited to a frequency of 5.6. It can be seen that the frequency found in node (5;2) is significantly higher than 5.6 however, these colours are not represented in the frequency map. Unlike the frequency map of NCEP data, the frequencies across the ECHAM4 SOM space are not uniform. In fact, the majority of the ECHAM4 SOM space has a low frequency of data mapped to it.

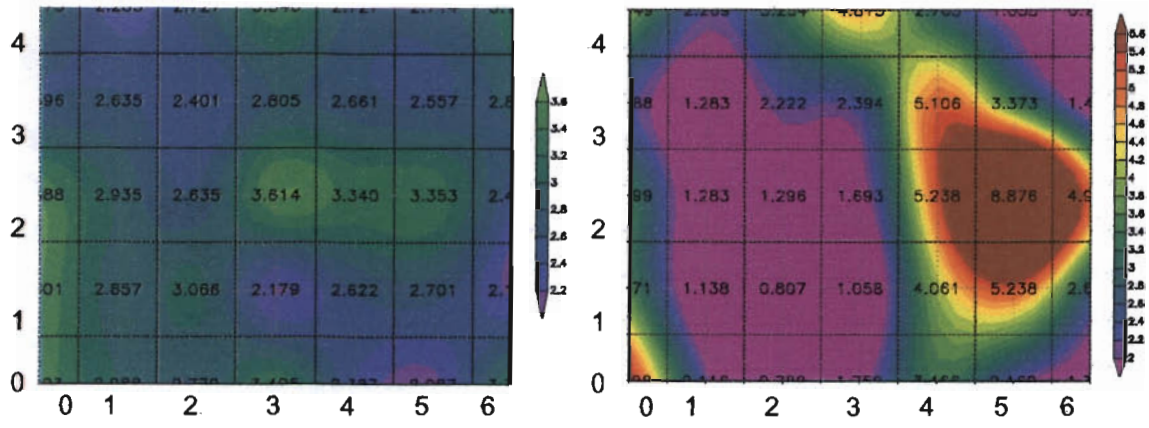

NCEP (a) **ECHAM4 (b)**

FIGURE 13 (a) and (b): Comparison between NCEP control and ECHAM4 control frequency maps

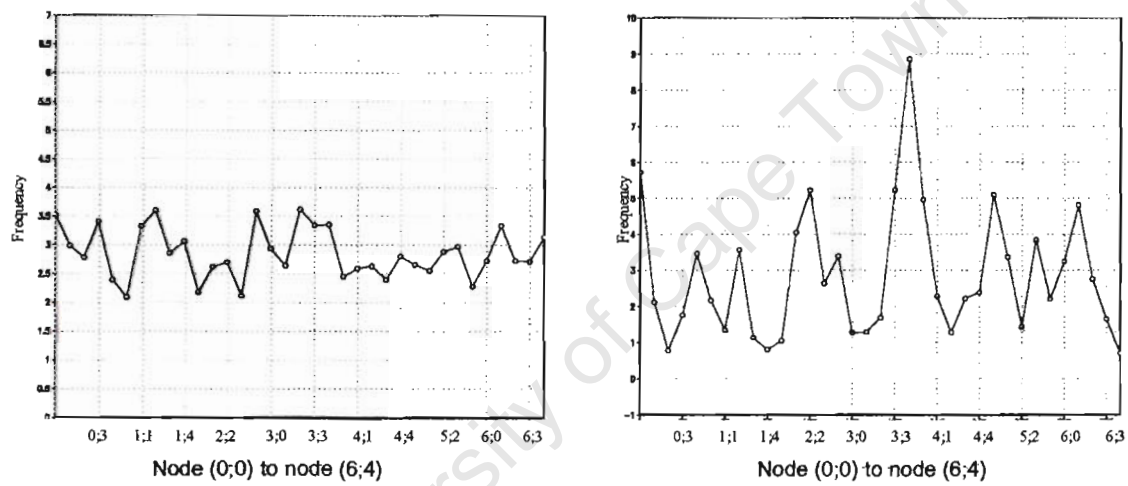

NCEP (a) **ECHAM4 (b)**

FIGURE 14 (a) and (b): Comparison between NCEP control and ECHAM4 control frequency line graphs

Comparison of the NCEP reanalysis data and the ECHAM4 GCM data shows that the predominant difference between the two frequency images (Figures 13 and 14) is that the high frequency SOM node is situated in node (3;2) in the NCEP-trained SOM whereas it falls into node (5;2) when the ECHAM4 control data is mapped onto the NCEP-trained SOM. It is concluded that the ECHAM4 control data depicts a higher occurrence of days that resemble the synoptic pattern of node (5;2). It happened that node (5;2) represents a synoptic condition that is predominantly associated with a summer day. This fact leads to the conclusion that the ECHAM4 data includes a majority of days that are representative of summer conditions, therefore, displaying a summer bias. In fact, ECHAM4 does not seem to map at all well to the SOM nodes created in the NCEP SOM training. Most of the ECHAM4 control data maps predominantly to seven nodes found around node (5;2). This error has to be taken into consideration when comparing the projected future GCM data to present conditions.

The greater uniformity in the distribution of data across the NCEP SOM space is confirmed in the comparison of the frequency line graphs of NCEP and ECHAM4 in Figure 14. The line graph of NCEP is relatively flat when compared to the ECHAM4 graph. This shows that ECHAM4 does not display a uniform distribution of data across the NCEP SOM space.

Once the error associated with the GCM data was established by analysing the GCMs representation of the present climate, it was possible to move on to the change in the predominant synoptic patterns projected by ECHAM4 from present to future. The results from the frequency maps represented in Figures 15 and 16 indicate that the ECHAM4-simulated A2 emission scenario data for 2079 to 2099 is very different from the ECHAM4 control data (1979 to 1999). This indicates a relevant change in the frequency pattern across the SOM space from the present to the future.

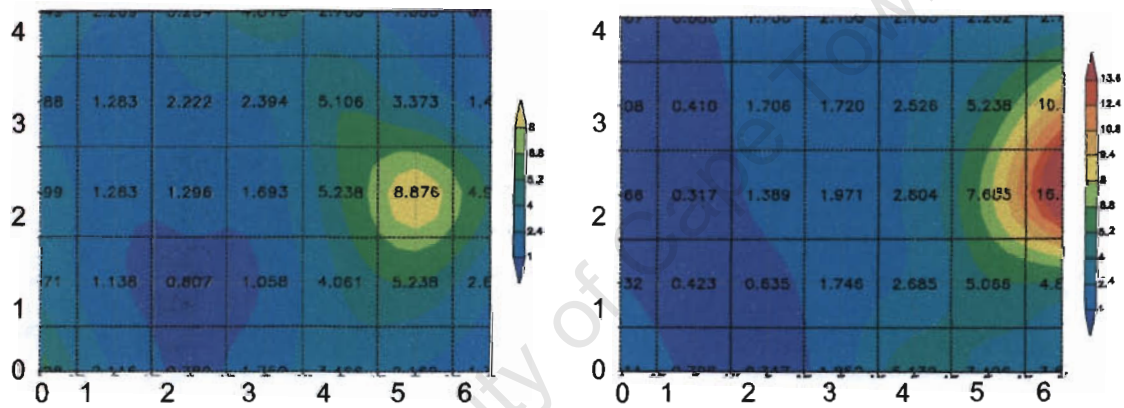

ECHAM4 control (1979 – 1999) (a) **ECHAM4 future (2079 – 2099) (b)**

FIGURE 15 (a) and (b): Comparison between ECHAM4 control and ECHAM4 projected future frequency maps

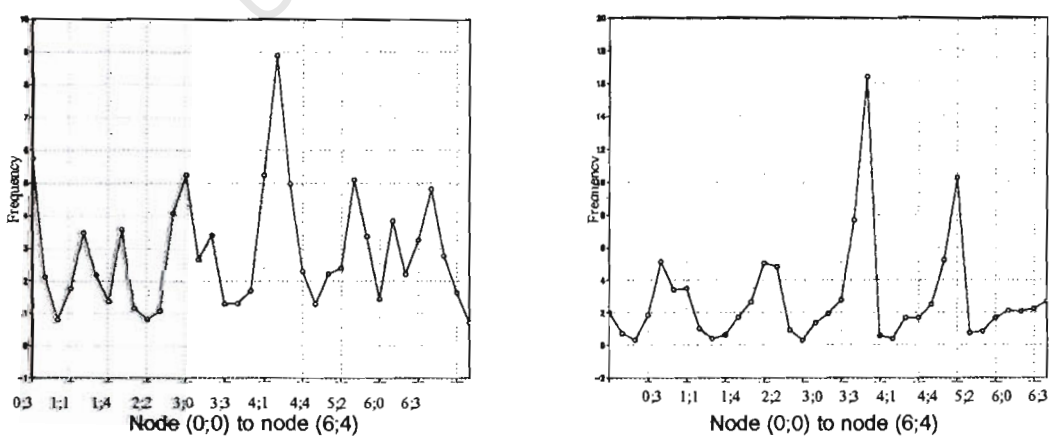

ECHAM4 control (a) **ECHAM4 future (b)**

FIGURE 16 (a) and (b): Comparison between ECHAM4 control and ECHAM4 projected future frequency line graphs

The projected future data shows a greater frequency and intensity of data falling into node (6;2) rather than node (5;2), which shows the majority of data mapping in the control frequency map. Therefore, the GCM-simulated future data projects a change in atmospheric conditions to a scenario that is represented by node (6;2), with ancillary nodes being node (6;3) and node (5;2). The intensity of data that is mapped to node (6;2) in the image depicting future conditions shows that there may be a decrease in day-to-day variability and could be interpreted as the future data 'falling off' the SOM space. This means that the projected future data would probably map better to a node lying to the right of node (6;2). Unfortunately, the data is constrained to mapping to a node within the NCEP-trained SOM.

The line graphs depicting frequency at each node across the SOM space (Figure 16) confirm that the control ECHAM4 data is more evenly dispersed over the SOM space than the projected future data because the profile of the control data is shown to be flatter when compared to the profile of the projected future data. The projected future data shows four spikes in the frequency signal. Furthermore, all the spikes correlate to nodes directly surrounding node (6;2).

In order to take into account the error that is evident in the model when compared to the NCEP reanalysis data, anomaly frequency maps were produced. Subtraction of the NCEP frequency map from the ECHAM4-simulated control and future frequency maps created the maps shown in Figure 17. This process shows the departure of the data generated in the ECHAM4 model from the NCEP model data.

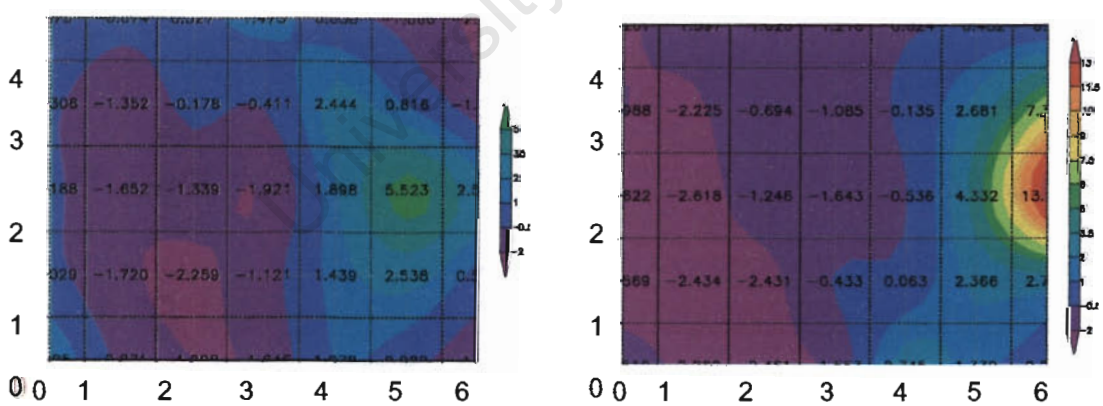

ECHAM4 control (a) **ECHAM4 future (b)**

FIGURE 17 (a) and (b): Comparison between ECHAM4 control and ECHAM4 projected future anomaly frequency maps

The two anomaly maps exhibit a very similar pattern to the non-anomaly maps. This confirms the statement that the NCEP data is quite uniformly distributed over the SOM surface. This deduction is possible because, if NCEP were not uniformly distributed over the SOM space, the pattern in the anomaly ECHAM4 frequency maps would have differed significantly from the original ECHAM4 frequency maps.

By examining the anomaly maps (Figure 17) it is seen that even when NCEP is subtracted there is still a change in the high frequency node from node (3;2) to node (6;2). This confirms that the deductions made when assessing the earlier frequency maps are still true.

Obviously, there is a degree of error when mapping each time step to only 35 atmospheric conditions. These errors are represented in the same format as frequency maps. Error plots are shown on the same colour range in Figures 18 and 19.

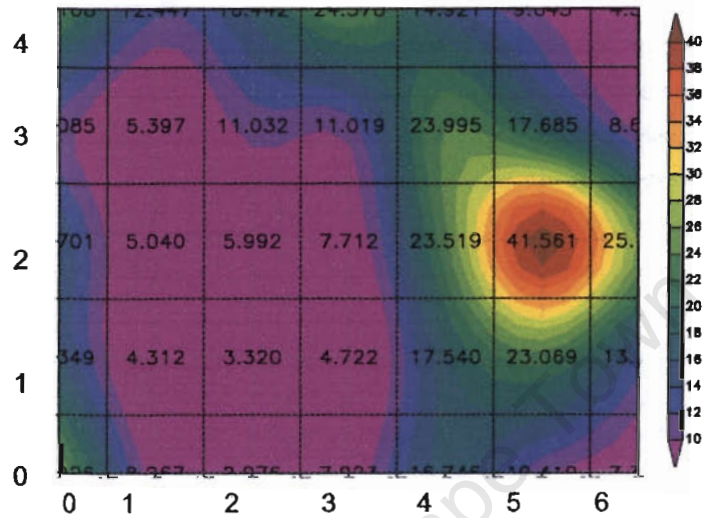

FIGURE 18: The error plot of the SOM of ECHAM4 control data

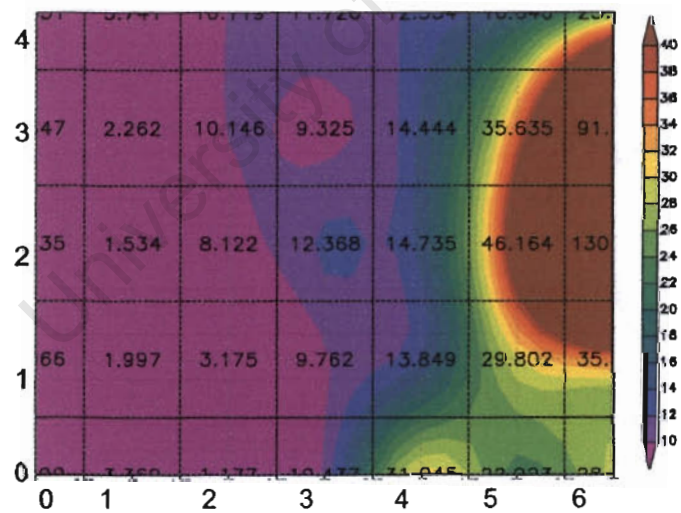

FIGURE 19: The error plot of the SOM of ECHAM4 projected future data

It is noticeable that the error plots are very similar to the frequency plots in pattern. They are similar because the high error nodes are the same as the high frequency nodes in the frequency maps. This is intuitive as the node where most of the data falls would have the greater degree of error because of the greater number of time steps falling into that node. This greater degree of error, in turn, leads to a greater average error for that SOM node. The within group variance is also increasing because synoptic states are moving further away from the pattern represented in the baseline NCEP SOM.

ECHAM4 shows the greatest error in the high frequency nodes of all the GCM data analysed with a SOM. This confirms that the ECHAM4 data does not map at all well to the NCEP-trained SOM. The reason that these high frequency nodes have a high error is because most ECHAM4 data is mapping to one semi-suitable node. This exhibits an inherent problem with forcing GCM data on to an NCEP-trained SOM because the current climate data represented in NCEP does not span enough of the climate data space. This may limit analysis of the future climate scenario.

2.4.2 CSIRO Frequency Analysis

Australia's Commonwealth Scientific and Industrial Research Organisation (CSIRO) developed the CSIRO GCM. CSIRO is Australia's largest program for the investigation of greenhouse gas induced climate change. The CSIRO model is based on the basic equations of physics with sub-systems for modelling boundary layer mixing, moisture advection, radiation and the formation of clouds (Watterson et al., 1997).

The CSIRO model is a Coupled Ocean-Atmosphere-Sea-Ice Model (CSIRO Coupled)[3]. This model includes the components of the atmosphere, ocean, sea-ice and biosphere elements. The grid cell has measurements of 625km by 350km with nine vertical levels in the atmosphere and 21 in the ocean. Due to the fact that it is a coupled ocean-atmosphere model representation it has a heat transfer scheme incorporated into the ocean model.

The CSIRO A2 scenario was the second set of model data to be analysed. The CSIRO data was mapped onto the NCEP-trained SOM in the same way as ECHAM4. This model has an advantage in that it displays a 365-day year whereas the other two GCMs have 360-day years. However, a disadvantage of CSIRO for use in the Western Cape is that it exhibits a bimodal distribution of rainfall throughout the year when there should be a unimodel distribution showing a predominance in winter rainfall. This downfall of the model is illustrated in a graph of average precipitation over the year (Figure 20). The fact that CSIRO does not model precipitation very well in the Western Cape does not mean that it does not have the ability to model other variables accurately.

[3] Hennessy http://ipcc-ddc.cru.uea.ac.uk/dkrz/dkrz_index.html

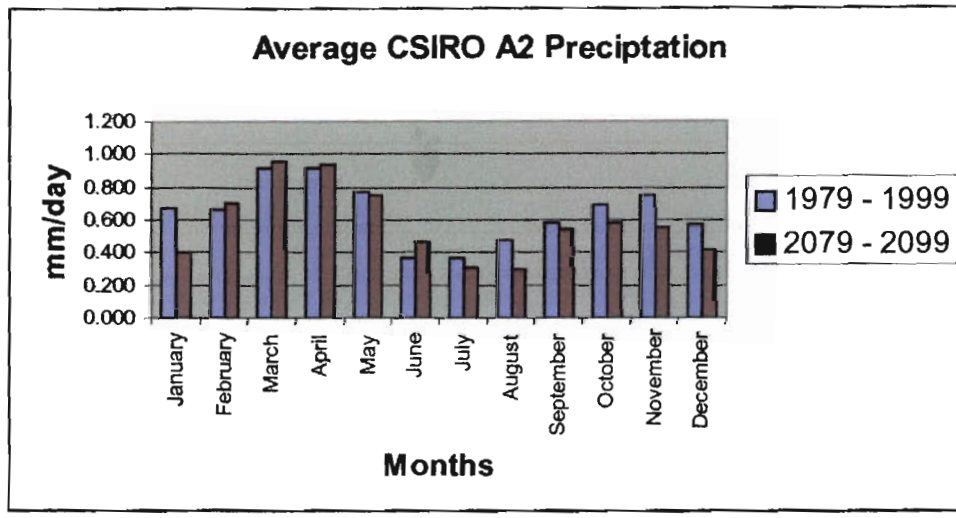

FIGURE 20: Bimodal distribution of the CSIRO A2 scenario precipitation

A frequency map was created for CSIRO in order to analyse the frequency of data mapping to each SOM node. The frequency map for the control data (1979 to 1999) is depicted in Figure 21.

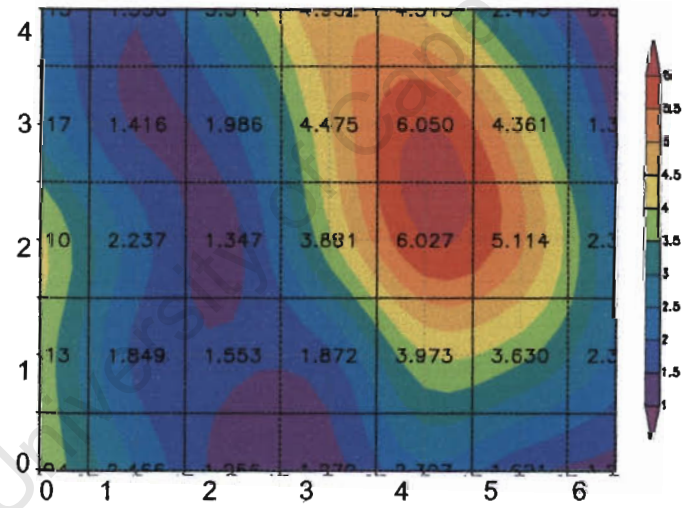

FIGURE 21: The frequency map of the CSIRO control SOM (1979 – 1999)

The SOM of CSIRO control data shows that the highest frequency of data falls into nodes (4;2) and (4;3) and the majority of other data is mapped to nodes surrounding the two high intensity nodes. Nodes (0;0), (0;1) and (0;2) also display a relatively high frequency of data mapped to them when compared to the rest of the SOM space but not as high as node (4;2) and (4;3).

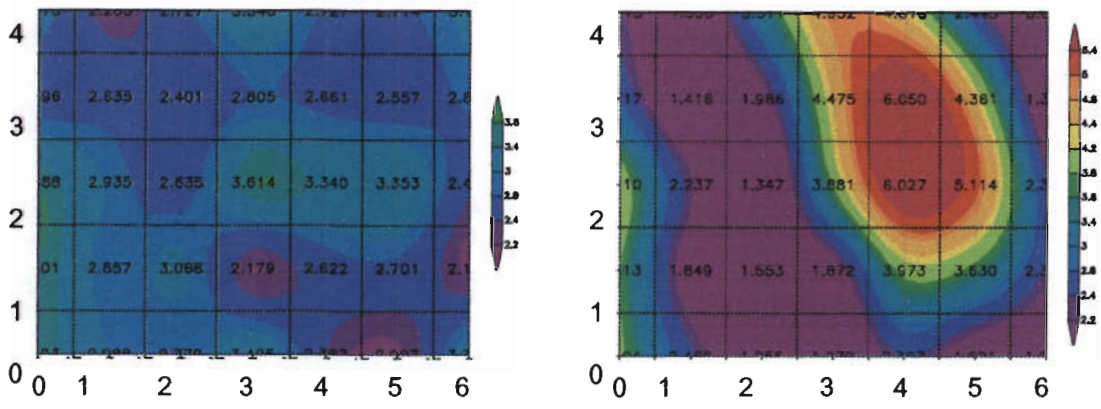

NCEP control (a) **CSIRO control (b)**

FIGURE 22 (a) and (b): Comparison between NCEP control and CSIRO control frequency maps

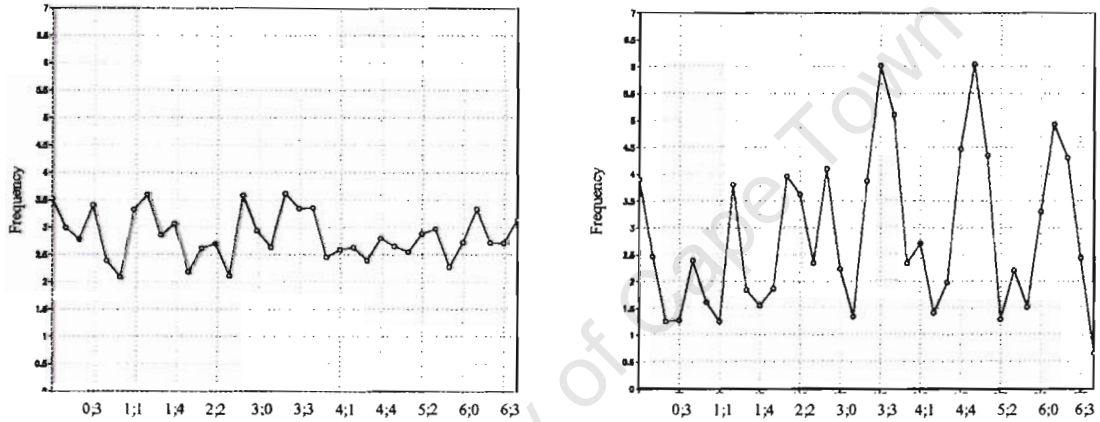

NCEP (a) **CSIRO (b)**

FIGURE 23 (a) and (b): Comparison between NCEP control and CSIRO control frequency line graphs

The predominant difference between the analysis using NCEP control data and the CSIRO control data is the uneven spread of data over the CSIRO SOM space (Figures 22 and 23). As discussed previously, the CSIRO data principally maps to the SOM nodes surrounding nodes (4;2) and (4;3), whereas NCEP has a slightly higher frequency in node (3;2). Again, it can be said that the CSIRO GCM, like ECHAM4, has a summer bias because the high frequency node, that has the majority of daily data mapped to it, displays a synoptic condition that is principally found in the summer season.

The line graph depicting the frequency found at each node (Figure 23) serves to confirm that NCEP, rather than CSIRO, maps more uniformly over the SOM space. This is seen by the flatter graph depicted by Figure 23(a) as opposed to Figure 23(b). The two predominant spikes seen in the CSIRO line graph correspond to nodes (4;2) and (4;3).

While taking into account the error of the CSIRO model in depicting the present climate, it is possible to analyse the change depicted from the CSIRO control data to the projected A2

emission scenario future data. The change from the frequency map of CSIRO control data (Figure 24(a)) to the frequency map of CSIRO projected future data (Figure 24(b)) is only slight. The control to future map indicates a change of high frequency nodes from nodes (4;2) and (4;3) in the control map into solely node (4;3) in the frequency map of projected future data. The future frequency map shows a change in frequency distribution with node (4;3) actually decreasing in frequency in the future climate. However, this still indicates that the predominant future daily synoptic state should exhibit an atmospheric pattern similar to that of node (4;3). The other high frequency areas in the SOM space stay very similar from the control data to the projected future data, except for a slight extension of high frequency into nodes (3;4) and (4;4) and a slightly higher frequency found in nodes (0;0), (0;1) and (0;2).

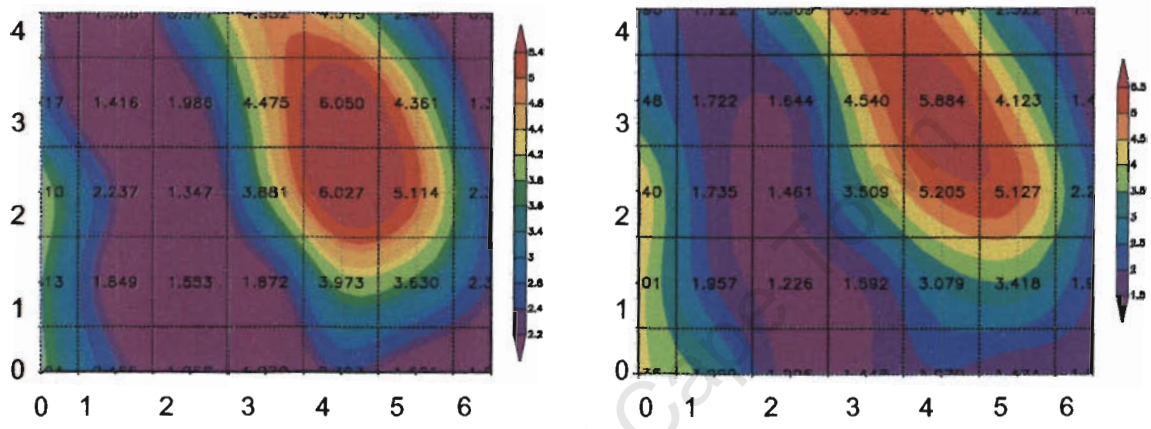

CSIRO control (1979 – 1999) (a) **CSIRO future (2079 – 2099) (b)**

FIGURE 24 (a) and (b): Comparison between CSIRO control and CSIRO projected future frequency maps

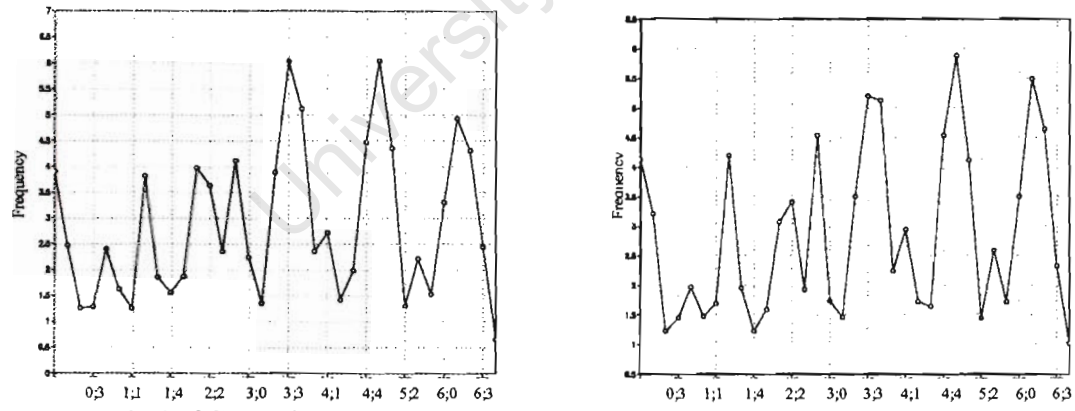

CSIRO control (a) **CSIRO future (b)**

FIGURE 25 (a) and (b): Comparison between CSIRO control and CSIRO projected future frequency line graphs

The line graphs of frequency at each node (Figure 25) show that there is one chief spike in the projected future data. This indicates that the high intensity data falls into one node. The two second highest spikes represent the two nodes on either side of the highest frequency node.

In order to fully account for the error incorporated into the CSIRO model, anomaly maps were created. These maps show the frequency maps of CSIRO-simulated control and future data after the subtraction of the NCEP frequency map. These show the true deviation from the actual observed data in both the control and GCM-projected future data.

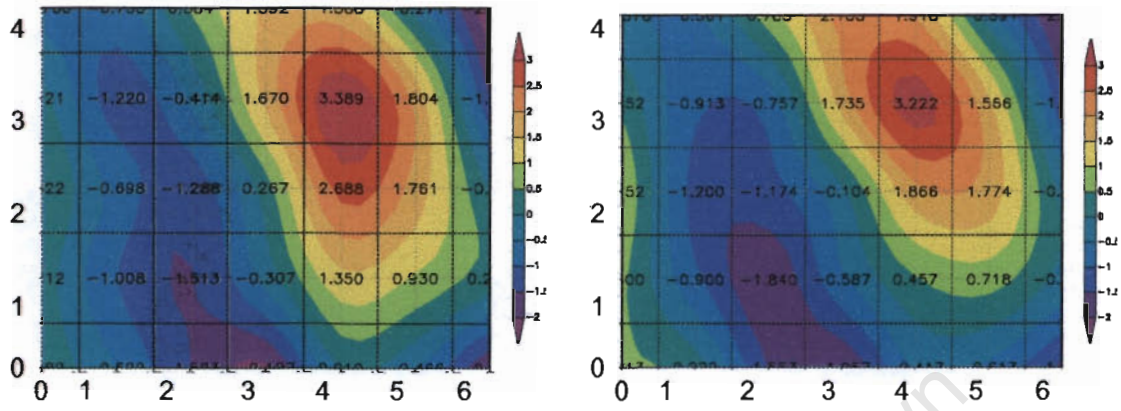

CSIRO control (a) **CSIRO future (b)**

FIGURE 26 (a) and (b): Comparison between CSIRO control and CSIRO projected future anomaly frequency maps

Again, the anomaly maps in Figure 26 have a very similar pattern to the non-anomaly maps because NCEP has a fairly even distribution of data over the SOM space. One significant difference between the anomaly maps and the non-anomaly maps is that node (4;3) represents a greater proportion of all the data on the SOM space, in both the control and future anomaly maps. This confirms the statement that node (4;3) is a dominant node and, even though it's data-mapping frequency decreases in the future map, it is still projected that most of the future daily atmospheric conditions should have a strong similarity to the conditions represented in node (4;3).

Maps showing the error of mapping CSIRO data to 35 nodes gives insight into how well the GCM data maps to the NCEP-trained SOM nodes. Error plots are shown on the same colour range in Figures 27 and 28.

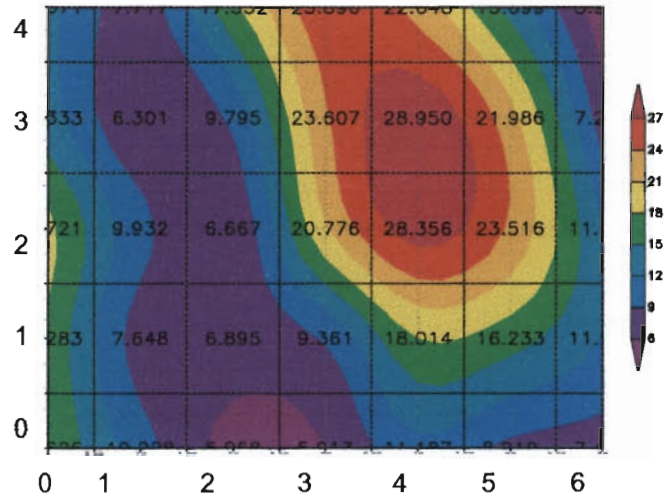

FIGURE 27: The error plot of the SOM of CSIRO control data

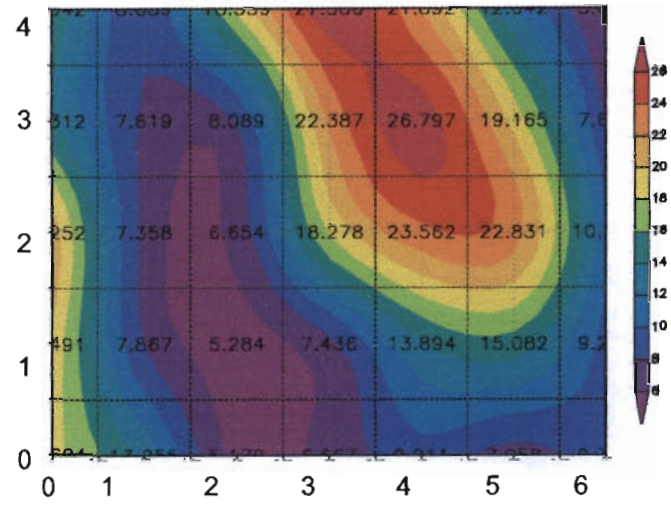

FIGURE 28: The error plot of the SOM of CSIRO projected future data

The CSIRO error plots (Figures 27 and 28) are similar to the ECHAM4 error plots and show a strong resemblance to the original frequency maps because more error occurs where more data is found. The only difference in the CSIRO error maps is that the points of high error are less defined and more dispersed over the nodes than the high frequency areas in the CSIRO frequency maps.

2.4.3 HadAM Frequency Analysis

HadAM was developed by the Hadley Centre for Climate Prediction and Research and was run as an atmosphere general circulation model[4]. The resolution of the model is 2.5° of latitude by 3.75° of longitude with nineteen atmospheric levels. The GCM is provided with baseline data for sea surface temperatures and sea-ice coverage but is not a fully coupled model

There are some components that are explicitly represented in the model, such as the radiative effects of lesser-known greenhouse gases and those of carbon dioxide, ozone and water vapour. The atmospheric component allows for processes such as emission, oxidation, transportation and deposition of sulphur and sulphur compounds. This makes the model unusual in that it models the effect of sulphur aerosols, which not all models include (Pope et al., 2000).

Using the same process as ECHAM4 and CSIRO, the HadAM data was mapped on to the NCEP-trained SOM and frequency maps of the control and A2 emission scenario projected future data were produced. The HadAM control frequency map is shown in Figure 29.

[4] http://ipcc-ddc.cru.uea.ac.uk/dkrz/dkrz_index.html

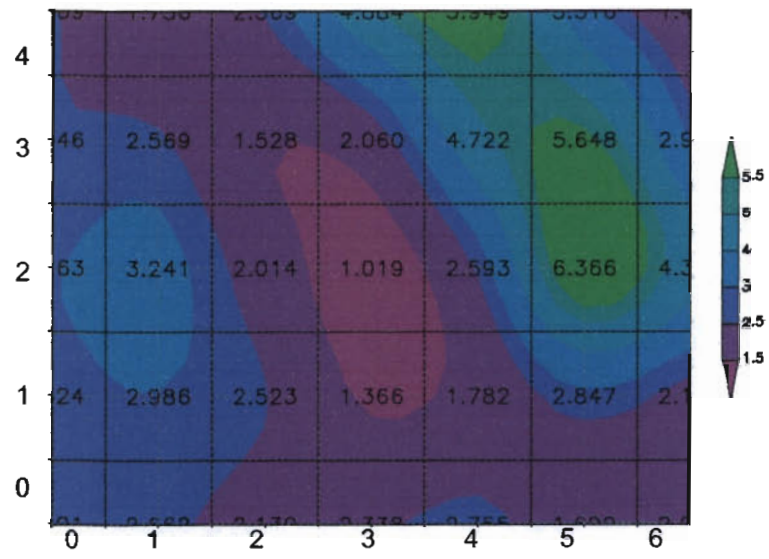

FIGURE 29: The frequency map of the HadAM control SOM (1979 – 1999)

The frequency map of HadAM control data (Figure 29) is very similar to the ECHAM4 control frequency map as it has a high frequency of data mapping to node (5;2). However, in the frequency map created using HadAM data there is an overflow of this high frequency into nodes (5;3) and (4;4). Again, the GCM data shows a predominance of data mapping to the right-hand side of the SOM space, hence showing a greater majority of days mapping to synoptic states associated with predominant summer conditions. Unlike the other models, HadAM displays the lowest frequency of data mapping to node (3;2), which is where the frequency map created with NCEP displays the highest frequency. This reinforces that the HadAM control data does not map perfectly to the NCEP-trained SOM.

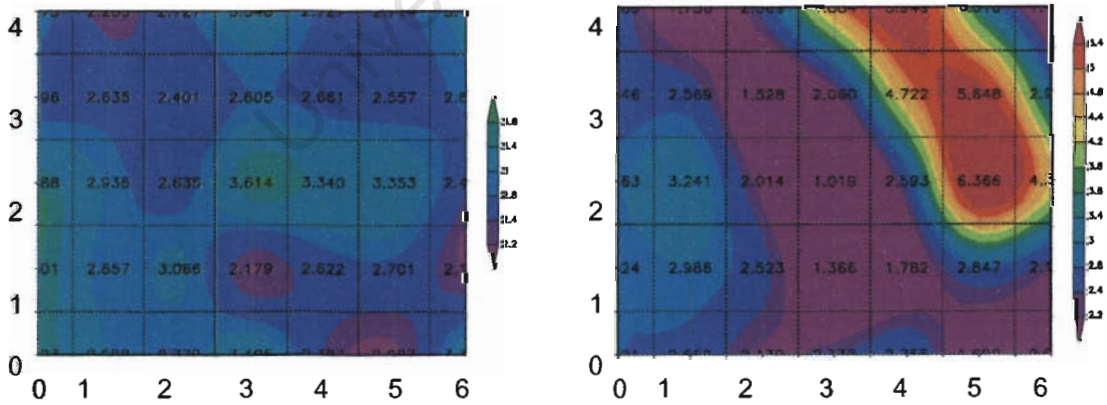

NCEP control (a) **HadAM control (b)**

FIGURE 30 (a) and (b): Comparison between NCEP control and HadAM control frequency maps

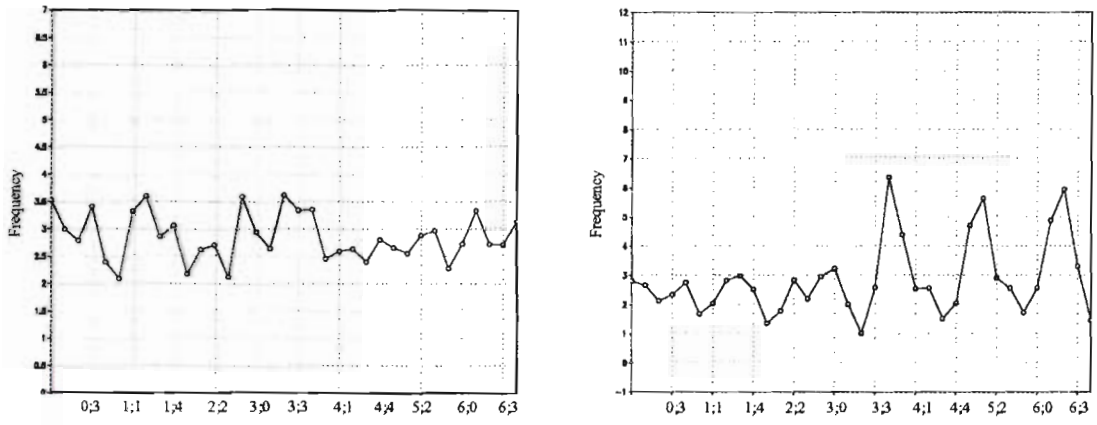

FIGURE 31 (a) and (b): Comparison between NCEP control and HadAM control frequency line graphs

By examining the NCEP control frequency map (Figure 30(a)) and the HadAM control frequency map (Figure 30(b)) on the same colour range, the difference between the two frequency maps are obvious. Not only does the HadAM data distribute unevenly across the NCEP-trained SOM space, but the areas of high and low frequency are much more intense than in the frequency map created with NCEP data.

The line graphs depicting frequency at each node (Figure 31) verify that HadAM-simulated control data (Figure 31(b)) has a more uneven distribution across the SOM space than NCEP and shows three areas of high intensity. These three spikes correlate to nodes (5;2), (5;3) and (4;4) which have the greatest intensity of data mapping to them.

To analyse the change in mapping frequency between the HadAM control and projected future data, it is necessary to take into account the error that the HadAM model shows in representing the control climate. Bearing this in mind, the projected changes in predominant atmospheric state from the control to projected future data are studied in Figures 32 and 33.

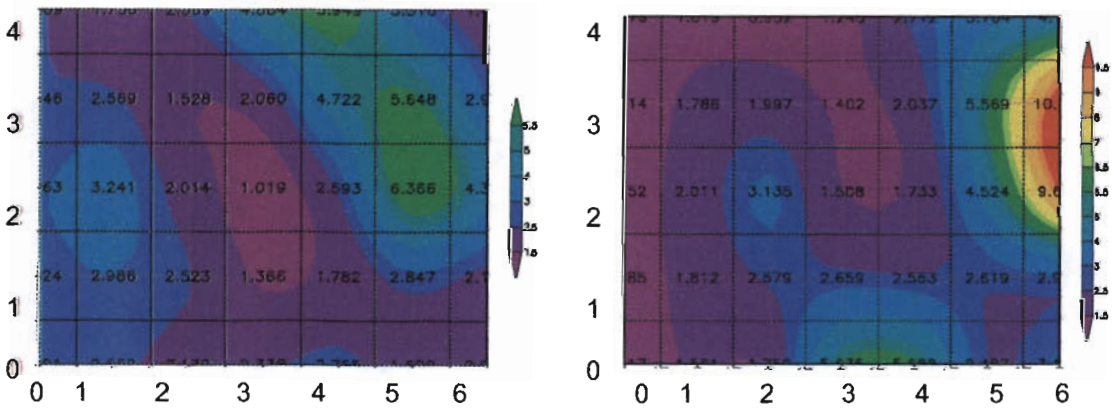

FIGURE 32 (a) and (b): Comparison between HadAM control and HadAM projected future frequency maps

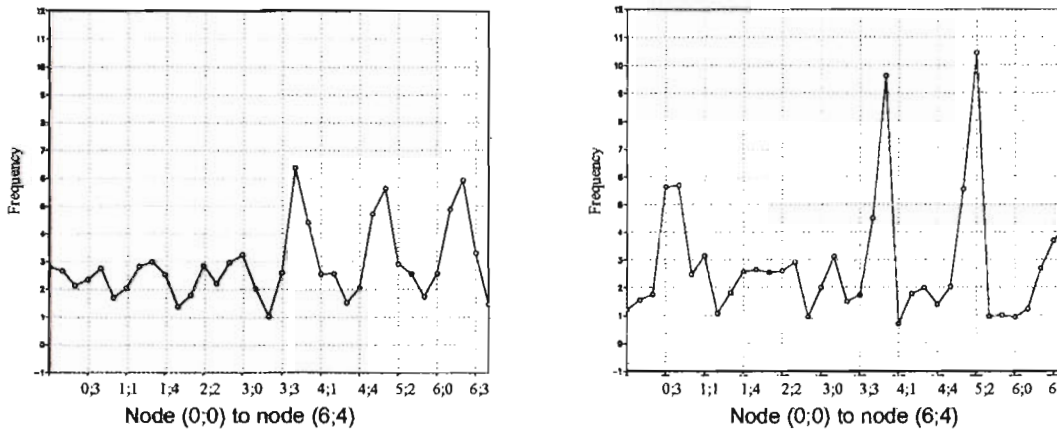

HadAM control (a) **HadAM future (b)**

FIGURE 33 (a) and (b): Comparison between HadAM control and HadAM projected future frequency line graphs

The most obvious difference between the two frequency maps in Figure 32 is the movement of the high frequency nodes from node (5;2) and (5;3) in the control data to nodes (6;2) and (6;3) in the projected future data. Added to this observation, the high frequency nodes in the projected future data frequency map are more intense than the high frequency nodes in the control data frequency map. The projected future atmospheric condition also seems to be representing a higher frequency of daily data in nodes (3;0) and (4;0). Similarly to the ECHAM4 data, the projected future data looks like it is almost 'falling off' the edge of the NCEP-trained SOM space. This indicates that the HadAM-simulated future data does not fit well to the NCEP-trained SOM nodes. The higher spikes in Figure 33b, when compared to Figure 33a, show a prominent mapping of data to only a few nodes in the projected future data, as well as a more uneven distribution of data over the SOM space than the control data.

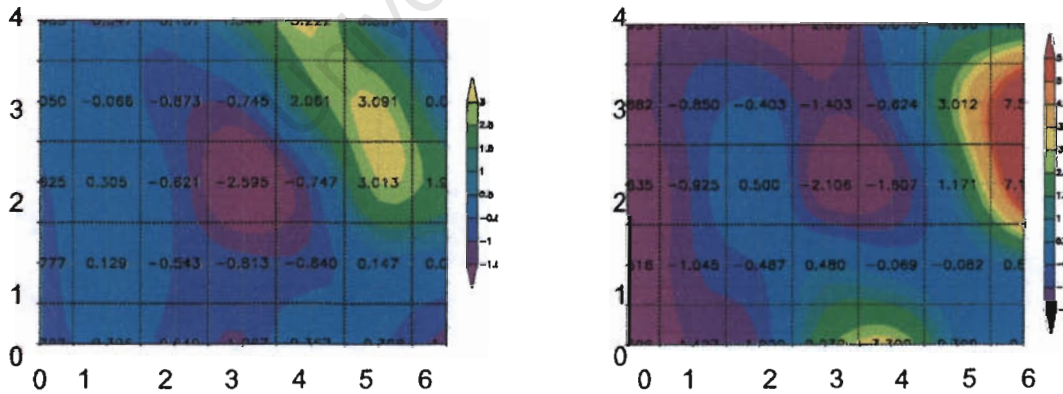

HadAM control (a) **HadAM future (b)**

FIGURE 34 (a) and (b): Comparison between HadAM control and HadAM projected future anomaly frequency maps

The anomaly maps (Figure 34), created by subtracting the NCEP frequency map from the HadAM frequency maps, show a similar pattern to the original frequency maps. There are small differences in the anomaly maps such as the slightly higher frequency in nodes (5;2), (5;3) and (4;4) in the control HadAM anomaly map compared to the rest of the SOM space.

There is also a much larger area of low frequency in the original HadAM control frequency map than the anomaly control frequency map.

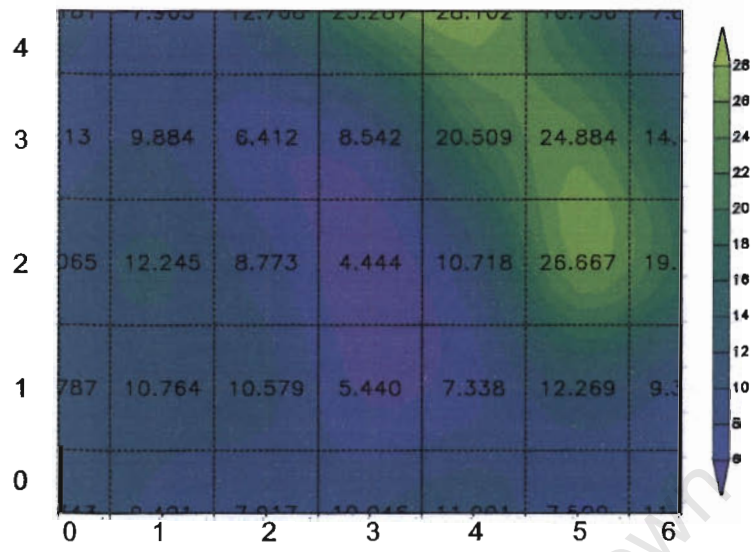

FIGURE 35: The error plot of the SOM of HadAM control data

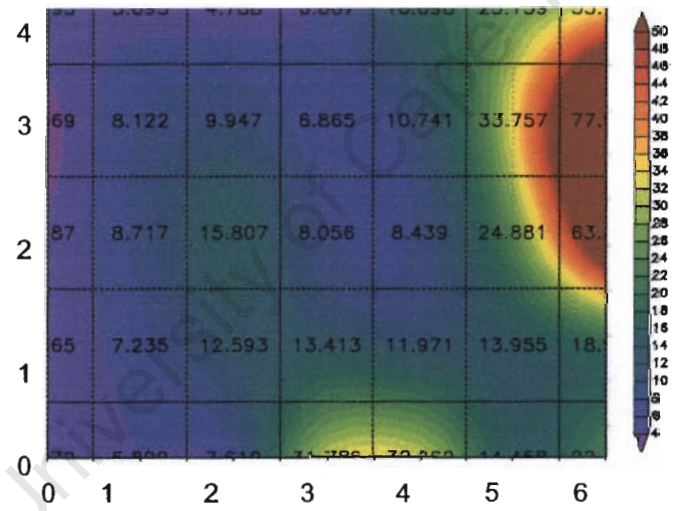

FIGURE 36: The error plot of the SOM of HadAM projected future data

The error maps in Figures 35 and 36 display a very similar pattern to the original frequency maps because a greater density of data usually equates to a larger error. However, HadAM displays the second greatest average error of all three GCMs when mapping to the NCEP-trained SOM, with ECHAM4 displaying the largest error. The largest error with using HadAM-simulated future data is found in node (6;3) in the SOM map. This confirms the earlier statement that the projected HadAM future data is almost 'falling off' the SOM space because it does not map well to any of the NCEP-trained nodes.

From inspection and analysis of all three GCMs, it is clear that there are problems with mapping GCM data to an NCEP-trained SOM. If these problems are accounted for in the analysis of runoff, the error of the GCMs in modelling both the control and future climate should be minimised. However, all the GCMs agree that there is a shift either up or towards

the right-hand side of the SOM space in the projected future data. When inspecting the original NCEP SOMs of specific humidity and geopotential height, in figures 7 and 8, one can see that there is a definite change in the synoptic pattern represented by the high frequency control nodes and the high frequency projected future nodes. The nodes that represent the majority of the projected future data show a greater intrusion of humid air than the control nodes. Also, greater geopotential heights are shown over the South African interior in the projected future nodes, which would result in a considerable climate difference. Overall, the difference in synoptic pattern as shown in the results of this section is a significant indication of the effects of climate change. By examination of the runoff associated with these projected future high frequency nodes, the future runoff in the catchment can be assessed.

CHAPTER THREE: RUNOFF ANALYSIS

This chapter makes use of the SOM analysis, performed in the previous section, to begin to understand the change in runoff associated with climate change. By first analysing the runoff associated with the SOM-identified synoptic states in the GCM control simulation, and then the GCM future simulation, it was possible to assess the predominant change in runoff from the control climate to the projected future climate as a function of changing frequencies of synoptic systems. For the purposes of this study, runoff was defined as the amount of water flowing in the river at a stream gauge.

3.1 Runoff Stations

Runoff data from five stations throughout the catchment was obtained from the Department of Water Affairs and Forestry (DWAF). As shown in Table 1, two of the stations are in the upper reaches of the catchment (H1H006 and H1H018), one in the middle reaches (H4H017) and two in the lower reaches (H6H009 and H7H006). This distribution of stations throughout the catchment leads to a holistic view of runoff within the whole basin.

TABLE 1: Location of Runoff Stations

Station Number	Place	Latitude	Longitude	Catchment Area	Record Period	Years
H1H006	Witbrug	33°25'18"	19°16'06"	753km^2	1950 - 1998	48
H1H018	Haweqias	33°43'24"	19°10'13"	113km^2	1969 - 1999	30
H4H017	Le Chasseur	33°49'05"	19°41'41"	4336km^2	1980 - 1998	18
H6H009	Reenen	34°04'32"	20°08'44"	2007km^2	1964 – 1998	34
H7H006	Swellendam	34°03'57"	20°24'15"	9842km^2	1967 - 1997	30

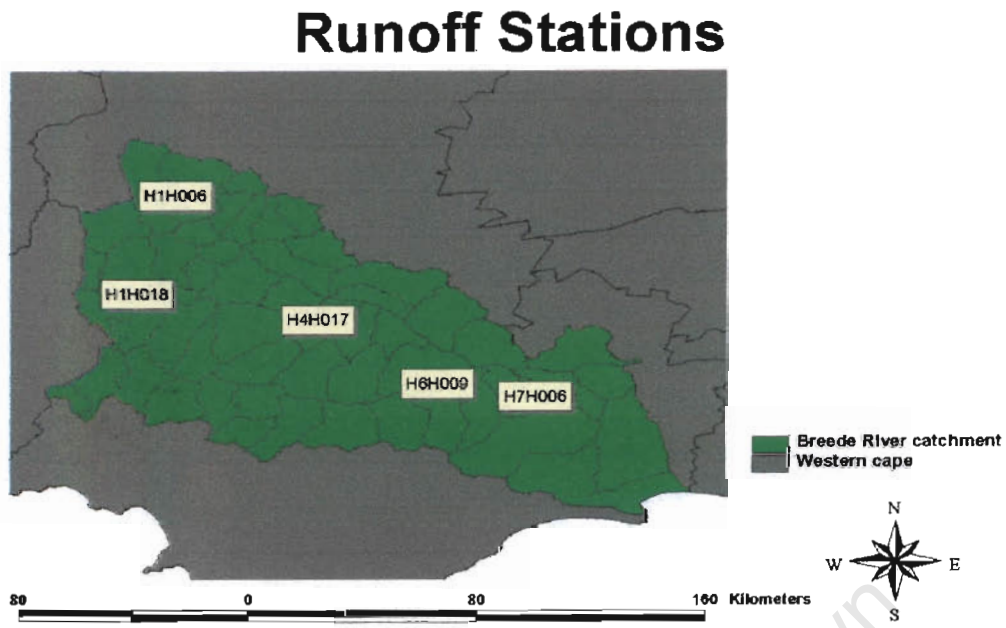

FIGURE 37: Map showing location of runoff stations (1:1319620)

Runoff stations H1H006 and H1H018 are both near the source of the Breede River flow (Figure 37). Station H1H006 has the longest record of all the stations used in this project. DWAF officials regard the data as trustworthy, although some high approach velocities and upstream pool siltation have been recorded (DWAFa, 2002). Station H1H018 has a thirty-year record and the data is reliable although there were intermittent problems with rocks inundating an upstream pool near the gauge (DWAFa, 2002).

The runoff station H4H17 is situated in the middle reaches of the catchment and just below the Brandvlei and Stettynskloof dams. DWAF officials rate the observed flow at this station as good because the data capturing procedure was thorough. This area also contains numerous farms that are intensely irrigated. The farmers in this area meet their water needs both through in-situ farm dams and run-of-river extraction (DWAFa, 2002).

The runoff stations H6H009 and H7H006 are located in the lower reaches of the catchment. H6H009 has reliable records and includes both the Theewaterskloof and Baviaanskloof catchments. Both stations are situated in areas that contain several farms and their irrigation needs are met either by farm dams, which are filled in winter, or by run-of-river abstraction. Station H7H006 has small areas of afforestation and alien vegetation so some water is utilised for these land uses. DWAF officials classify the records at the station as good with the exception that peak flows were not recorded very accurately (DWAFa, 2002).

3.2. A Methodology towards understanding runoff-atmosphere relationships

A methodology was developed in order to associate runoff data with atmospheric conditions by using the SOM-based classification of the atmospheric circulation. The fundamental principle incorporated into a SOM is that each of the time steps over the twenty-one year period is associated with a node in the SOM space. By identifying which dates are associated with each SOM node, the runoff for those dates can be associated with a specific atmospheric pattern. When the possibility of a lead-lag relationship between rainfall and runoff is accounted for, this provides the capability of identifying the typical runoff for a given atmospheric state.

By grouping together all the dates that fall into each SOM node, a box and whisker plot, showing the non-outlier ranges of the data at each station, could be drawn. Outliers are, by definition, data points that do not appear to follow the characteristic distribution of the rest of the data. These may either reflect genuine properties of the data, or be due to measurement errors or other anomalies that should not be modelled. Generally, it is assumed that outliers depict a random signal that one would like to be able to control. In this case, the non-outlier data range was defined as above and below the 75^{th} and 25^{th} percentile. This range was decided upon because it appeared to remove most of the outliers in the majority of cases.

A median or middle value was also depicted on the runoff graphs. Showing the median, rather than the mean, was chosen because the mean value is more influenced by extreme values than the median value. Observation of the median value confirmed that, as expected, SOM nodes with a synoptic condition conducive to rainfall would show a higher median runoff than those SOM nodes with atmospheric states not conducive to rainfall. For instance the 6^{th} of February 1979 mapped to node (6;3) in the NCEP-trained SOM. This node depicted a predominantly summer condition with low specific humidity and average geopotenital heights over the Western Cape. The runoff associated with this node at station H1H006 was 0.523 million m^3/annum. On the other hand, the 15^{th} of July 1979 mapped to node (0;0). This node was associated with predominantly winter conditions with high specific humidity and low geopotential heights over the Western Cape. This date had a much higher associated runoff of 3.26 million m^3/annum at station H1H006, which was to be expected in the winter rainfall region of the Western Cape.

Before the box and whisker plots could be drawn, a determination had to be made as to whether there was a significant time lag between the particular atmospheric condition and the resultant runoff. This information was important because it pertained to which node in the SOM space each date in the runoff file corresponded to and therefore it was required when creating box and whisker plots of each node or synoptic state. By assessing the time lag between precipitation events and runoff, i.e. the response time of the catchment, the temporal relationship between rainfall and runoff was investigated. This assessment of the temporal

relationship is, by virtue of daily resolution data, somewhat crude. Nonetheless, it serves to provide a basic assessment of the first order lags.

To assess the lag, precipitation data was extracted from a 10km gridded data set generated by Hewitson and Crane (2004). Precipitation was only extracted for the upper reaches of the catchment (basin H1). Due to interference from extraction and dams in the lower reaches, the lag was only assessed for the catchment region upstream. This omission should not have any implications for the lower catchment regions because the direct lag between rainfall and runoff should be the same throughout the catchment. Only the direct lag between rainfall and runoff were assessed in this project because the indirect impacts on lag time are too variable. The lags were assessed through simple lagged correlation analysis.

The correlation figures from the lagged correlation analysis show the multiple R, R squared and the standard error of estimate. The multiple R value assesses the correlation of the actual value, such as precipitation, with the value that needs a correlation assessment, such as runoff. In this case, the number 'one' indicates a perfect fit. The R squared value is similar to the multiple R value but incorporates an adjustment to take into account the length of the time series. Again, the number 'one' indicates a perfect fit. The standard error of estimate is the square root of the variance, which is how much the error term differs from the average. No error indicates a perfect fit.

TABLE 2: H1H006 lagged correlation analysis

H1H006	Time lag	Multiple R	R squared	Standard Error of Estimate
	On day	0.304702	0.09284314	45.016493917
	One day lag	0.489788	0.23989570	41.209060841
	Two days lag	0.365058	0.13326893	44.007335509

TABLE 3: H1H018 lagged correlation analysis

H1H018	Time lag	Multiple R	R squared	Standard Error of Estimate
	On day	0.56678713	0.32124765	39.149705627
	One day lag	0.63684670	0.40557372	36.639346211
	Two days lag	0.40018064	0.16014454	43.553882995

In the upper catchment, (Tables 2 and 3) a one-day lag shows the best correlation between precipitation and runoff. This correlation is not very strong because the data sets of runoff and precipitation were not derived in the same way; however, the greatest correlation for both the multiple R and the R squared is seen in the one-day lag. The lowest standard error of estimate is also seen in the one-day lag.

As purely an introduction to the runoff stations used in the project, box and whisker plots were tested for their usefulness while depicting the range of runoff related to the atmospheric state of each SOM node. These show how the runoff changed, at each gauging station, across the range of atmospheric states as represented by the SOM space. A significant change in runoff between SOM nodes was expected because each node depicts an atmospheric state that may or may not be associated with rainfall. If the synoptic state depicted by the SOM node is conducive to rainfall, this should lead to an increase in runoff, whereas a lack of rainfall would lead to a decrease in runoff.

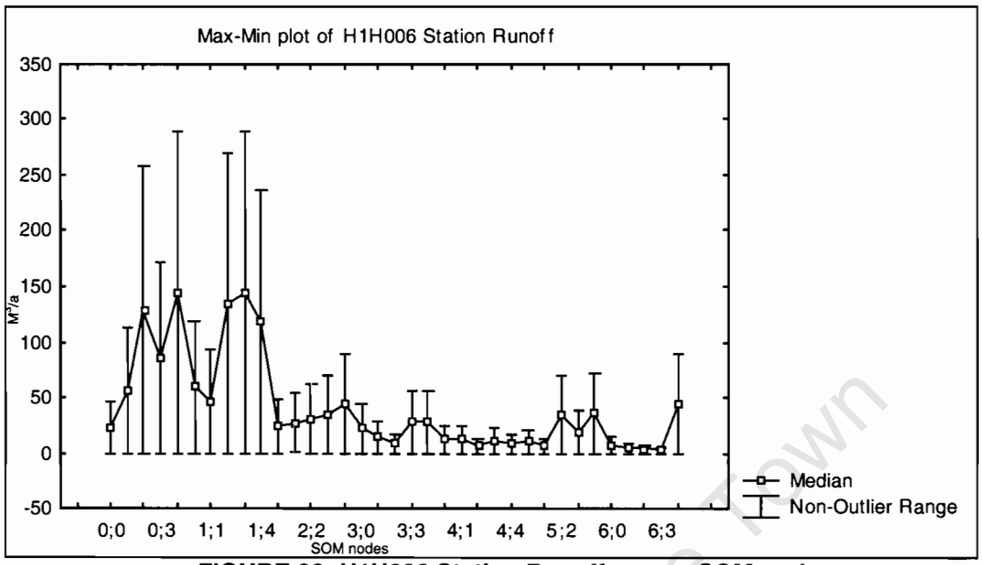

FIGURE 38: H1H006 Station Runoff across SOM nodes

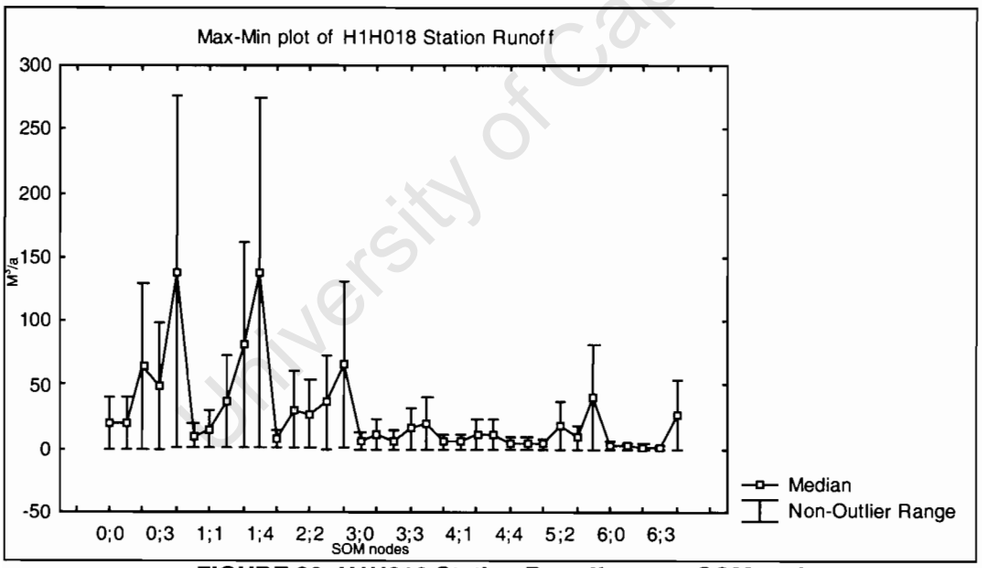

FIGURE 39: H1H018 Station Runoff across SOM nodes

Stations H1H006 and H1H018 (Figure 38 and 39) have a low overall maximum runoff across all synoptic states. One would expect this pattern from stations situated at the source of the river because the gauges are fed purely by rainfall and do not include any stream confluences. Bearing in mind the discussion in chapter two which found that the left-hand side of the SOM space represented predominantly winter synoptic states and the right-hand side of the SOM space depicted predominantly summer synoptic states, the runoff pattern of winter to summer rainfall can be clearly seen across the nodes.

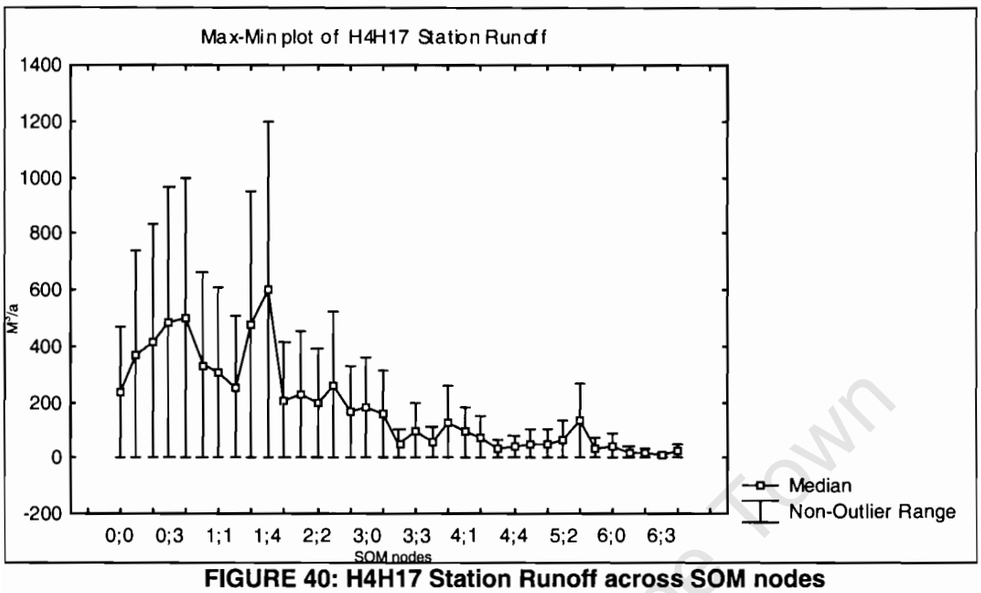

FIGURE 40: H4H17 Station Runoff across SOM nodes

Runoff station H4H17 (Figure 40) shows the highest maximum values of all the stations. This is to be expected as station H4H17 integrates upstream sub-catchments, and also reflects release from the dam situated above the station; consequently this will, to some degree, decrease the strength of the relationship to atmospheric forcing because of the human induced high runoff values. However, the dam does not appear to interfere too significantly with the station runoff data although the graph is significantly smoothed due to an external factor moderating the flow. It is concluded that there is not much interference because the runoff pattern still suitably represents nodes predominantly associated with winter conditions and nodes predominantly associated with summer conditions, over the SOM space.

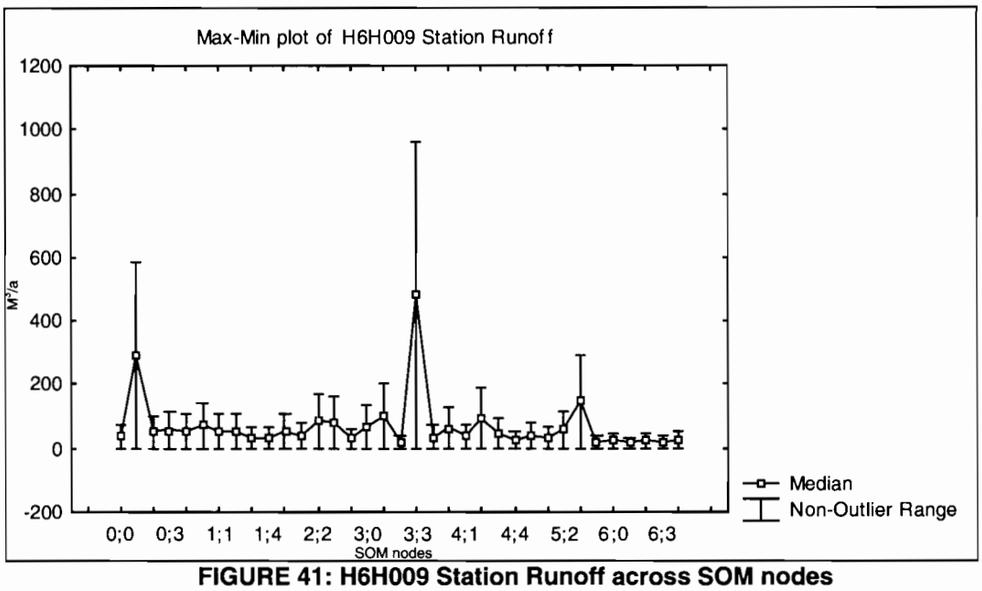

FIGURE 41: H6H009 Station Runoff across SOM nodes

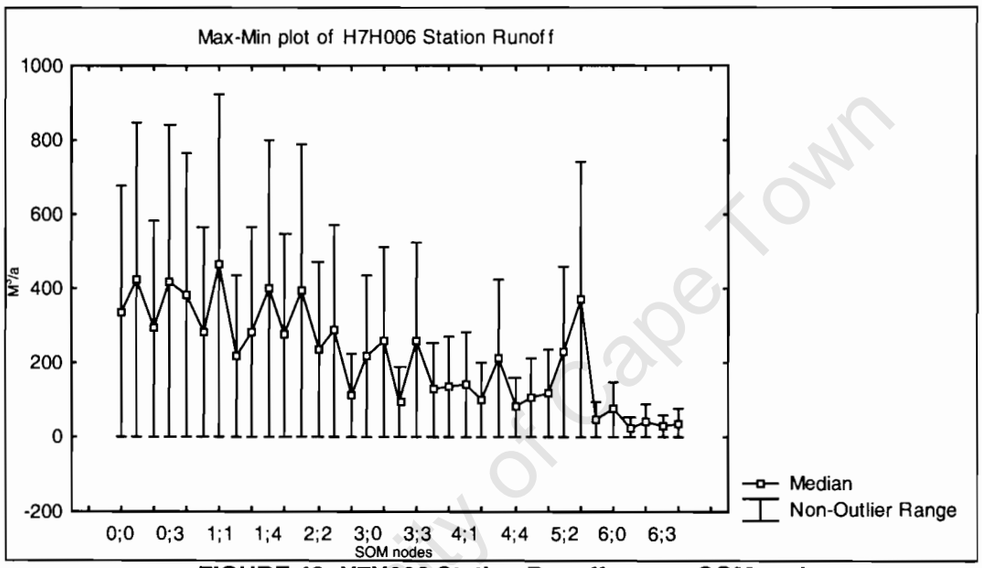

FIGURE 42: H7H006 Station Runoff across SOM nodes

Both stations H6H009 (Figure 41) and H7H006 (Figure 42) contain records with high maximum values. This is expected as the stations are in the lower reaches of the catchment and confluence of water from the tributaries would have taken place higher in the catchment. H6H009 does not seem to correctly represent the runoff values that should be associated with the winter to summer continuum across the nodes. This anomaly may have been due to the withholding and timely release of water from the Theewaterskloof dam that lies upstream from the runoff station.

In the next section, the SOM nodes that show the highest frequency of data mapping in the control and projected future data, for each GCM, are analysed with box and whisker plots,

which have proven to be a useful tool in runoff analysis. The box and whisker plots, in the next section, vary slightly from the plots already analysed in that they depict a specific SOM node rather than a runoff station. The plots are used to assess the change in runoff associated with the high frequency nodes from control to projected future. By first analysing the change in runoff associated with the high frequency nodes it is possible to get, at least, a first order impression of the change in runoff under climate change. Once the first order analysis is completed, analysis of the change in Mean Annual Runoff over the whole SOM space can be undertaken.

3.3 Analysis of the runoff associated with high frequency nodes

The runoff associated with the SOM nodes that display the highest frequency of data mapping were analysed, for each GCM. First, the frequency maps of the control of each GCM were compared to the frequency maps produced with NCEP reanalysis data in order to assess the GCMs ability to capture current circulation. Second, the runoff associated with the high frequency node(s) in the control data was compared with the runoff associated with the high frequency node(s) in the projected future scenario. By association of the runoff with the circulation states and the change in frequency of data mapping to each circulation state, one could infer, at least a first order, consequence on runoff of the projected changes in the atmosphere.

This was just the first step in the analysis of the change in runoff from the control to the projected future data. It was recognised that the high frequency nodes are not the only nodes likely to show a change in runoff under climate change. If a currently low frequency node became a somewhat higher frequency node under climate change this could have a significant effect on projected future runoff. To account for this fact, section 3.4 included an assessment of the change in Mean Annual Runoff over the whole SOM space. This did not serve to supersede the analysis of high frequency nodes but merely complemented it. The analysis of high frequency nodes, alone, was still a necessity because the change in predominant synoptic states, represented by the change in the high frequency nodes, enabled representation of whether the predominant synoptic states presently associated with each season will become more or less prominent under future conditions. This will give an indication of whether there may be an increase in extreme events under climate change. Only analysing the change in Mean Annual Runoff could not depict this possible change. The box and whisker plots also incorporated a range of runoff values and their associated median, rather than simply a Mean Annual Runoff value as expressed in section 3.4.

3.3.1 High frequency node analysis of ECHAM4 data

3.3.1a Comparison between NCEP and ECHAM4 control data

Initially, it was necessary to examine the difference between the frequency map of NCEP and the ECHAM4 frequency map in order to assess how well ECHAM4 simulates the current

climate. Only high frequency areas of both frequency plots were used for the comparison because the frequency map created with ECHAM4 data exhibited the same regions of low frequency in the SOM space as NCEP.

Frequency maps (Figure 31(a) and (b)) show which SOM nodes require the most pressing inspection. It is observed that the NCEP data displays a more uniform data mapping frequency pattern over the SOM space than the ECHAM4 control data, because the SOM was trained with the NCEP data and the ECHAM4 data was mapped on to the NCEP-trained SOM.

The NCEP nodes displaying the highest frequency of data mapped to them are nodes (0;0), (0;1), (0;2) and (3;2). It was hypothesised earlier that the left-hand side of the SOM space represented winter conditions over the South Western Cape whereas the right-hand side represented summer patterns (see chapter 2). This could be extrapolated to infer that the NCEP data represents a high frequency of present day winter conditions, which map to a few preferred states, because the high frequency nodes predominantly fall into the left-hand side of the SOM space.

Winter in the South Western Cape should exhibit a higher precipitation value than the summer months, therefore resulting in a greater runoff. By examining the box and whisker plots of the high frequency NCEP nodes, (Figures 43, 44 and 45) it is ascertained whether this hypothesis is indeed valid. The box and whisker plots take into account the time lag between rainfall and runoff, hence time plus 24 hours as represented in the titles.

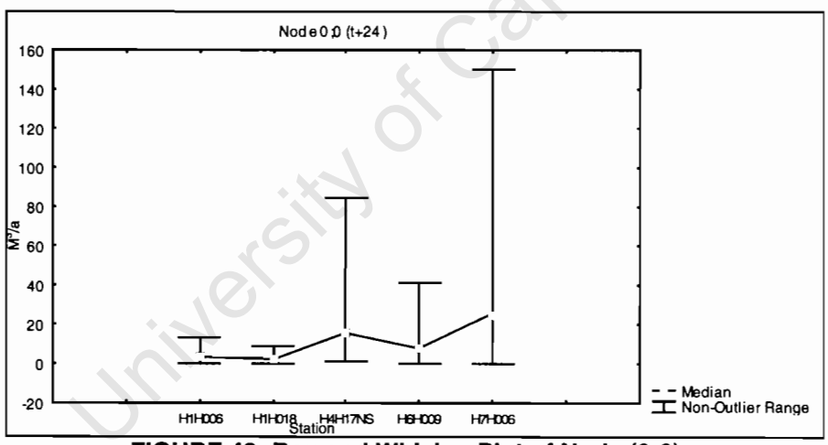

FIGURE 43: Box and Whisker Plot of Node (0;0)

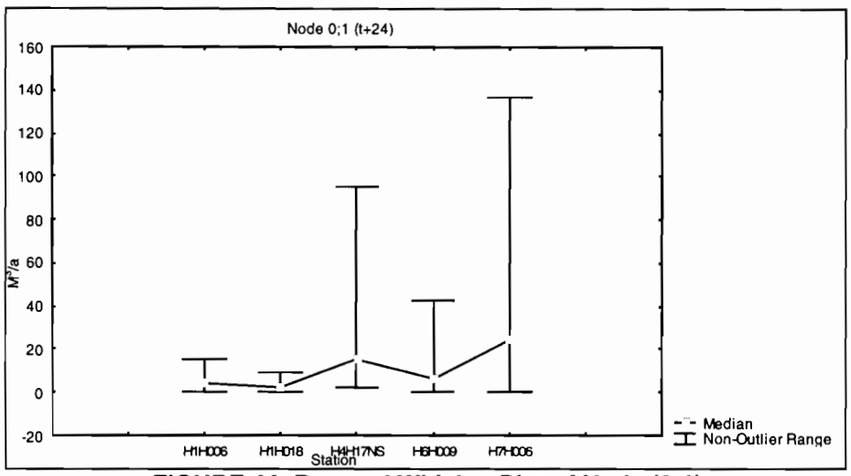

FIGURE 44: Box and Whisker Plot of Node (0;1)

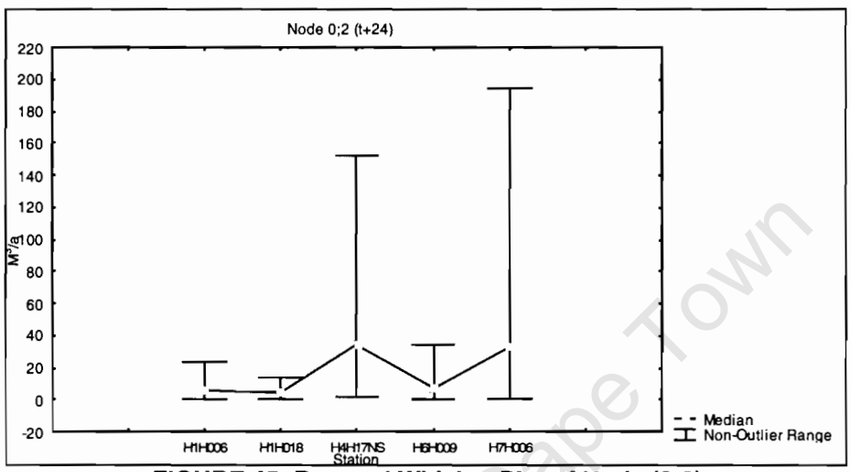

FIGURE 45: Box and Whisker Plot of Node (0;2)

All of the nodes of (0;0), (0;1) and (0;2) exhibit high runoff ranges, especially in the lower catchment station of H7H006. The upper limits of the runoff values associated with these SOM nodes are much higher than on the right-hand side of the SOM space, as seen when examining the runoff associated with these nodes. In addition, the median values are higher than on the right-hand side of the SOM space. This indicates that these SOM nodes represent synoptic conditions that can be associated with winter in the Western Cape due to the higher winter rainfall.

The fact that the ECHAM4 data exhibits a much lower data mapping frequency than NCEP, in these nodes (apart from node (0;0)), indicates that ECHAM4 models a lower amount of winter synoptic patterns than NCEP. The lack of high frequency SOM nodes in the winter months, in the ECHAM4 model, are compensated for by the very high frequency represented in node (5;2) (Figure 12). The frequency of this node is significantly higher than any of the high frequency nodes found in the NCEP frequency map.

In addition to the high frequency NCEP nodes already discussed, node (3;2) in NCEP also exhibits a high frequency of data mapped to it. This node is found along the same left to right continuum on the SOM space as the control ECHAM4 high frequency node (5;2) (Figure 13). Figures 46 to 48 examine the difference in runoff along this left to right continuum, in the SOM space.

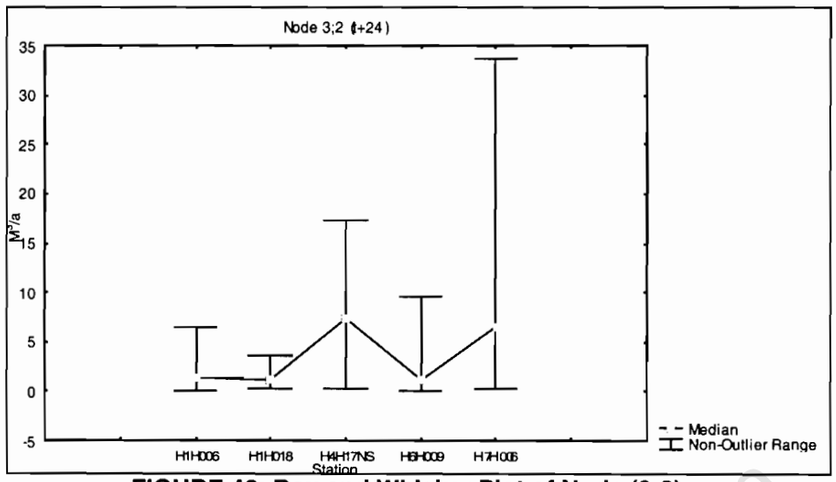

FIGURE 46: Box and Whisker Plot of Node (3;2)

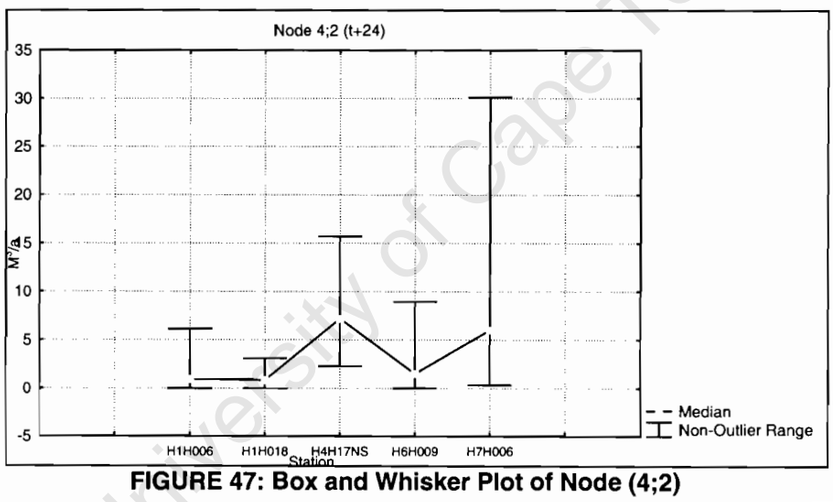

FIGURE 47: Box and Whisker Plot of Node (4;2)

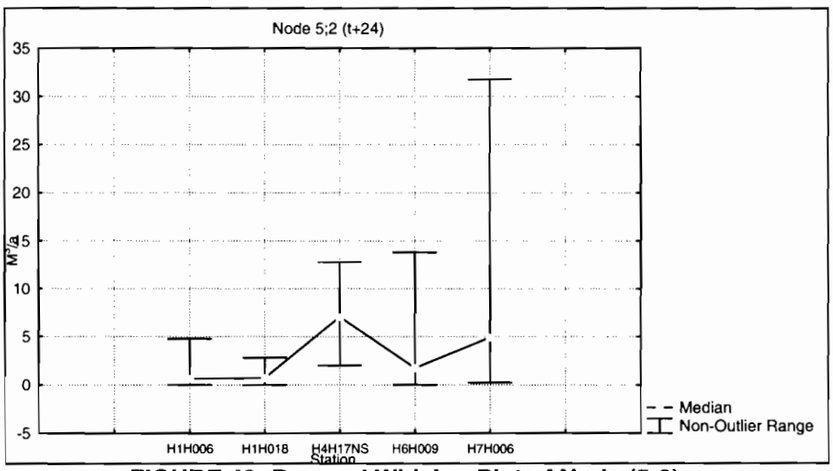

FIGURE 48: Box and Whisker Plot of Node (5;2)

A noticeable difference between the runoff associated with nodes (3;2), (4;2) and (5;2) (Figures 46 to 48) and nodes (0;0), (0;1) and (0;2), examined on the left-hand side of the NCEP SOM space, is that the nodes towards the right-hand side of the SOM space have a lower upper limit of runoff. The nodes on the right-hand side of the SOM space were explained earlier as being 'summer' SOM nodes therefore exhibiting a predominant atmospheric condition associated with less precipitation in the Western Cape. This assumption explains the lower upper limit of runoff present in nodes (3;2), (4;2) and (5;2).

Another prominent difference along the left to right continuum from node (3;2) to node (5;2) is the decrease in median runoff. The median runoff either decreases slightly or stays the same across all the stations along the continuum. The synoptic patterns displayed in these SOM nodes are consistent with this result showing synoptic states associated with decreased precipitation along the left to right continuum and therefore less runoff. The SOM of specific humidity shows decreasing specific humidity from node (3;2) to node (5;2) and the SOM of geopotential height shows an increasing high pressure over the interior from node (3;2) to node (5;2). Neither of these changes in synoptic state would be conducive to rainfall.

The presence of the high frequency of data mapping to node (5;2) in ECHAM4 infers that the ECHAM4 GCM depicts control atmospheric conditions resulting in less overall runoff than in reality. This is inferred while bearing in mind the decrease in runoff shown in the left to right continuum from node (3;2) to (5;2) and that the NCEP data, used as a representation of current climate, shows a high frequency in node (3;2). This is a significant error of the ECHAM4 model that had to be taken into account when looking at the projected future atmospheric conditions as modelled by ECHAM4.

3.3.1b Comparison between ECHAM4 control and projected future data

Once the error between the current and GCM-modelled data had been accounted for, the difference in data mapping frequency between the ECHAM4 control and projected future data was considered. Frequency maps (Figure 15 (a) and (b)) indicate which SOM nodes in the ECHAM4 control and ECHAM4 projected future data require the most pressing inspection. The frequency maps indicate that the high frequency node (5;2) in the control data shifts to node (6;2) in the projected future data. Not only does the high frequency node shift but the amount of data mapping to node (6;2) in the GCM-simulated future data is far greater than the amount of data mapping to node (5;2) in the control frequency map. Therefore, the projected future data displays even less uniformly distributed data over the SOM space.

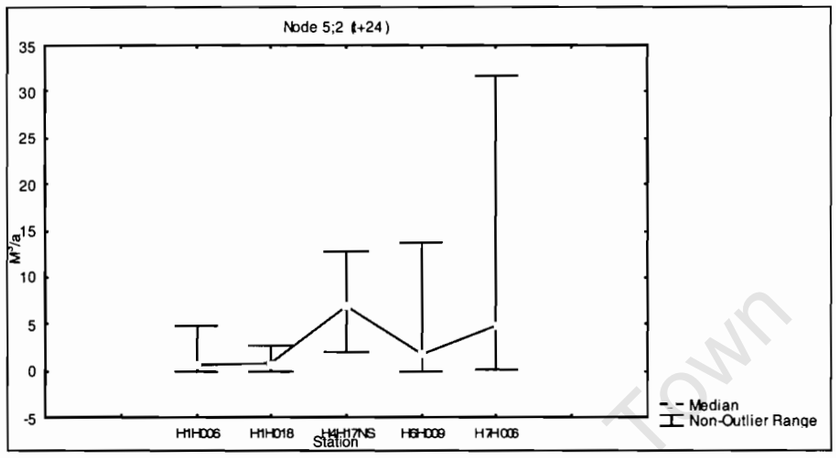

FIGURE 49: Box and Whisker Plot of Node (5;2)

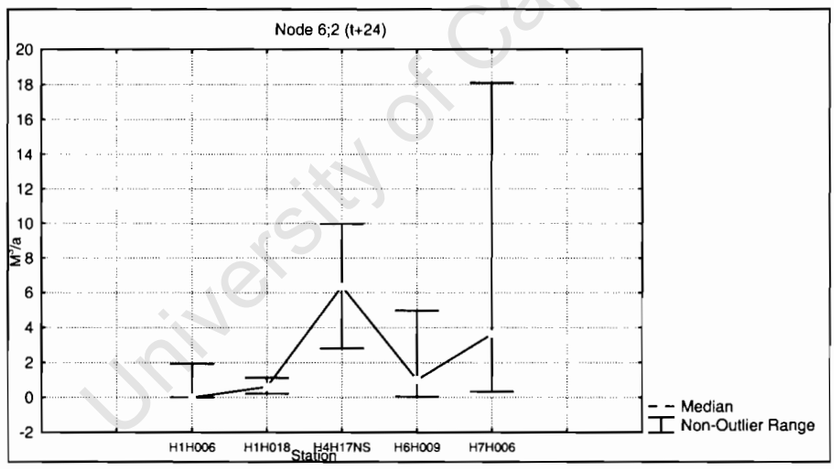

FIGURE 50: Box and Whisker Plot of Node (6;2)

Box and Whisker plots of runoff, that are not on the same scale, (Figures 49 and 50) reveal the magnitude of the change in runoff that could be expected in the catchment as a result of ECHAM4-modelled climate change. A decrease in runoff at all stations in node (6;2) when compared to node (5;2) is found. This decrease is shown not only in the median runoff but

also in the non-outlier range. This result is consistent with the theory that there is a decrease in runoff along the left to right continuum from node (3;2) to node (6;2). The decrease in runoff between node (5;2) and node (6;2) is quite distinct in comparison to the decrease across the rest of the continuum.

Each runoff gauging station's percentage decrease in runoff from node (5;2) to node (6;2) is shown in Table 4. The decrease is first calculated for the median and then for the maximum of the non-outlier range.

TABLE 4: Decrease in runoff represented from node (5;2) to node (6;2)

Median	**5;2**	**6;2**	**Decrease**	**% Decrease**
H1H006	0.65 m^3/s	0 m^3/s	0.65m^3/s	100
H1H018	0.74 m^3/s	0.6 m^3/s	0.14 m^3/s	18.59
H4H17NS	7.05 m^3/s	6.37 m^3/s	0.68 m^3/s	9.65
H6H009	1.76 m^3/s	0.1 m^3/s	0.76 m^3/s	43.38
H7H006	4.91 m^3/s	3.62 m^3/s	1.29 m^3/s	26.17
Non-outlier (maximum)	**5;2**	**6;2**	**Decrease**	**% Decrease**
H1H006	4.76 m^3/s	1.93 m^3/s	2.83 m^3/s	59.45
H1H018	2.82 m^3/s	1.12 m^3/s	1.7 m^3/s	60.28
H4H17NS	12.8 m^3/s	9.98 m^3/s	2.82 m^3/s	22.03
H6H009	13.8 m^3/s	4.97 m^3/s	8.83 m^3/s	63.99
H7H006	31.8 m^3/s	18.1 m^3/s	13.7 m^3/s	43.08

The ECHAM4 model projects dominant atmospheric conditions under climate change to be very similar to those depicted in node (6;2). Seeing as though every station in node (6;2) throughout the catchment, has an atmospheric condition that is associated with a lower runoff than at present, it is expected that climate change may result in less water flowing in the Breede River. The two stations that require the greatest scrutiny are stations H1H006 and H1H018, because these are in the upper catchment and close to the source of the river. Significant projected decreases in runoff at these stations would have an impact on the catchment as a whole. The median runoff for these stations at node (6;2) is a little lower than node (5;2) with the non-outlier ranges significantly lower at both of the stations. This partly explains the decreased runoff throughout the catchment.

While accounting for the error of the ECHAM4 model when compared to the control NCEP data, it can still be concluded that there may be a decrease in the projected future runoff, under climate change. This is due to the fact that node (3;2) to node (6;2) lie along the same continuum of decreasing runoff. Since the ECHAM4 projected future data has, in fact, been constrained to within the training of the NCEP SOM it may, in reality, be mapping to a SOM node outside that of (6;2). This is assumed because the data appears to be 'falling off' the SOM space in the frequency map. Due to this feature, it is hypothesized that the ECHAM4 projected future data would map better to a node that is to the right of node (6;2) in the SOM space, which would result in an even greater expected decrease in runoff in the future Breede River flow.

3.3.2 High frequency node analysis of CSIRO data

3.3.2a Comparison between NCEP and CSIRO control data

When a comparison was performed between the NCEP control frequency map and the CSIRO control frequency map, the accuracy of the GCM in portraying the current climate was assessed. It was discussed above that node (3;2) is the high frequency node in the SOM of NCEP data. The high frequency nodes in the SOM of CSIRO control data are represented by nodes (4;2) and (4;3) (Figure 21). No additional analysis was needed for the comparison of the NCEP frequency map with the CSIRO control frequency map because it was already concluded in section 3.3.1a that there is a decrease in runoff along the left to right continuum from node (3;2) to node (4;2). Hence, the high frequency nodes as represented by the CSIRO control data exhibit a lower overall runoff than the high frequency node in NCEP control (apart from node (0;0)).

The following section shows that node (4;3), which is the high frequency node in the SOM of CSIRO projected future data, exhibits an even lower median runoff than node (4;2). This is discussed while assessing the future runoff but also applies to the high frequency nodes in the CSIRO control SOM. The analysis shows that both the high frequency nodes in the CSIRO control SOM exhibit a lower associated runoff than the NCEP high frequency node (3;2).

3.3.2b Comparison between CSIRO control and projected future data

The highest frequency of data mapping in the projected future scenario is concentrated into node (4;3) (Figure 24(b)). Therefore, it is necessary to examine the runoff associated with nodes (4;2) and (4;3) to understand the characteristics of the change in predominant projected future runoff. There is also a slight increase in the frequency of data mapping to nodes (0;0), (0;1) and (0;2) but the predominant change is present in the nodes discussed below.

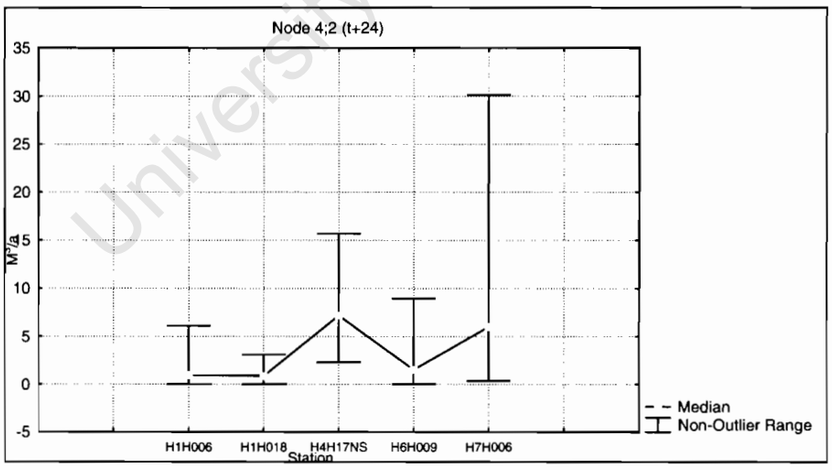

FIGURE 51: Box and Whisker Plot of Node (4;2)

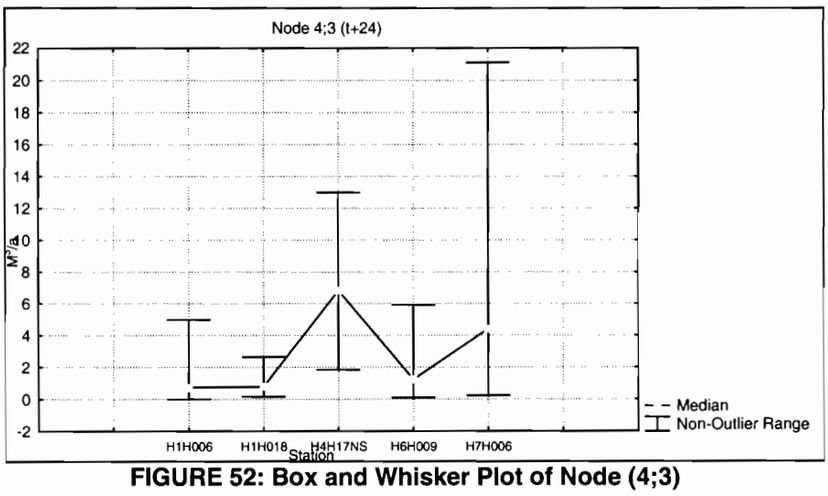

FIGURE 52: Box and Whisker Plot of Node (4;3)

Throughout all the gauging stations there is a decrease in median runoff from node (4;2) to node (4;3) (Figures 51 and 52). The decrease in median runoff is confirmed due to the decrease in all the maximum non-outlier ranges. Table 5 shows the actual decrease and the percentage decrease in runoff, throughout all stations, both in the median value and in the maximum non-outlier range.

TABLE 5: Decrease in runoff represented from node (4;2) to node (4;3)

Median	**4;2**	**4;3**	**Decrease**	**% Decrease**
H1H006	0.96 m^3/s	0.71 m^3/s	0.25 m^3/s	25.64
H1H018	0.85 m^3/s	0.8 m^3/s	0.05 m^3/s	6.24
H4H17NS	7.19 m^3/s	6.82 m^3/s	0.37 m^3/s	5.08
H6H009	1.53 m^3/s	1.24 m^3/s	0.29 m^3/s	18.95
H7H006	6.01 m^3/s	4.41 m^3/s	1.6 m^3/s	26.64
Non-outlier (maximum)	**4;2**	**4;3**	**Decrease**	**% Decrease**
H1H006	6.11 m^3/s	4.99 m^3/s	1.12 m^3/s	18.33
H1H018	3.1 m^3/s	2.64 m^3/s	0.46 m^3/s	14.84
H4H17NS	15.7 m^3/s	13 m^3/s	2.7 m^3/s	17.2
H6H009	8.93 m^3/s	5.91 m^3/s	3.02 m^3/s	33.82
H7H006	30.1 m^3/s	21.1 m^3/s	9 m^3/s	29.90

It is recognised that projections from the CSIRO model show the future scenario to exhibit a greater proportion of days with atmospheric conditions similar to those in node (4;3). The runoff associated with node (4;3) is lower than the associated runoff in node (4;2) therefore, a lower overall runoff in the catchment may be expected in the future. This also confirms the inference, made at the beginning of the section, that both nodes (4;2) and (4;3) depict a lower overall runoff than the high frequency NCEP node (3;2).

If it is assumed that there is a shift 'up' in nodes from the present to the projected future condition as modelled by the CSIRO data, it is possible to take into account the error of the

GCM data. The error is accounted for by assessing the runoff associated with the NCEP node directly above node (3;2), which is the high frequency node in the NCEP data. If node (3;3), which is directly above node (3;2), has a lower runoff than node (3;2), it can be assumed that the inferences made with the GCM data are correct. A cursory glance at the runoff associated with node (3;3) shows a median runoff that is either the same or less than node (3;2). Therefore, it can be assumed that the inferences made from the GCM data are correct, even with the associated error of the model.

3.3.3 High frequency node analysis of HadAM data

3.3.3a Comparison between NCEP and HadAM control data

The Hadley model displays a more distributed area of high frequency in the SOM of control data than the other GCMs. There are three SOM nodes that have a high frequency as modelled by the HadAM control data, being nodes (5;2), (5;3) and (4;4) (Figure 29). These nodes are then concentrated into nodes (6;2) and (6;3) in the frequency map of projected future data.

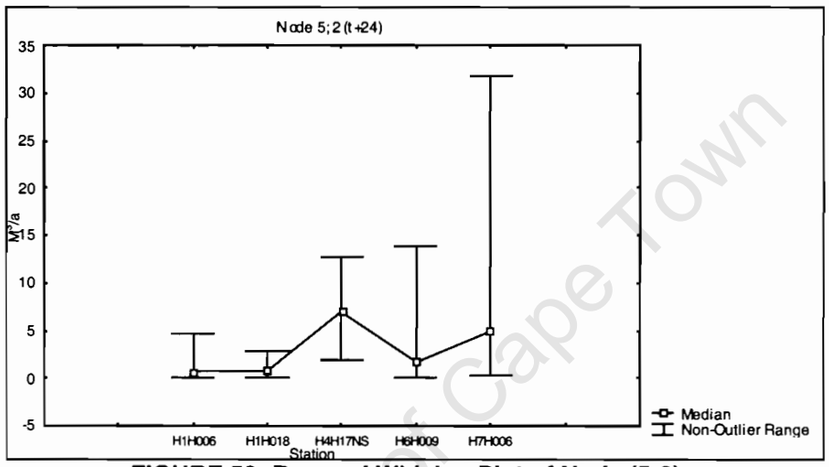

FIGURE 53: Box and Whisker Plot of Node (5;2)

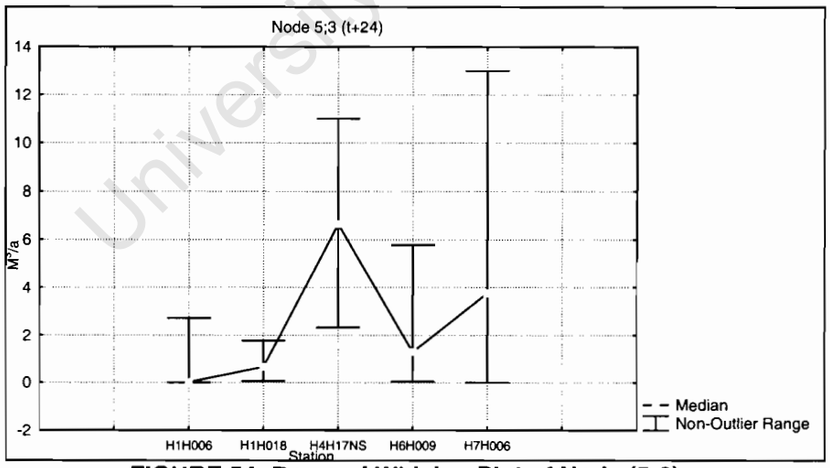

FIGURE 54: Box and Whisker Plot of Node (5;3)

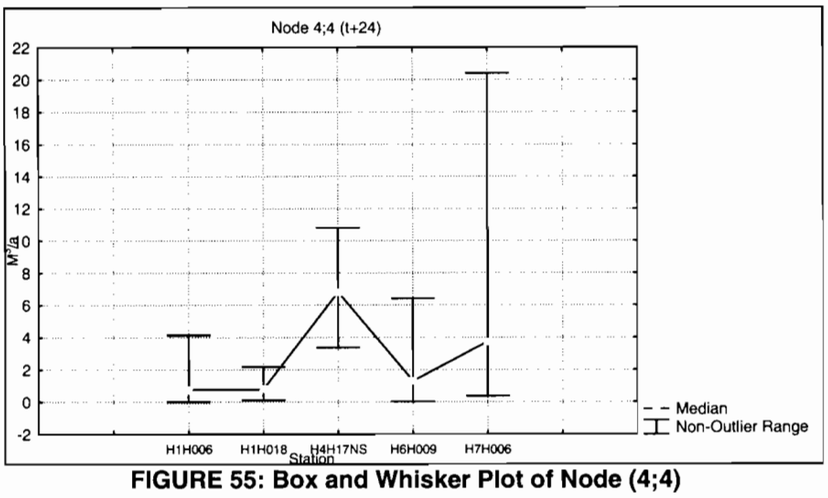

FIGURE 55: Box and Whisker Plot of Node (4;4)

Of the three high frequency control nodes (Figures 53, 54 and 55), node (5;2) displays the highest runoff values and (5;3) the lowest runoff values. Therefore, intuitively, if the projected future high frequency nodes exhibit an associated runoff less than that of the lowest valued runoff node, (5;3), the projected future high frequency nodes would have a lower associated runoff than all the high frequency control nodes. This conclusion can be used to assess the change in runoff from present day to projected future. If the runoff in the projected future scenario exhibits overall runoff values that are less than those associated with node (5;3) it can be assumed that this GCM projects a possible decreased runoff under climate change.

3.3.3b Comparison between HadAM control and projected future data

The two high frequency nodes in the projected future scenario are nodes (6;2) and (6;3) (Figure 32(b)). Analysis of the runoff associated with the synoptic state depicted in these two nodes enables a first order assessment of possible future runoff in the catchment.

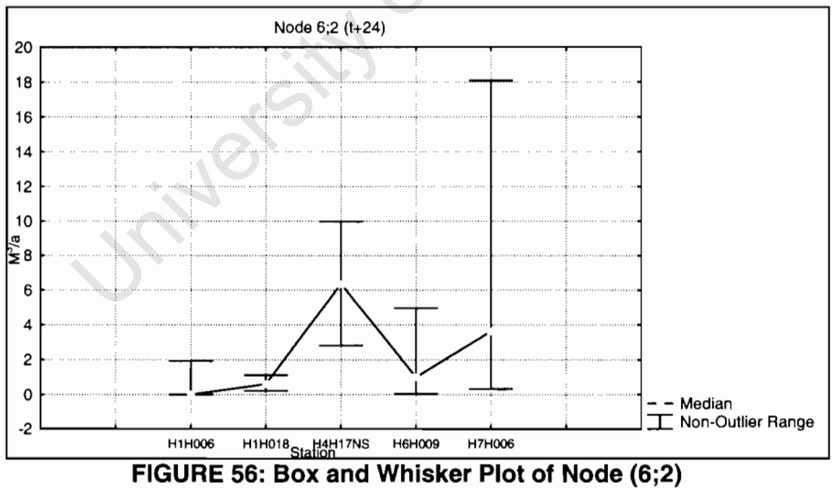

FIGURE 56: Box and Whisker Plot of Node (6;2)

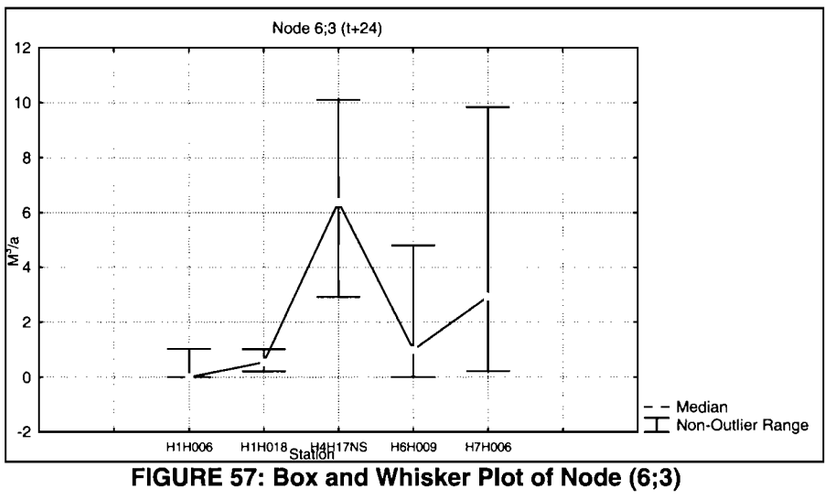

FIGURE 57: Box and Whisker Plot of Node (6;3)

All of the values of median runoff in node (6;2) and (6;3) are less than the values of median runoff in node (5;3) (Figures 56 and 57). Therefore, remembering the conclusion that was attained in section 3.3.3a, the projected future scenario might exhibit a lower median runoff than the present condition. Another way of examining the change in runoff is by looking at the non-outlier ranges of runoff. In this case all the non-outlier ranges are lower than node (5;3) except for station H7H006 in node (6;2). The median runoff is lower at this station than the median at the same station in node (5;3) so this anomaly can be discounted and the original statement that runoff is projected to decrease under the future climate remains valid.

To create a table of runoff values showing the magnitude of the decrease in runoff from the present to the projected future it was necessary to combine the runoff values of (5;2) and (5;3) to represent the present runoff. Node (4;4) was omitted because it appeared, from the SOM map, that the predominant shift was along the horizontal continuum from nodes (5;2) and (5;3) to nodes (6;2) and (6;3). The runoff values in nodes (6;2) and (6;3) were also combined to represent the future runoff. Using this method, the decrease in the runoff associated with the high frequency nodes can be examined (Table 6).

TABLE 6: Decrease in runoff represented from node (5;2) and (5;3) to node (6;2) and (6;3)

Median	**5;2 + 5;3**	**6;2 + 6;3**	**Decrease**	**% Decrease**
H1H006	0.66 m^3/s	0 m^3/s	0.66 m^3/s	100
H1H018	1.4 m^3/s	1.14 m^3/s	0.26 m^3/s	18.24
H4H17NS	13.7 m^3/s	12.76 m^3/s	0.94 m^3/s	6.86
H6H009	3.06 m^3/s	1.99 m^3/s	1.06 m^3/s	34.71
H7H006	8.67 m^3/s	6.56 m^3/s	2.12 m^3/s	24.39
Non-outlier (maximum)	**5;2 + 5;3**	**6;2 + 6;3**	**Decrease**	**% Decrease**
H1H006	7.47 m^3/s	2.97 m^3/s	4.5 m^3/s	60.24
H1H018	4.59 m^3/s	2.14 m^3/s	2.45 m^3/s	53.38
H4H17NS	23.8 m^3/s	20.08 m^3/s	3.72 m^3/s	15.63
H6H009	19.57 m^3/s	9.77 m^3/s	9.8 m^3/s	50.08
H7H006	44.8 m^3/s	27.93 m^3/s	16.87 m^3/s	37.66

It is possible to account for the error in the HadAM model using the same technique as used to assess the error in the ECHAM4 model. In the ECHAM4 analysis it was shown that there is a continuum of decreasing runoff from node (3;2) to node (6;2). This statement suggests that there would still be a decrease in runoff whether the high frequency node in the SOM of control data is found at node (3;2) (the NCEP high frequency node) or further along the continuum, for example node (5;2). This statement holds true for the HadAM data, which shows a shift in the high frequency nodes along the same continuum from present to projected future. In this way, the error in the HadAM model is accounted for because the high frequency nodes still shift along the left to right continuum.

These results may not bode well for the future of the Breede River's agricultural sector. The projected decreases in runoff may be slight but, over time, the impact of this projection could have severe effects on agriculture. More concerning is the pressure that is already being placed on the Breede River's water resources from all land uses throughout the catchment. Lowered runoff will only increase these pressures over time. Also concerning is the potential change in the predominant synoptic pattern depicted by all the GCMs. It was discussed earlier that the left-hand side of the SOM space depicts predominantly winter synoptic states whereas the right-hand side depicts predominantly summer synoptic patterns. All three GCMs show a shift in the high frequency SOM node either up or to the right of the high frequency SOM node in the present data. This shift shows a projected change towards synoptic states predominantly associated with summer conditions. The increase in "summer state" conditions may have severe ramifications other than simply a decreased runoff, such as an increase in average temperature, which may hamper the growth of many crops in the catchment.

3.4 Calculation of Mean Annual Runoff

In the preliminary discussion, in section 3.3, it was determined that the nodes depicting a high intensity of data displayed a predominant decrease in runoff from the control to the projected future condition. This analysis showed that there might indeed be a decrease in future runoff in the river. However, in order to quantify the change in Mean Annual Runoff (MAR) another approach must be employed.

The high frequency nodes alone cannot be used to calculate MAR as only one runoff regime is displayed in each SOM node. In order to quantify the average runoff over the entire year it is necessary to consider every SOM node. The synoptic conditions found in all the seasons of the year and their associated runoff are incorporated into the final analysis when using all the SOM nodes.

The previous sections daily runoff values are averaged and converted from million m^3/s into million m^3/a by multiplying the figure by the number of seconds in a year. The second part of the calculation uses the frequency maps for NCEP, ECHAM4, CSIRO and HadAM generated in the previous section. Each SOM node in the frequency maps is assigned a value of frequency, which represents a percentage of the data present across the SOM space. Therefore, by dividing these values by 100 the proportional contribution of each SOM node can be determined.

If the proportional contribution of each SOM node is multiplied by the appropriate associated runoff and the results from each node across the SOM space summed together, the result is the MAR. Repetition of this process for each daily runoff gauging station determines the MAR for each station.

At the end of this process, the MAR values calculated using the NCEP reanalysis data should be representative of the original MAR data supplied by DWAF. The supplied DWAF MAR values have been inserted into Table 7 for use as a reference. It is important to note that the sampling points for the supplied DWAF MAR data are not at exactly the same points as the gauging stations for daily runoff data used in the previous section (Figure 58). However, they are close enough for comparison with the daily runoff data. The ECHAM4, CSIRO and HadAM data represent the modelled control and projected future MAR in the catchment.

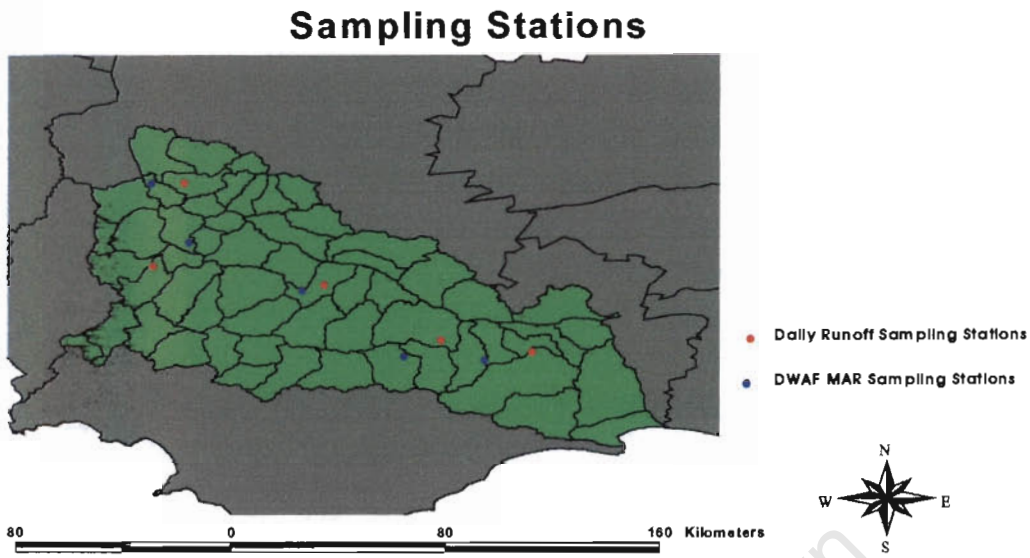

FIGURE 58: Comparison between the positions of daily runoff sampling stations and Mean Annual Runoff sampling stations (1:1371283)

There are some small discrepancies between the calculated NCEP MAR data and the supplied DWAF MAR data (Table 7) for two reasons. The first reason is that the stations used to measure the DWAF MAR are only in approximately the same positions as the original daily station data (as mentioned above), some measurement stations are several kilometres away from the stations used to measure daily runoff. The second reason is that NCEP utilises reanalysis data and not observed climate data. Although constrained by observations, NCEP data is still a product of an atmospheric model (Tennant, 2003).

The following table presents DWAF values for the MAR presently observed in the river, what the runoff would be if there were no extractions or disturbances in the river (Natural MAR) and what level of runoff the ecology of the river needs to be able to sustain life and to provide a functioning ecosystem.

TABLE 7: Comparison between the observed MAR data and the GCM-simulated MAR data. (units in million m^3/a)

MAR (mil m^3/a)					
DWAF (original)	**H1H006**	**H1H018**	**H4H017**	**H6H009**	**H7H006**
Present MAR	287.00	131.00	763.00	94.00	1059.00
Natural MAR	333.00	158.00	1210.00	347.00	1720.00
Ecological Requirement	84.00	79.00	552.00	134.00	623.00
Models	**H1H006**	**H1H018**	**H4H17NS**	**H6H009**	**H7H006**
NCEP (control)	234.01	176.61	975.76	319.24	1178.27
ECHAM (control)	218.58	160.67	917.42	289.11	1053.37
CSIRO (control)	192.32	147.19	854.64	295.32	1039.86
HADAM (control)	208.84	158.81	887.16	302.87	1079.19
ECHAM (future)	94.90	76.03	424.06	180.33	565.23
CSIRO (future)	204.9	154.48	902.24	298.90	1075.46
HADAM (future)	140.34	113.24	625.53	263.44	842.09

The MAR data, as analysed with the NCEP-trained SOM, should be a good approximation of the supplied DWAF present MAR because, for the purposes of this project, the observed environment is represented using NCEP data. It can be seen in Table 7 that the runoff at stations H1H006, H4H017 and H7H006 is well represented by the NCEP data. Stations H1H018 and H6H009 are not so well represented. These two DWAF MAR sampling points are the furthest away from the original DWAF daily runoff gauging stations. The DWAF MAR sampling point that represents station H1H018 is approximately 20 kilometres away from the original daily runoff station and the DWAF MAR sampling point that represents H6H009 is approximately 30 kilometres away from the original daily runoff station. This non-correlation in sampling points between the supplied MAR data and the daily runoff data may be the reason for these discrepancies. This is an uncertainty that needs to be taken into account in the final total MAR results. The calculated control MAR data from the ECHAM4, CSIRO and HadAM GCMs is also not exactly the same as the calculated NCEP MAR data because GCM data is modelled data and each model uses different physics.

The future MAR values in Table 7 are not the final values because they are the product of a GCM. The runoff changes from present to projected future, as seen in Table 7, need to be incorporated into the supplied DWAF MAR values to get the absolute value for projected future MAR under each GCM. The most reliable method of getting an absolute value for future MAR under each GCM is to calculate the change in MAR between the control and the future GCM data. The percentage change from the control to the future has to be calculated for each GCM before the changes in future MAR can be incorporated into the present MAR. By subtracting the percentage change from the present MAR, a future MAR value can be achieved. The associated biases in the GCMs are taken into account by using the percentage change values and not the absolute values.

In equation form this is written as

$$NCEP + \left[\frac{GCMfut - GCMcon \times NCEP}{100} \right] \quad (1)$$

TABLE 8: Calculation of Future MAR

MAR change	**H1H006**	**H1H018**	**H4H17NS**	**H6H009**	**H7H006**
ECHAM	-123.68	-84.65	-493.4	-108.79	-488.14
CSIRO	12.58	7.29	47.60	3.58	35.61
HADAM	-68.51	-45.57	-261.64	-39.43	-237.09
% change	**H1H006**	**H1H018**	**H4H17NS**	**H6H009**	**H7H006**
ECHAM	-56.58	-52.68	-53.78	-37.63	-46.34
CSIRO	6.54	4.95	5.57	1.21	3.42
HADAM	-32.80	-28.69	-29.49	-13.02	-21.97
Future MAR	**H1H006**	**H1H018**	**H4H17NS**	**H6H009**	**H7H006**
ECHAM	124.61	61.99	352.68	58.63	568.25
CSIRO	305.77	137.49	805.5	95.14	1095.26
HADAM	192.86	93.41	537.98	81.76	826.34

CSIRO reflects an increase in the MAR whereas both the other GCMs show the opposite result (Table 9). This can be partly explained by the small increase in frequency of data seen in nodes (0;0), (0;1) and (0;2) in the future SOM map. These nodes were explained earlier to be "winter" nodes, therefore exhibiting winter rainfall patterns of elevated rainfall. There is also a slightly higher frequency of the other "winter" nodes in the future SOM in comparison to the control SOM which may be contributing to the overall increase in MAR.

The ECHAM4 and HadAM models exhibit a decrease in the MAR from the present to the projected future scenario. An assessment can now be made as to whether the future projected MAR for these models already falls below the ecological requirement expressed in Table 7. This is before the impact of the agricultural sector is taken into account, in the next section.

Station H1H006, in the upper catchment, reveals that none of the models exhibit a projected MAR that falls below the ecological requirement of 84 million m^3/a. However, at the other upper catchment station, H1H018, the ECHAM4 model does show a projected future MAR that is lower than the ecological requirement of 79 million m^3/a, with the other models still demonstrating an ecologically sustainable runoff. At the middle catchment station of H4H17NS both the models of ECHAM4 and HadAM exhibit a projected future MAR that is less than the ecological requirement of 552 m^3/a. The lower catchment station H6H009 already displays a current MAR of less than the ecological requirement of 134 m^3/a. Obviously, this deficit will only worsen across most of the models in the projected future

scenario. At the final station, H7H006, ECHAM4 shows a future runoff that is projected to be lower than that of the 623 m^3/a ecological requirement.

Once the increased irrigation from the agricultural sector is taken into account this deficit in runoff associated with ecological sustainability could only worsen, hence creating more areas in the river that would not be ecologically sustainable under climate change. Part two of the project investigates the quantifiable increase in irrigation that would be required for sustainable agriculture under climate change while taking this water loss into account in the future runoff.

PART TWO

Watermod3 - simulated agricultural water demand under future conditions

CHAPTER FOUR: AGRICULTURAL WATER DEMAND IN THE BREEDE RIVER

4.1 Introduction

The objective of part two of the study is to assess the increased irrigation demand under a future climate, together with its resultant impact on runoff. A critical assumption that is required in this process is that farming practices, farm sizes and population will not change into the future. This is highly unlikely to be the case, however, trying to project future farming practices and population size would only introduce more uncertainty.

Firstly, using data from part one, the increase in irrigation demand was assessed using the Watermod3 biophysical crop simulation model. The Watermod3 model was selected for, amongst other reasons, its ability to provide detailed outputs for simulated irrigation amount and application. The simulated amount of increased irrigation was then converted into a value that could be subtracted from the projected future runoff levels in the river as determined in part one. This, in turn, was translated into a final value of projected future runoff after agricultural water usage.

The Department of Water Affairs and Forestry (DWAFb, 2002; 2003) have assessed that agriculture is the most important source of primary production in the Breede River catchment. Products of agriculture alone account for 36% of the Breede River's Gross Geographical Product. It follows that irrigated agriculture accounts for the greatest percentage of water use in the basin, with a total of 66%. The prominence of the agricultural sector has even prompted the development of secondary industries in the basin, such as canning factories and wineries.

The Breede River basin possesses many qualities that make it particularly suitable for agriculture. The climate is that of mild Mediterranean which is appropriate for a wide variety of crops. There is, at present, an abundance of good quality water for irrigation. Additionally, there is a wealth of good soils close to water sources and the basin is in close proximity to harbours for export of harvested crops. However, recent declines in the financial situation of many of the farmers in the catchment are a concerning factor in the future planning for water allocation in the basin because these financial losses may prompt substantial changes in land use in the foreseeable future. The financial losses have been attributed to factors such as the escalation in competing export agencies, slow adjustment to market preferences and a series of dry and warm winters (Kriel, 2004).

Crops currently grown in the basin can be divided into three main groups. The first category, with an area of 13 880ha, is irrigated C4 crops. C4 crops differ from C3 crops in that they use a method of carbon dioxide uptake that forms a 4-carbon molecule instead of 3-carbon molecules (Starr and Taggart, 1998). In this case, irrigated C4 crops consist mainly of grazing and fodder crops. The second biggest category is orchards (29 049ha). This group

consists of fruit such as stone fruit, pome and citrus and is the industry that has been under the greatest financial pressure in the export market in the past few years (Wand and Midgley, 2003). Finally, the most prominent agricultural group, covering a total area of 35 000ha, is the irrigated vineyards, which incorporates both wine and table grapes.

DWAF (2001) indicated where each crop is grown within the basin and each region's suitability for that crop. Knowledge of these factors is critical for the assessment of irrigation usage in the future. C4 crops are suited to the lower Breede River regions of Riviersonderend, Buffeljagts and Barrydale. They differ from the other crops grown in the basin as they are harvested every five to six weeks from the end of October until the beginning of winter, if they are not grazed (Dall, 2004).

Orchard fruit can be divided into pome fruit, citrus and stone fruit. Pome fruit are generally poorly adapted to soils that have high pH values and contain free lime. This requirement results in the growth of these fruits in areas of the Breede River such as the Ceres basin, Koo valley and Villiersdorp-Vyeboom.

There are certain sections in the Breede River that are more suitable for growing citrus than others. For instance, the Robertson-Ashton-Swellendam area is very suitable for soft citrus. The only limitation of this area is that the soils have a high pH. Swellendam is good for late cultivars and varietals because of the low winter rainfall and is also ideal for satsumas. Rawsonville and De Doorns are perfect because of their sandy soils and low incidence of false codling moth (*Cryptophlebia leucotreta*). The Grabouw area is less suitable for citrus as the early winter rainfall is too high and the temperatures are cooler. Finally, the Riviersonderend valley is too windy, resulting in wind abrasion marks on the fruit.

Stone fruit grow well throughout the basin because they do reasonably well in a wide range of soils; however, a soil with a slightly alkaline pH is ideal. They are also very tolerant of wet environments and high salinity soils. However, they are particularly sensitive to trace element deficiencies in the soil, especially iron. Their high tolerance of most climatic conditions makes them an ideal crop to grow anywhere in the basin.

Vineyards are found throughout the Breede River valley but table grapes are more suited to regions such as the Hex valley where warmer temperatures enhance early ripening. For instance the Hex valley is particularly suited to the production of late black seeded grapes. There does not seem to be much competition for this type of grape so the potential exists for this to become a niche product (DWAFb, 2002)

Taking the growing conditions of these crops into account, the Department of Water Affairs and Forestry are currently determining what the future allocation percentages of water will be.

There are plans to transfer water out of the Breede River into the greater Western Cape system. This policy decision will depend on the forecasted need for water in the agricultural sector since agriculture is such an important industry in the Breede River basin. The benefits of the transfer of water will therefore have to be offset against the benefits of agriculture. Climate change and the relevant change in runoff in the river needs to be taken into account in this respect due to the impact that it will have on water availability.

Chaves and Pereira (1992) propose that if temperature and potential evapotranspiration increase under climate change, which they are expected to do, irrigated crops will require additional water. By taking the three main crop categories into account it is possible to assess what will happen to their agricultural viability and irrigation requirements under climate change. These crops are assessed using both their characteristics as a crop variety and their position in the basin. By evaluating the increase in need for irrigation for each crop type under climate change, an assessment of the direct impact on the future runoff in the basin can be made.

4.2 Introduction to the Watermod3 Biophysical Crop Simulation Model

Watermod3 is a windows-based biophysical crop simulation model that is used, in this project, to investigate the change in irrigation required for agricultural crops under climate change. Although the model is not designed to simulate crop growth under climate change it does lend itself to this project by giving insight into the change in crop growth under changing temperature and rainfall conditions. It is a user-friendly agricultural/biophysical crop simulation model for all environments because it allows the user to insert external climate data (Johnson, 2003). It predominantly models soil water dynamics, crop growth and evapotranspiration and was designed for the specific utilisation of researchers and agricultural or environmental managers (Johnson 2003). The model is actually based on a cereal crop, although it can be adapted to other crops. Nevertheless, despite of some of the underlying simplifications, the model is robust and flexible, and interacts with the water dynamics in the desired way (Johnson, 2003).

Due to the recent development of the Watermod3 biophysical crop simulation model there is no published documentation on its use in research projects, however, an attempt to validate the model is undertaken later in this chapter, in section 4.4.1, by comparing Watermod3-simulated data to supplied observed DWAF irrigation data. This process of validation is undertaken because Thornley and Johnson (2000) state that initial validation of the model can be achieved by comparing model outputs with observed measurements. However, this process can sometimes produce the 'right' results for the 'wrong' reasons. Popper (1958) discusses validation of a theory as attempting to falsify it. Each failed attempt at falsifying the model results in a greater confidence in the model.

Testing and evaluating this or any model involves examining the model parameters, structure and climatic inputs used to drive the model. In this case, Watermod3 incorporates and accounts for all the water in the system and therefore provides a useful structure for analysing all the different fluxes that are involved (Johnson, 2003). One of the reasons Watermod3 is a suitable crop simulation model for use in this study is because, apart from its simplicity, it gives detailed results of irrigation application and amount. This is accompanied by crop growth and net crop yield. Both these elements under present and projected future conditions are crucial elements required for the calculation of future runoff. For use in scientific research, the model can be utilised to assess the behaviour of water dynamics for different crop types. It can also be used to investigate the response of different irrigation strategies and analyse experimental data.

Watermod3 allows for separate variables for soil water, crop type and irrigation to be inserted into the model (Johnson, 2003). The soil water component uses either the Richards equation (Johnson, 1996) or Capacitance model (Johnson, 1996) to describe infiltration and distribution of water. The Capacitance model is used for the purposes of this project because it is generally computationally faster and less subject to water mass balance problems, however, the effect of suction is not included (Johnson, 2003). Soil types can be entered in four different levels for representation of the soil profile. Data pertaining to the optimal soil type required for each vegetation category was obtained from DWAF (2001). Above the soil, the canopy and litter interception are modelled by entering values for water storage capacity. Data is not readily available for this variable so the generic Watermod3 value of 1mm per leaf area index was used. Topographical information is used to simulate water lost as runoff, the amount of water available for runoff being derived from the bare soil water storage capacity.

The crop growth module allows the user to enter parameters for crop type and growth. The specific growth characteristics for each crop type used in this module are discussed further on in this chapter. Crop types have to be separated into either C_3 or C_4 plants but individual growth characteristics can be entered into the model for each crop. The crop growth module includes the date of emergence of the plant, the date of anthesis and the date of maturity. Entering these dates into the model allows the user to specify how many days encompass emergence to anthesis and anthesis to maturity. It is also necessary to enter the latitude (33° South) and diurnal temperature range in this module. This gives information about the average temperature and amount of sunlight available for growth. Values for maximum root depth and 50% root distribution are indicative of the amount of water entering the plant and hence the amount available for plant growth and rejuvenation.

Irrigation can be applied according to three different application strategies. The first strategy applies water according to plant water status. Irrigation is only applied in this regime if the plant is assessed to lack a suitable level of water content. The second regime of irrigation,

which is the most common in the Breede River valley, is irrigation due to soil water deficit. The level of soil water is determined by the use of neutron probes, a diviner or even tensiometers (Stipp, 2004). Watermod3 allows the user to decide the critical soil water deficit and depth for calculation. The user also defines the months when irrigation is necessary. The third irrigation strategy is regular interval irrigation. Watermod3 allows the user to specify how much and how often to irrigate.

The irrigation strategy employed in the case of the Breede River is irrigation due to soil water deficit. This irrigation regime is employed because it is the method employed by the majority of farmers interviewed in the area. Throughout all irrigation strategies there is an option to either irrigate on top of the canopy or apply the water directly onto the soil while also setting the time of day for irrigation.

The data file allows for data of rainfall, temperature, relative humidity, solar radiation and potential evaporation to be drawn into the model in Excel spreadsheets. The program allows for external rainfall input files at intervals from one day up to one hour to be inserted. User-specified data is not a prerequisite for use in the model but insertion of localised data produces more reliable results for the area of study. This feature allows for very detailed simulations.

If user-defined data is not available, the model can use its own approximated data, as defined by fairly simply generic distributions, to create the climatic environment (Johnson, 2003). Approximated rainfall data is defined by millimetres of rainfall per month, number of rain days in the month and duration of rainfall per day. Average minimum and maximum temperatures define temperature, with a sinusoidal approximation throughout the year (Campbell, 1977; List, 1971). Soil temperatures can either be set at the same temperature as the air or at a user-defined temperature. Radiation inputs are defined in three sections; clear sky conditions, net radiation and albedo. Yearly relative humidity is approximated by the minimum, maximum and diurnal range. A value for wind speed can be set at a constant value throughout the year and the canopy height can be set to approximate the amount of potential evapotranspiration.

While the simulation is running, graphs of the different variables are viewed. This feature enables a quick check of the data and growth patterns. Upon completion of the simulation, detailed yearly data or longer-term summary data can be extracted into an Excel spreadsheet. The compatibility of Watermod3 and Excel makes data extraction and analysis significantly easier.

The principle objective of the model is to supply a dynamic interaction between crop growth and the water dynamics in the system and is not intended as a detailed model of crop growth.

Results are obtained for crop yield and irrigation under both present and future climate conditions by inserting the basic parameters of each crop type into the model. In this way, an assessment can be made about the amount of additional irrigation required under climate change to sustain the same crop yield as present. This, in turn, is translated into a value of runoff decrease due to irrigation and subtracted from the projected future runoff.

Unfortunately, the model does not take into account the affect of water use efficiency changes when crops are exposed to climate change. This may have a significant effect on how much irrigation needs to be applied, especially in C4 crops, which are expected to increase water use efficiency under a high CO2 environment.

4.3. Setting up Watermod3

4.3.1 Data

Climatic inputs for observed and projected future climate are required for insertion of the user-defined data into the Watermod3 agricultural model. However, prior to extraction of this climate data, the catchment was divided into 3 sections; the upper, middle and lower catchment. The upper catchment consists of sub-catchments H1 and H2, the middle catchment contains H3, H4, H5 and H6 and the lower catchment H7. These sub-regions are represented by running Watermod3 three times for each crop, a different data file for climatic inputs corresponding to a particular sub-region loaded for each run. The simulations thus produce crop simulation statistics for the upper, middle and lower catchment. This is important, as some of the crops are more prominent in one area of the basin than others. The basin cannot be divided into smaller sections because of the coarse nature of the climate data.

The data for the control climate was obtained from a number of sources. Daily temperature data from 1/1/1979 to 29/11/1997 was derived from the Computing Centre for Water Research (CCWR) station data set. This is a reasonable data set for use because of its high resolution of 0.25° in latitude and longitude. However, one limitation is that data is only present until 29/11/1997. Ideally, a longer time span would be optimal in formation of a base climate. The second climatic parameter of observed rainfall was obtained from conditionally interpolated observed station data (Hewitson and Crane, 2004). Rainfall figures from this data set were extracted for the same years as temperature with the added advantage of the data set's high resolution of 10 kilometres.

The simulation data of future climate change was obtained from each of the CSIRO, HadAM and ECHAM4 GCM simulations. However, given that the GCM spatial resolution is coarse, perturbing the observed CCWR high-resolution data with the climate change anomalies from the GCM data derived the projected future temperature for the region. Average temperature per month was calculated for the GCM simulation of present day climate and the simulation of the future climate (nominally 2079 to 2099 using the SRES A2 scenario for greenhouse gas

forcing). This average monthly temperature increase was then converted into an overall average increase in temperature over all the years to show what increase in temperature can be expected in the twenty year period from 2079 - 2999. This projected increase in temperature for each GCM was added to each observed daily temperature obtained from CCWR to attain a perturbed future climate change estimate of daily temperature. The result was a projected future temperature that could be entered into the agricultural model.

Statistically downscaled precipitation data is available for the models of CSIRO and ECHAM4 for the projected future climate (Hewitson, pers. comm.). Statistical downscaling was achieved through the development of a stochastic procedure conditioned by the large-scale circulation fields, providing a statistical relationship between observed large-scale variables and local, site-specific precipitation. Once extracted, this data could be entered straight into the model at a resolution of 0.25° in latitude and longitude. Unfortunately, downscaled data is not yet available for the HadAM model. In this case, the percentage value showing the decrease in runoff determined during the SOM analysis was used to determine a value of precipitation that could be subtracted from the conditionally interpolated observed precipitation data, in each sub-catchment.

It is important to remember here that the intention is to explore the impact of future climate perturbations on the regional system. As such the GCM simulations are used in this approach as guided perturbations (Hewitson, pers. comm.) rather than a definitive climate change projection.

4.3.2 Crop parameters used in Watermod3

Watermod3 has to be set up with the specific parameters for each crop in order to undertake each simulation of crop growth, yield and irrigation. This data was inserted into the biophysical crop simulation model as user-defined data. The parameters for each crop were researched mainly via communication with farmers (interviews in appendix A). Relevant experts that have worked in each field and/or have done extensive research about each field were also consulted. Both of these sources were combined with literature about each crop. In general, the consultation with farmers and relevant experts proved to correspond well with the literature. In cases when the literature was not consistent with the farmer interviews, the inputs from farmers superseded the literature.

In addition to specifying these parameters for each crop in Watermod3, the crop growth module was divided into the three sub-regions of the upper, middle and lower catchment. The majority of each crops parameters, specified in the tables below, are the same throughout all the sub-catchments with only the user-specified rainfall and temperature input data differing for each sub-catchment, however, the inclination of the profile differs from the upper to the lower sub-catchments. This is because farms found in the mountainous upper

catchment region should have a steeper runoff profile than farms found in the flatter valley region.

The parameters used for each crop are as follows:

Orchards

In the respect of orchards (Table 9) information was acquired with the kind participation of farmer A from Worcester, farmer B from Robertson and farmer C from Riviersonderend. Information was also obtained with the help of Stephanie Wand of Stellenbosch University and Peter Dall, previous head of the Deciduous Fruit Producers Trust and present consultant to the fruit industry.

TABLE 9: User-specified parameters for Orchards inserted into Watermod3

C_3 / C_4 Plant	C_3
Soil	Sandy-Clay (DWAF, 2001)
Maximum Root Depth	250cm (Pair, 1969)
Depth for 50% root distribution	100cm
Date of Emergence	15 September
Date of Anthesis	15 October
Date of Maturity	2 February
Date of Harvest	February to May
Irrigate on soil / canopy	Soil
Irrigate according to soil water status/ plant water status / regular intervals	Soil Water Status
Critical Soil Water Deficit	50mm
Depth for Calculation of Soil Water Deficit	250cm
Time of day of irrigation	5am – 9am
Months of Irrigation	1 September to 30 April
Profile Length	500m
Inclination of Profile	5% (upper) 4% (middle) 3% (lower)
Average Diurnal Temperature Range	8° - 28°
Infiltration time step factor	5

Vineyards

The relevant people consulted in order to gather parameters for use in vineyard growth simulation (Table 10) were farmer D of Worcester, Payter Botha and Briaan Stipp of Vinpro and Peter Dall.

TABLE 10: User-specified parameters for Vineyards inserted into Watermod3

C_3 / C_4 Plant	C_3
Soil	Sandy-Clay-Loam (DWAF, 2001)
Maximum Root Depth	100cm (Cape Wine Academy, 2002)
Depth for 50% root distribution	50cm
Date of Emergence	15 September
Date of Anthesis	4 November
Date of Maturity	12 February
Date of Harvest	February to april
Irrigate on soil / canopy	Soil
Irrigate according to soil water status/ plant water status / regular intervals	Soil Water Status
Critical Soil Water Deficit	50mm
Depth for Calculation of Soil Water Deficit	100cm
Time of day of irrigation	5am – 9am
Months of Irrigation	1 September to 31 May
Profile Length	500m
Inclination of Profile	5% (upper) 4% (middle) 3% (lower)
Average Diurnal Temperature Range	8°- 28°
Infiltration time step factor	5

C4 crops

The experts consulted in the respect of C4 crops (Table 11) were farmer E from Worcester, farmer F from the Riviersonderend Valley and Peter Dall.

TABLE 11: User-specified parameters for C4 crops inserted into Watermod3

C_3 / C_4 Plant	C_4
Soil	Clay-Loam (DWAF, 2001)
Maximum Root Depth	125cm (Janick, 1931)
Depth for 50% root distribution	70cm
Date of Emergence	15 Sept, 31 Oct, 16 Dec, 31 Jan, 18 Mar
Date of Anthesis	10 Oct, 25 Nov, 10 Jan, 25 Feb, 12 Apr
Date of Maturity	30 Oct, 15 Dec, 30 Jan, 17Mar, 2 May
Date of Harvest	30 Oct, 15 Dec, 30 Jan, 17Mar, 2 May
Irrigate on soil / canopy	Soil
Irrigate according to soil water status/ plant water status / regular intervals	Soil Water Status
Critical Soil Water Deficit	50mm
Depth for Calculation of Soil Water Deficit	125cm
Time of day of irrigation	5am – 9am
Months of Irrigation	1 September to 30 April
Profile Length	500m
Inclination of Profile	5% (upper) 4% (middle) 3% (lower)
Average Diurnal Temperature Range	8° - 28°
Infiltration time step factor	5

4.4 Watermod3 results

Once all the data of rainfall, temperature and each crops parameters had been inserted into Watermod3, it was run for each crop type, catchment and year. A summary for each year was made available for extraction at the end of each run. The summary includes variables such as irrigation inputs, yield, growing season rain and total rainfall, amongst others. For detailed summary results see appendix B.

4.4.1 Observed Data

The first step in the analysis is to assess how closely the Watermod3-modelled irrigation data resembles the original, observed irrigation data supplied by DWAF. This process can be used as an attempt to validate the use and suitability of the model. Temperature data from CCWR and observed conditionally interpolated rainfall data were used for insertion into Watermod3 for the control run.

The original supplied DWAF data has values for the volume of water utilised during irrigation per annum and the irrigated area. The Watermod3-modelled data gives values in millimetres of water per annum. Therefore, the supplied DWAF data required conversion into a value comparable to the Watermod3-modelled data. The results of the converted DWAF data are presented in Table 12. The conversion was achieved using the following equation:

$$\textit{Volume of water per year } (m^3/a) \textit{ / area } (m^2) \textit{ x 1000 = mm/a} \quad \textbf{(2)}$$

TABLE 12: Original DWAF irrigation data (DWAFb, 2002)

Units mm/a	**Upper Catchment**	**Middle Catchment**	**Lower Catchment**
Orchards	696	627.5	330
Vineyards	875.5	812.5	460
C4 crops	1673	1326	927

TABLE 13: Watermod3-modelled observed irrigation data

Units mm/a	**Upper Catchment**	**Middle Catchment**	**Lower Catchment**
Orchards	591.61	566.56	640.13
Vineyards	570	606.06	610.67
C4 crops	1401.56	1633	1622.78

This comparison between supplied irrigation data and Watermod3-simulated irrigation data can be used as a form of model validation because if the Watermod3-modelled data is similar to the observed data it shows that Watermod3 generates a good simulation of crop growth patterns. It is seen that similar magnitudes of irrigation are exhibited between the original DWAF supplied data (Table 12) and Watermod3-modelled data (Table 13) for orchards, although the Watermod3-simulated lower catchment shows almost double the amount of irrigation as the DWAF-supplied observed data.

Watermod3 simulates too little irrigation for vineyards, except in the lower catchment, where the agricultural model again exhibits a high water usage. In the original DWAF data, the orchards exhibit a lower irrigation requirement than the vineyards whereas in the Watermod3-simulated data the vineyards seem to show a slightly lower overall requirement. However, in general, Watermod3 is not too erroneous when simulating vineyard irrigation.

The Watermod3-simulated C4 crops data shows a similar magnitude of irrigation to the original DWAF data. However, the Watermod3-simulated data exhibits an increase in irrigation requirements from the upper catchment to the middle and lower catchment whereas the original DWAF data exhibits decreased irrigation reliance. Again, the lower catchment demonstrates a large error in the Watermod3-modelled data set. The Watermod3-simulated data shows a value almost twice as large as the original DWAF data in this catchment.

It must be noted that the lower catchment CCWR temperature data set has a significant amount of missing data in the years spanning 1995 to 1997 resulting in these years not being included in the analysis. This will most likely have had an impact on the inaccuracy of the lower catchment Watermod3-modelled data. There could also be other factors at play that are not taken into account in the Watermod3 model. Perhaps there is less runoff in the lower catchment due to the flatter topography, this may result in less need for such regular irrigation. Whatever the source of the error, it is isolated to this region and must be accommodated in the project.

Overall, the agricultural model simulates the observed conditions well. Apart from some large errors in the lower catchment, there seems to be a relatively good correlation between the modelled data and the original DWAF data. This validates the use of the model to some extent because Watermod3 simulates a reasonable representation of observed irrigation amounts. Therefore, the areas that have to be taken into account in the analysis of the results are where the model is either overestimating or underestimating the quantity of irrigation. This is predominantly in the lower catchment.

4.4.2 ECHAM4

It is necessary to complete a control (1979 – 1997) Watermod3 crop growth simulation for each crop and for each GCM. The control run creates a set of base growing conditions, which can then be used in comparison to the projected future (2079 – 2099) growing conditions generated by Watermod3, using data from each GCMs A2 emission scenario.

By creating a table of results depicting the change in some of the Watermod3 output variables for each crop it is possible to observe the projected changes in crop growth under climate change. It must be noted that this section only deals with the guided perturbations of the ECHAM4 GCM and thus only demonstrates one projection of future climate change.

TABLE 14: Watermod3-modelled future data (average 2079 - 2097) – control data (1979 – 1997) generated with ECHAM4

Crop	Variable	Upper Catchment	Middle Catchment	Lower Catchment
Orchards	Yield	-1.12	-1.02	-1.17
	Growing Season Rain	-7.78	-0.28	43.87
	Irrigation	179.45	111.61	-54.87
	No. of irrigations	3.45	2.17	-1.13
Vineyards	Yield	-1.17	-1.26	-1.42
	Growing Season Rain	-17.22	-3.62	44.07
	Irrigation	102.73	74.56	-28.93
	No. of irrigations	2	1.44	-0.6
C4 crops	Yield	0.31	0.23	0.15
	Growing Season Rain	-95.83	-56	29.54
	Irrigation	1168.28	391.78	-188.8
	No. of irrigations	22.83	7.61	-3.73

The change in agricultural performance under future conditions (Table 14) is depicted by the difference values between the control and future data. This is achieved by subtracting the control values from the projected future values as generated by Watermod3. Negative values indicate a decrease and positive values an increase.

The yields are projected to decrease slightly from the control to the projected future in orchards and vineyards and projected to increase slightly in C4 crops. The magnitude of the change in yields is only slight and is not considered to be statistically significant.

Unlike the data generated using the other GCMs, irrigation is not projected to increase across every catchment and crop. It is projected to increase in the middle and upper catchments for all three crop types. However, a decrease is projected in the lower catchment for all crops. This discrepancy was not entirely unexpected as it was shown in section 4.4.1 that Watermod3 shows a large error in modelling the irrigation inputs in the lower catchment in comparison to the observed data. The magnitude of this decrease exhibited in the lower catchment, using ECHAM4 data, is very small and it can therefore be assumed that irrigation levels may not change into the future.

Obviously the growing season rain and number of irrigations corresponds accordingly with the increase or decrease in irrigation amount. When there is a projected decrease in irrigation amount, the growing season rain is seen to increase and the number of irrigations decrease. Conversely, when there is a projected increase in irrigation amount, the growing season rain is shown to decrease and the number of irrigation events increase. Given the fact that the

sole difference between the control and future Watermod3 runs is the insertion of different temperature and rainfall values, it can be said that the changes described above are only driven by factors of temperature and rainfall.

4.4.3 CSIRO

Data from the CSIRO GCM is the second set of data used for simulation of crop growth in Watermod3. A GCM simulation of present climate is necessary for use in comparison with the projected future A2 scenario data. These two simulations were then differenced from each other to obtain the change in crop growth projected under future conditions.

TABLE 15: Watermod3-modelled future data (average 2079 – 2097) – control data (1979 – 1997) generated with CSIRO

Crop	Variable	Upper Catchment	Middle Catchment	Lower Catchment
Orchards	Yield	-2.56	-2.73	-2.86
	Growing Season Rain	-68.05	-30.22	0.07
	Irrigation	407.66	247.16	150.54
	No. of irrigations	5.73	4.72	2.87
Vineyards	Yield	-2.91	-3.31	-3.43
	Growing Season Rain	-67.28	-29.61	-2.54
	Irrigation	309.83	203.44	95.33
	No. of irrigations	5.95	3.89	1.87
C4 crops	Yield	-0.05	0.06	0.11
	Growing Season Rain	-94.89	-36.94	-13.67
	Irrigation	1315.27	662.39	436.47
	No. of irrigations	25.72	12.89	8.4

The use of CSIRO data in Watermod3 depicts a larger discrepancy in the crop yield of orchards and vineyards from the control to the projected future than either of the other GCMs (Table 15). This is a concern and, in all probability, means that more than the Watermod3-simulated amount of irrigation would need to be applied to reach an acceptable yield for those crops.

Even though the projection shows a decrease in the yield of orchards and vineyards, Watermod3 projects irrigation amount to increase across all the catchments and crops. The magnitude of the increase is significant across all crop types, especially in the upper catchment.

Again, the growing season rain is projected to decrease across most of the catchments; the only exception to this statement is the lower catchment orchards where the growing season rain is predicted to increase by 0.07mm. This does not seem to have a dramatic effect on the

irrigation requirements as they are still projected to increase into the future. The reason for this could be due to the elevated temperatures in the future projection or due to a change in intensity and timing of the rainfall. The number of irrigations are projected to increase with the increase in total irrigation in the future scenario. This is intuitive as the farmer is more likely to increase the number of irrigations than increase the amount of water applied per irrigation as too much water applied at once may stress the plant.

4.4.4 HadAM

Unfortunately, statistically downscaled precipitation data is not available for the future A2 scenario of the HadAM model. Data was obtained for insertion into Watermod3 by calculating a percentage decrease in precipitation shown by the change in the high frequency node in the SOM for each runoff station. This was then differenced from the observed conditionally interpolated precipitation data.

It must be reinforced here that these results cannot be directly compared to the ECHAM4 and CSIRO results because the downscaling processes used to derive the input precipitation data is different. It is a viable technique for assessing the change in irrigation requirements. It is not, however, as robust as the technique used in ECHAM4 and CSIRO. The downscaling technique performed to produce the ECHAM4 and CSIRO precipitation incorporates a statistical relationship between observed large-scale variables and local, site-specific precipitation. The downscaling process should produce a closer approximation of future climate than perturbing present climate by a standard amount. An important implication of the process used to calculate HadAM values for precipitation under future climate is that it does not allow for a possible increase in precipitation. However, even though the data cannot be analysed in the same way, this method is still a useful tool in reinforcing the simulations obtained from CSIRO and ECHAM4.

TABLE 16: Watermod3-modelled future HadAM data (average 2079 – 2097) – observed data (1979 - 1997)

	Variable	Upper Catchment	Middle Catchment	Lower Catchment
Orchards	Yield	-1.27	0.79	-0.28
	Growing Season Rain	-44.44	-60.28	-74.07
	Irrigation	205.17	523.44	363.74
	No. of irrigations	3.89	9.95	6.94
Vineyards	Yield	-1.71	-1.11	-1.45
	Growing Season Rain	-45.66	-61.95	-78.53
	Irrigation	133	273.83	229.66
	No. of irrigations	2.56	5.22	4.34
C4 crops	Yield	0.07	0.7	0.33
	Growing Season Rain	-79.94	-109.89	-143.8
	Irrigation	640.72	2877.06	2058.95
	No. of irrigations	12.61	56.44	40.41

When using HadAM data, Watermod3 shows that although most of the yields exhibit a decrease from the observed to the projected future data (Table 16), this decrease is not sizeable. In fact, most of the projected future yields lie around similar values as the control yields. It can be accepted, therefore, that the projected future yield is held at an acceptable level by increasing the irrigation inputs.

Watermod3 shows a significant increase in the amount of irrigation throughout all the catchments and crop types in order to produce a comparable yield. This is especially evident in the C4 crops as the irrigation is projected to increase, on average, more than two-fold.

There is also a corresponding projected increase in the number of irrigations applied throughout the growing season in every crop type and catchment. This shows that there is a projected change in the amount of irrigation being applied as opposed to the intensity of irrigation. Intuitively, the growing season rainfall also decreases substantially from the observed to the simulated future data. This is already evident in the input data file.

This confirms the results shown in the Watermod3 simulations completed with the CSIRO and ECHAM4 data. All the GCM-forced Watermod3 simulations show a projected future increase in irrigation across most of the catchments and crops. They also show a predominant decrease in growing season rain and a corresponding increase in the number of irrigation events.

In summary of this section, it was discovered that Watermod3 displays a projected increase in irrigation in every catchment and crop except for the lower catchment crops in ECHAM4. This

gave a cohesive view of the predominant changes projected for the future and that the changes are principally showing an increase in irrigation amount. The variable showing the change in the amount of irrigation is considered the most important as it has a direct effect on runoff in the river.

CHAPTER FIVE: IRRIGATION WATER EXTRACTION EFFECTS ON RUNOFF

The effect on runoff from irrigation water extraction has to be dealt with in a slightly different manner from the method used to assess the change in runoff under purely atmospheric conditions. This is due to the fact that the simulated irrigation data is area data whereas the runoff data is point data. The change in irrigation amount cannot be incorporated directly into the runoff exhibited at each station in the sub-catchment because all the water for a particular sub-catchment is not extracted at exactly the same point. For the purposes of this project it is assumed that 100% of the water used in irrigation is drawn from the river and neglects the existence of on-farm dams. Obviously this is not strictly true but most of the farmers interviewed in the Breede River valley said that they rely solely on the Brandvlei dam pipe transfer scheme for their irrigation needs and do not have on-farm dams.

To avoid the potential confusion, the following logic was employed. It is logical that the two runoff stations in the upper catchment (H1H006 and H1H018) will not be affected by the change in irrigation because water is not drawn for irrigation at the source of a river. It is also reasonable to assume that the runoff station H7H006 will exhibit the cumulative effects of water drawn both from the upper and middle catchment. Therefore, in order to calculate runoff at station H7H006 all the irrigation inputs from the upper and middle catchments are subtracted from the Mean Annual Runoff (MAR) at station H7H006. Due to the fact that the other two runoff stations (H4H017 and H6H009) are situated around the centre of the middle catchment, it is necessary to make an approximation of their irrigation affected runoff. To make this approximation, the same percentage decrease that is present in the lower catchment station of H7H006 is applied to the middle catchment stations of H4H017 and H6H009.

Unfortunately, there is no runoff data available at the mouth of the river, so it can only be assumed that the irrigation required in the lower catchment is subtracted from the river flow after the H7H006 station and would only serve to further decrease the runoff levels in the lower catchment, the magnitude of which is not known. This assumption may result in an overestimation of water in the lower catchment under climate change therefore biasing the results towards a situation with a more favourable level of runoff in the lower catchment.

The simulated future MAR modelled under purely the change in atmospheric conditions is required to start the calculation of runoff incorporating increased irrigation demands. This was first calculated in chapter 3. The future MAR under atmospheric climate change conditions is given in Table 17. This is used as a base from which to subtract the simulated future change in water amount used for irrigation.

TABLE 17: Calculated future MAR (million m^3/a)

Future MAR	H1H006	H1H018	H4H017	H6H009	H7H006
ECHAM	124.61	61.99	352.68	58.63	568.25
CSIRO	305.77	137.49	805.5	95.14	1095.27
HadAM	192.86	93.41	537.98	81.76	826.34

5.1 Runoff results

5.1.1 ECHAM4

The results of the control and projected future irrigation simulations from Watermod3 are available in chapter 4 and in more detail in appendix B. The difference between the ECHAM4-forced control and projected future irrigation results give a value depicting the change in irrigation between the GCM-simulated present climate and the GCM-simulated future climate, as shown in Table 18. Where the values in Table 18 are shown as positive, there is a projected increase in irrigation expected for the future. Where the values are shown as negative there is a projected decrease in irrigation requirement.

TABLE 18: The increase in irrigation in response to forcing by the ECHAM4 model (mm/a)

ECHAM future irrigation – ECHAM control irrigation	Upper Catchment	Middle Catchment	Lower Catchment
Orchards	179.45	111.61	-54.87
Vineyards	102.73	74.56	-28.93
C4 Crops	1168.28	391.78	-188.8

ECHAM4 exhibits an increase in irrigation requirement in both the upper and middle catchments, however, there is a decrease in irrigation demand present in the lower catchment. This is unexpected as there is a projected "drying" in the whole catchment under projected future conditions as shown by the SOM analysis. This should, in turn, lead to an increase in irrigation requirement. This projected decrease in irrigation has to be taken into account, however, it can possibly be explained, to a certain extent, by the error shown in Watermod3 whilst modelling the lower catchment. This was investigated in chapter 4 as most likely being due to missing data in the years 1994 to 1997 in the CCWR temperature data set or other unknown factors. The decrease in precipitation may also be due to a uninvestigated potential bias in the conditionally interpolated rainfall data or the downscaled rainfall data, which were used for the observed and projected future data sets, respectively.

The greatest change in simulated irrigation demand under the projected future climate is shown in the C4 crops. This is not unexpected as C4 crops have the greatest demand for irrigation at present (see Table 12). This is because they are generally harvested every five

to six weeks resulting in up to six harvestings a year and a greater overall yield. Due to this fact the number of irrigations and irrigation amount required to sustain the present yield is greater than the other crops. For this reason it is expected that, under a changing climate, C4 crops will have a greater impact on irrigation demand than the other crops. However, Watermod3 does not model the potential change in water use efficiency of the crops under climate change. It is expected that C4 crops may increase their water use efficiency under higher CO2 levels which may counteract this high level of irrigation demand, to some extent.

To convert these values pertaining to changes in irrigation requirement into an amount that is compatible with runoff it is necessary to perform the calculation in equation 2;

Increased irrigation (mm/a) / 1000 x crop area / 1 000 000 = runoff in million m^3/a **(3)**

The result is a volume of runoff, shown in Table 19, that requires subtraction from the simulated future MAR in Table 17 in order to get runoff after irrigation usage. The positive values in Table 19 indicate a decrease in runoff whereas a negative value indicates an increase in runoff.

TABLE 19: Calculated decrease in runoff due to irrigation in response to forcing by ECHAM4 (million m^3/a)

Runoff decrease	Upper Catchment	Middle Catchment	Lower Catchment
Orchards	17.9	19.2	-1.03
Vineyards	16.41	14.07	-0.04
C4 Crops	17.63	35.74	-6.13
TOTAL	51.94	69.01	-7.2

Due to the fact that some crops have a greater proportion of plantation than others in each sub-catchment it is expected that each crop would not have a similar proportional contribution to the change in runoff as to the change in irrigation demand. This is because the area of plantation of each crop is incorporated into the equation of conversion from irrigation amount to runoff value. As seen in Table 19, in the upper catchment, orchards have a greater impact on runoff than C4 crops, even though C4 crops have a much higher simulated irrigation demand under the projected future climate. This is because plantation of orchards is more predominant in the upper catchment than C4 crops.

The total change in simulated runoff for all crops in each sub-catchment can then be used to calculate the projected future runoff at each station. As stated above, stations H1H006 and H1H018 will not be affected by water extracted for irrigation because they are at the source of the catchment. H7H006 shows a 120.95 million m^3/a (21.28%) decrease in runoff due to water extracted in the middle and upper catchments. Hence, stations H4H017 and H6H009

are decreased by the same percentage. The final runoff values at all stations are shown in Table 20.

TABLE 20: Final runoff available in response to forcing by the ECHAM4 climate model (million m^3/a)

Future MAR including irrigation	H1H006	H1H018	H4H017	H6H009	H7H006
ECHAM4	124.61	61.99	277.61	46.15	447.3

These final runoff values represent the amount of water that is projected to flow in the Breede River under future conditions (2079 to 2099) as forced by the ECHAM4 GCM. These values take into account both the Watermod3-simulated projected increase in irrigation demand and the SOM-analysed projected future runoff values.

5.1.2 CSIRO

The process of running both the CSIRO control and projected future data through Watermod3 was repeated to generate values of simulated irrigation. The difference between the future and control irrigation is again calculated with positive values in Table 21 indicating an increase in irrigation.

TABLE 21: The increase in irrigation in response to forcing by the CSIRO model (mm/a)

CSIRO future irrigation – CSIRO control irrigation	Upper Catchment	Middle Catchment	Lower Catchment
Orchards	407.66	247.16	150.54
Vineyards	309.83	203.44	95.33
C4 Crops	1315.27	662.39	436.47

The Watermod3 simulations driven with CSIRO differ from the ECHAM4 driven simulations because the simulated irrigation demand is projected to increase in every catchment under the CSIRO GCM. Although all the catchments indicate a projected increase in Watermod3-simulated irrigation demand, the lower catchment shows the lowest increase. Again, this inconsistency with the rest of the data may be due to the error of the agricultural model in modelling the lower catchment. It may also be due to the downscaled rainfall data predicting a higher rainfall in the lower catchment, in comparison to the other catchments, in the projected future. This projection would seem unlikely because, generally, higher precipitation areas are seen in mountainous areas such as the upper catchment.

Again, the C4 crops exhibit the greatest increase in simulated irrigation demand, followed by orchards and then vineyards. However, the present irrigation requirements actually show vineyards to have a greater current irrigation demand than orchards, so the fact that orchards are showing a greater increase in irrigation demand under future conditions may be due to many reasons. Considering that Watermod3 is set with parameters requiring that vineyards be irrigated from September to May and orchards from September to April, there is a possibility that the GCM-simulated future rainfall regimes are simulating a greater amount of rainfall in the month of May than at present. This increased rainfall might result in less required irrigation in the month of May under future conditions. This scenario, however, is unlikely and it is more likely that Watermod3 is not entirely accurate in modelling the irrigation requirements of vineyards because it does not take into account the potential change in water use efficiency under climate change. This is evident in the initial validation of the model (see Tables 12 and 13) where it can be seen that Watermod3 does not always simulate a greater irrigation demand for vineyards than orchards. If this is the case, it is an error that needs to be taken into account when assessing the certainty of the final runoff results.

The decrease in runoff in Table 22 is calculated using equation 2. This converts the Watermod3-simulated irrigation demand from mm/a to m^3/a, making it comparable with a value for runoff.

TABLE 22: Calculated decrease in runoff due to irrigation in response to forcing by CSIRO (million m^3/a)

Runoff decrease	Upper Catchment	Middle Catchment	Lower Catchment
Orchards	40.66	42.51	2.83
Vineyards	49.49	38.4	0.14
C4 Crops	19.85	60.42	14.18
TOTAL	110	141.33	17.15

Under the CSIRO GCM, orchards and vineyards have a much greater impact on runoff in the upper catchment than C4 crops. This is not evident under the ECHAM4 GCM, in which each crop in the upper catchment contributed similar values of runoff decrease. In the middle and lower catchments, however, there is a greater proportional impact on runoff from the C4 crops. This is also evident in the simulations as forced by the ECHAM4 GCM.

Lastly, the runoff after irrigation water extraction is calculated and displayed in Table 23. The lower catchment shows the cumulative effects of water extracted throughout the basin, which is calculated to equal a 251.33 million m^3/a (22.95%) decrease in runoff. Therefore, the H4H017 and H6H009 stations are decreased by the same percentage, giving the final runoff levels.

TABLE 23: Final runoff available in response to forcing by the CSIRO climate model (million m^3/a)

Future MAR including irrigation	H1H006	H1H018	H4H017	H6H009	H7H006
CSIRO	305.77	137.486	620.66	73.31	843.94

The final runoff results after irrigation water extraction show greater projected future levels of runoff than the ECHAM4 GCM, at all the stations. However, the CSIRO GCM simulates high levels of runoff in the original atmospherically perturbed MAR data (Table 17) so the high runoff levels are expected. The high CSIRO MAR is due to winter rainfall and the irrigation changes happen at other times of the year, which may be partly why the CSIRO runoff remains high.

5.1.3 HadAM

The results obtained using the HadAM GCM have to be treated in a different manner because statistically downscaled precipitation data is not available for this model. Future precipitation data is derived by calculating a percentage decrease in precipitation shown by the change in the high frequency nodes in the SOM analysis. The percentage decrease is then subtracted from the current conditionally interpolated precipitation data.

Irrigation was simulated with the Watermod3 agricultural model for both the observed data and the GCM-perturbed data. The observed data simulation acts as the HadAM control run. Once the simulated irrigation amount under projected future conditions is known, the observed irrigation amount can be subtracted to show an increase in irrigation under climate change.

TABLE 24: The increase in irrigation in response to forcing by the HadAM model (mm/a)

HadAM irrigation – Observed irrigation	Upper Catchment	Middle Catchment	Lower Catchment
Orchards	205.17	523.44	363.74
Vineyards	133	273.83	229.66
C4 Crops	640.72	2877.06	2058.95

The Hadley model is consistent with the other GCMs in showing that there is an expected increase in irrigation requirement under projected future conditions (Table 24). The HadAM model also reveals that the increase in water extracted for use from all catchments is more consistent for each crop than the other GCMs. This is probably due to the manner in which the input precipitation data was produced, which was by perturbing the observed data with a

standard percentage change. It is thus also evident that the inconsistencies with the lower catchment values in the ECHAM4 and CSIRO models are associated with the downscaled rainfall data rather than Watermod3 because downscaled rainfall data is not used in the HadAM analysis.

TABLE 25: Calculated decrease in runoff due to irrigation in response to forcing by HadAM (million m^3/a)

Runoff decrease	Upper Catchment	Middle Catchment	Lower Catchment
Orchards	20.46	90.03	6.83
Vineyards	21.24	51.69	0.35
C4 Crops	9.67	262.45	66.87
TOTAL	51.37	404.17	74.05

Using equation 2 the decrease in runoff is calculated (Table 25). Utilising the accumulated runoff decrease from the upper and middle catchment, the decrease in runoff at station H7H006 is determined to be 455.54 million m^3/a (55.13%). This shows that the decrease in runoff in the lower catchment is more than half of its present level. It is also double the amount exhibited by either of the other GCMs. This result makes the magnitude of decrease in runoff as simulated by the Hadley model somewhat questionable because the results produced with the other two GCMs, with downscaled rainfall data, are very different. As discussed earlier the downscaling process is thought to produce a more accurate rainfall data set. Therefore, the larger value, as simulated by HadAM, may be due to the dissimilar derivation of Watermod3 input data. H4H017 and H6H009 are decreased by 55.13% in order to determine their projected runoff under climate change. The final results are shown in Table 26.

TABLE 26: Final runoff available in response to forcing by the HadAM climate model (million m^3/a)

Future MAR including irrigation	H1H006	H1H018	H4H017	H6H009	H7H006
HadAM	192.86	93.41	241.39	36.69	370.80

Due to the fact that HadAM can only be used to confirm the results of the other GCMs no firm inferences can be made from the final runoff results except that the final runoff values are more similar to the ECHAM4 final runoff values than the CSIRO values. The Watermod3 simulations with data derived from the HadAM GCM serve to confirm that runoff is expected to decrease under projected future conditions.

The decrease in runoff across all GCMs is due to a change in irrigation patterns, which are brought about by a change in rainfall and temperature under projected future conditions. However, it is critical to remember that it was assumed, at the beginning of the process, that farming activities will not change in the catchment from the present to the future. This is obviously not the case and a change in crop proportion in each sub-catchment, amount of farmed land, farming techniques and introduction of new crop varieties are amongst several factors that could seriously impact these results. It is highly unlikely that farmers will not try to adapt to the changes in rainfall and temperature.

It is also assumed that the farmers have a 100% reliance on the river water for their irrigation needs. This was assumed for the purposes of this project because the majority of the farmers interviewed are in consensus about this fact, at present. However, under changing climate conditions it is highly likely that farmers will change their strategy for obtaining water and may have a greater reliance on on-farm dams than at present.

Taking into account these assumptions, throughout all the models there is a predominant decrease in projected runoff. The magnitude of decrease varies across the models, with ECHAM4 and CSIRO displaying a similar percentage decrease. The initial assumptions may affect the magnitude of runoff decrease, however, unless there is no extraction from the river for agricultural purposes in the future, agriculture will certainly have a depleting effect on the runoff in the river.

Even though there is a difference in the magnitudes of decrease, the most important factor is the agreement across all GCMs that runoff is projected to decrease. The agreement shows that even though the models are predicting slightly different future conditions and have different input physics, they all show the same broad projection, which, in turn, enforces the probability of the projections being accurate.

PART THREE

Assessment of ecological sustainability

CHAPTER SIX: EVALUATION OF ECOLOGICAL SUSTAINABILITY

6.1 Ecological Flow Requirements

Part three of the study uses the information already obtained in parts one and two to determine the ecological sustainability of the river under future conditions. Ecological sustainability determines the ability of the river to support a variety of life by maintaining a symbiotic relationship between the species. The ability to maintain the species ecology depends on the level of flow in the river because different lifecycle phases require different levels of runoff. Additionally, the runoff needs to be maintained at a suitable minimum level throughout the year.

All riverine environments require a certain amount of water-flow in the river to be ecologically sustainable. The South African water act stipulates that enough water must be left available in the river after transfer for the sustained ecological functioning of the river (Hughes and Hannart, 2002). The act also refers to the need for assurance that requirements for basic human needs and the environment are met before licenses are issued for water abstraction (DWAF, 1997). Rivers are ranked according to their present ecological state and how their condition differs from the natural or pristine condition. Rankings range from State 'A', which is classified as natural, to state 'E', which denotes extensive loss of habitat, biota and ecosystem functioning (Hughes, 2001). Rivers can also be ranked as 'F', this is considered unacceptable and these systems require restoration (DWAF, 2003).

Not only is the volume of flow important in ecosystem functioning but also the level of flow at different times of the year. Different flow regimes support various stages of species lifecycles (McKnight et al., 1996) and also affect which species occur at separate places along the river (Tharme and King, 1998). During the different stages of the species lifecycles they may exist as eggs, seeds or spores if the environmental condition or flow level is temporarily unsuitable. This allows no species to reach pest proportions in an ecologically balanced environment. (Tharme and King, 1998).

A riverine environment that supports a particular local hydraulic, thermal and chemical condition is known as a hydraulic biotype. The number of hydraulic biotypes present in a river is directly proportional to the number of species that can exist in the river (Tharme and King, 1998). Biotypes are created by high and low flows throughout the year. High flows dictate the mean size of bed particles, which, generally decrease in size as the river evolves to the mouth. High flows can be divided into freshes and floods. Freshes are slight elevations of water level during the wet season and floods are large increases in water level (Tharme and King, 1998). Each flow regime has a particular function in the lifecycle of species living in the river.

The first floods decrease the amount of dissolved oxygen and improve the water quality because the fine sediments are flushed out (Tharme and King, 1998). They also instigate fish spawning and migration. Peak flood flows are important because they work the bed particles into different sizes throughout the catchment, thereby increasing the number of hydraulic biotypes (Davies and Day, 1998). Floods also recharge the groundwater and inundate the surrounding vegetation area, allowing fish to move onto the floodplains. Pests are controlled and habitat diversity increased (Tharme and King, 1998). When the base flows return to normal after the rains, there is an increase in growth and productivity of both aquatic species and riparian vegetation as new seedlings are established (Tharme and King, 1998).

Dry season freshes stimulate spawning and renew the water quality. A sustained baseflow in the remaining times of the year supports the habitat and keeps pests under control (Tharme and King, 1998). Therefore, it can be seen that not only is the volume of water in a river important for maintaining an ecosystem but also the magnitude, velocity and return period of the flows (Tharme and King, 1998).

The Breede River is one of the few permanently open estuaries on the South African coast. At present the biodiversity is high and even though the water entering the river is only of average water quality it is still classified, overall, as a category 'B' (good) estuary. The reason for the category 'B' classification, as opposed to an 'A', is mainly due to the extensive development that has taken place upstream (DWAF, 2003). An understanding of ecological sustainability and the conditions necessary for ecosystem functioning are vitally important in the light of a changing climate.

6.2 Ecological Sustainability of the Breede River under climate change

A critical aspect of this project is to determine whether the river is projected to be ecologically sustainable at different points throughout the catchment. Ecological sustainability is assessed at the five stations of study using the level of projected future MAR runoff. The future runoff levels are compared to ecologically sustainable MAR levels. This assessment of ecological sustainability only takes into account the MAR levels and does not include intra-annual variations in runoff due to seasonal forcing. The runoff levels at different times of the year may have a significant impact on the ability to maintain ecological sustainability at a particular station. Without accounting for intra-annual variations of runoff levels, only a first order assessment of ecological sustainability can take place.

Data was supplied by DWAF, which shows the MAR levels required to sustain ecological functioning at various stations throughout the catchment (Table 27). These stations do not fall at exactly the same point in the river as the MAR stations (Table 28) but are close enough to be used as a comparison data set.

TABLE 27: Runoff level required for ecological sustainability (million m^3/a) (DWAF, 2003)

	H1H006	H1H018	H4H017	H6H009	H7H006
Ecological Requirement	84	79	552	134	623

TABLE 28: Present MAR (DWAF, 2003)

	H1H006	H1H018	H4H017	H6H009	H7H006
Present MAR	287	131	763	**94**	1059

At present only one of the stations (H6H009) shows a runoff level that falls below that required for ecological sustainability. This is represented in bold in Table 28. The part of the river that incorporates station H6H009 is the most degraded due to the upstream construction of the Theewaterskloof dam (DWAF, 2003). Water flowing past this station gauge has consequently decreased due to the containment of water in the dam.

All the GCMs are in agreement that there is a predominant projected decrease in runoff due to both atmospheric climate change and the simulated change in demand for irrigation water extracted from the river. The number of stations expected to fall below ecologically sustainable levels are expected to change dramatically into the future due to the simulated changes in runoff levels. The values in bold in Table 29 are the stations that are projected to fall below the ecologically sustainable level under future conditions.

TABLE 29: Projected Future MAR after irrigation extraction

	H1H006	H1H018	H4H017	H6H009	H7H006
ECHAM4	124.61	**61.99**	**277.61**	**46.15**	**447.3**
CSIRO	305.77	137.49	620.66	**73.31**	843.93
HadAM	192.86	93.41	**241.39**	**36.69**	**370.8**

The projected future MAR simulated using the ECHAM4 model depicts four out of the five gauging stations to fall below the runoff level required for ecological sustainability under future conditions. The only station that is projected to remain ecologically sustainable is the upper catchment station, H1H006. This is logical as it will have the least influence from water extracted for agricultural use because it is situated at the source of the river. ECHAM4 projects the most severe impact on ecological sustainability in comparison to the other GCMs. Hewitson (pers. comm.) rates the ECHAM4 model as the most reliable model when depicting precipitation over the Western Cape region. This would suggest that the impacts on ecological sustainability may be particularly large.

The HadAM model projects three of the five stations to fall below ecologically sustainable levels. Again, the stations that are projected to remain ecologically sustainable are those in the upper catchment. However, the middle and lower catchment stations that are projected to be ecologically unsustainable under future conditions have even lower runoff values than the same ECHAM4-simulated stations. This may be related to the process that was used to generate the simulated change in irrigation demand under the HadAM model, which showed very high amounts of projected water used for irrigation.

The CSIRO model shows only station H6H009 to fall below the required ecologically sustainable levels. This is not unexpected, as this station presently displays runoff levels that fall below the level required for ecological sustainability. The SOM analysis showed that this model simulates an increase in MAR under atmospheric climate change. This was stated earlier as possibly being a result of a slight increase in data mapping frequency to some of the "winter" nodes. If this is the case it would bias assessments for other times of the year. This could be the reason for the simulated increase in rainfall and hence the reduced impact on ecological sustainability.

The projected reduction in ecologically sustainable areas may have a serious impact on the river and the people who rely on it. As runoff decreases the temperature of the water flowing in the river will increase thereby decreasing the Oxygen levels available for organisms living in the river. Turbity may result in the river because of the lack of fast flowing water, which may, in turn, cause the river to silt up. A lack of a thriving ecology in the river will cause the river to become degraded and it will no longer be able to provide fresh water to the users (Davies and Day, 1998). Degraded rivers are significantly less economically valuable than normal rivers (Carpenter and Cottingham, 1997).
Aside from the obvious conservational concern this projected lack of ecological sustainability may have a serious economic impact. There will be ramifications for the tourism industry in the area because the Breede River is a prime fishing region and without the river being able to support a thriving ecology, the lifecycles of all fish species will be affected. This factor accompanied with the decline in the aesthetic value of the region will have a major economic impact due to a drop in tourism. The subsistence fisherman will also be affected by the changing ecology, which could create large sectors of unemployment.

New species, such as the Water Hyacinth, that proliferate in stagnant water, will be able to thrive in the slower flowing, lower water levels. The attraction of new species will have resonating effects throughout the basin, affecting all life in the river.

It must be noted that these conclusions were derived solely by taking into account the atmospheric impact due to climate change and the increase in extraction from increased irrigation requirements. It was not possible, in the time allocated for completion of the study,

to note all land-use impacts on the runoff in the catchment. Other impacts on the runoff will include extraction for human usage (depending on the population number) and water consumed by alien and natural vegetation, amongst others. If alien vegetation is allowed to proliferate unchecked this could become a major factor for consideration in future runoff projections.

SUMMARY, CAVEATS AND CONCLUSIONS

Summary

A key initial outcome from the research revealed that changing agricultural practices, necessitated by changing climate, are likely to have an added impact on the river and the life contained within it. This discovery prompted the project to assess the magnitude of impact that agriculture would have on the runoff under future conditions and whether this would influence the ability of the river to remain ecologically sustainable. Consequently, due to the change in runoff, from both atmospheric and agricultural influences, it was concluded that there might be a major impact on the river under climate change conditions. This was a significant discovery because of the strong human reliance on the river. Any impact will resonate through not only primary users but also many other secondary and tertiary users.

The project was undertaken in three parts. The first part encompassed the use of SOMs in assessing runoff under climate change. It was thought that SOMs would be a useful technique for analysis in this study as it has the ability to cluster large amounts of data into a specified amount of archetypal synoptic patterns, thereby rendering the data more manageable for analysis. This characteristic quality of SOM analysis allowed for the convenient assessment of the change in climate patterns from present to future.

The SOM nodes that showed the highest frequency of data mapping were analysed according to their associated runoff. It was determined that all the nodes with a high intensity of data mapping showed a decrease in runoff from the present to the future, throughout all the GCMs. This method was used as a first order analysis of the change in runoff because the node showing the highest frequency of data mapping would, by nature, exhibit the most predominant synoptic pattern. To check this result the Mean Annual Runoff (MAR) was calculated.

Using the SOM circulation-MAR relationship, the MAR related to the atmospheric circulation of the control period (1979 to 1999) was compared to the MAR of the circulation simulated for the future (2079 to 2099). It was concluded that two of the three GCMs showed a significant runoff decrease associated with the change in circulation patterns from present to future, whereas one GCM showed an increase in runoff. The GCM that showed an increase in runoff (CSIRO) displayed an increase in MAR in winter which renders it's MAR projections less relevant to the agricultural usage and flow at other times of the year.

.

Part two of the project used the Watermod3 biophysical crop simulation model to analyse the impact of an altered future runoff on irrigation supply to the agricultural sector. Watermod3 was chosen because of its user-friendly interface while modelling water usage in every aspect of plant growth. A major drawback of using this model was its simplicity. The user is only

given the choice of specifying plant types into either a C3 or C4 growth type. However, an attempt to counteract this simplicity was made by inserting detailed growth parameters into the model. Watermod3 produced results for all aspects of plant growth, but most importantly, irrigation amounts were calculated in production of an optimum yield. For the purposes of this study the output of Watermod3, in terms of water usage and plant yield, was considered a reliable estimate under future conditions because the model performed reasonable well while representing the current agricultural outputs.

All the models and catchments exhibited an increase in the irrigation requirement under climate change, with one exception. The use of ECHAM4 data in Watermod3 showed a decrease in irrigation requirement in the lower catchment. It was significant that Watermod3 showed most of the data, apart from the aforementioned ECHAM4 data, to be in agreement towards a predominant increase in irrigation demand because it indicated that agriculture may have an added effect on the depletion of water available for future runoff.

The third and last part of the project was the assessment of the ecological sustainability of the river under climate change. The Department of Water Affairs and Forestry supplied data pertaining to the runoff levels required for ecologically sustainability. If the projected future runoff levels fall below the specified amount, the river may no longer be ecologically sustainable at that station. The final data set showed the ECHAM4 model projecting four stations to fall below the required level for ecological sustainability, HadAM three stations and CSIRO one station.

This was of added consequence to all the land uses that rely on the Breede River for their water supply. The final scenario expressed in this research is only projected to take place over a 100-year time span but, if the GCMs are realistic, and if the circulation-runoff relationships are stable, the situation in the catchment could be expected to deteriorate at a steady rate until that point.

Caveats

Uncertainty is an integral part of any climate change research because it is never possible to perfectly predict the future. There are a number of necessary uncertainties in this project that make the research possible. Firstly, the project makes use of only the SRES A2 emission scenario because data is readily available for this scenario. SRES A2 forms one of the four scenario families that comprise the SRES scenario set, with each family being equi-plausible (Nakic´enovic´ et al, 2000). Although the use of only the SRES A2 scenario results in an assessment of a solitary climate change scenario, the use of only one scenario also allows for a common basis for comparison between the GCMs.

Moving on to uncertainties present in the second part of the project. There are uncertainties associated with using a specific crop simulation model, as would be necessary with any crop simulation model used in the project. Watermod3 forces one to assume that a crop is categorized into either C3 or C4 crops, however, with the input of specific crop parameters this becomes manageable. It is also assumed, in the crop modelling process, that farming practices, farm sizes and population will not change in the future. This assumption is obviously not correct, as it is highly likely that, if nothing else, the population will change within the next one hundred years. However, trying to project future farming practices and population size would only introduce more uncertainty so it is viable to keep these amounts unchanged in the analysis. This assumption does not invalidate the results because the baseline results will still be relevant. It may, however, result in a slight difference in magnitude of change, either worsened by a growing population or mitigated, to some extent, by adapting farming practices.

Farmers have differing opinions on farming practices; these include differences in irrigation timing, amount and reliance on the river for their water. Unfortunately, it is only possible to use one set of parameters for each crop type. This forces the creation of an average set of parameters that are used by farmers. For instance, it is assumed that every farmer relies fully on the river and municipal dams for their water supply. This is not strictly true as some of the farmers spoken to do extract some water from on-farm dams. However, the majority of farmers expressed that they rely entirely on the Brandvlei dam transfer scheme. Due to this fact, 100% reliance on the river is assumed for all farmers, which is not the case for some. This assumption will not invalidate the final results because a first order impact assessment of irrigation water extraction from the river is still achieved.

Lastly, there is debate about the best methodology to use in subtracting the future additional water used in irrigation (calculated in Watermod3) from the runoff stations. The runoff stations do not fall at exactly the same points as those used for the irrigation change calculations. Also, the irrigation data is area data and the runoff data is point data so the runoff decrease due to irrigation cannot be subtracted directly from the runoff stations. It was ultimately decided that the two upper catchment stations would not be affected, but the lower catchment would exhibit a decrease in runoff as accumulated from both the upper and middle catchments. The two middle catchment stations were decreased by the same percentage as the lower catchment station. This is not a strictly correct method of calculation and probably slightly overestimates the decrease in the middle catchment, but it is the only available method of calculating change at these stations. If one is mindful of the possibility of an overestimation of runoff decrease in the middle catchments and an underestimation of runoff decrease in the lower catchment, these results remain valid.

Conclusions

Despite the necessary assumptions made throughout the project, there are some very significant results arising out of it for use in water management. The climate change projections show some devastating effects on the runoff in the catchment. Even though these are long-term projections, if the projections are correct, the effects may be felt in the near future.

This is not the only research that has shown similar consequences on water supply in the Western Cape. Amongst other research, a study conducted by New (2002) concluded that the decrease in water supply and increase in demand in the Western Cape would exacerbate the existing water resource problems in the region. Even with 'moderately effective' water demand management it is likely that future water demand will exceed supply (CMC, 2001). New (2002) also stressed the need for the inclusion of climate change projections in long-term planning. This is already a requirement in the United Kingdom and is urgently needed in water-stressed regions such as the Western Cape (OFWAT, 1998).

The Department of Water Affairs and Forestry (DWAF) are candid about the fact that "any future abstractions would negatively affect (the Breede River's) environmental status" (DWAF, 2003). However, it is stated that; "if arrangements are made to ensure that sufficient water passes abstraction points the negative impact should be small enough to be acceptable" (DWAF, 2003). This statement was made without cognizance of climate change projections and in the light of potential water transfer schemes out of the Breede River system. To this end, it is recognised that without water transfer schemes out of the Breede River catchment, the Cape Town metropolitan region will experience a substantial future water stress.

DWAF bears realisation to the fact that future projections of water demand are uncertain and an element of conservatism needs to be employed in the decisions made about transfer schemes (DWAF, 2003). It is, however, of great concern that climate change projections have not been accounted for in their factor analysis, given the conclusions of this research. DWAF expressed an interest in the findings of this project and, hopefully, will take these results into account in future research concerning the Breede River.

The agreement of this research with similar research conducted on other Western Cape rivers demonstrates that SOMs are an effective method for use in hydrological research. SOMs are statistically based but require less computational knowledge than using a specific hydrological model. SOMs also have a greater variety of uses than a single hydrological model. The SOM method applied in this project presents a relatively new methodological option for future hydrological research.

The door has been left open for further work in this area. For instance, other land use impacts on runoff should be further investigated in order to reduce uncertainty in projected runoff. These were not included in this project due to time constraints, however, even without including the other land use impacts, it is still evident that climate change will have a significant impact on runoff in the Breede River.

REFERENCES

- Andreae, M, Annegarn, H, Barrie, L, Feichter, J, Hegg, D, Jayaraman, A, Leaitch, R, Murphy, D Nganga, J, Pitari, G, Boucher, O, Haigh, J, Hauglustaine, D, Haywood, J, Myhre, G, Nakajima, T, Shi, G, Solomon, S. 2001. *Aerosols, their Direct and Indirect Effects,* In: IPCC Climate Change 2001: the Scientific Basis, A contribution of Working Group 1 to the Third Assessment report of the Intergovernmental Panel on Climate Change. Cambridge University Press, Cambridge, United Kingdom, and New York, NY, USA, 881pp
- Arnell, N. 1999. Climate Change and Global Water Resources. *Global Environmental Change.* 9(1): 31 – 49
- Boonzaier, A. 2000. *The role of water demand management in integrated water resource management: constraints and opportunities in Southern Namibia.* Thesis (MPhil). University of Cape Town. pp 29 - 37
- Braune, M and Wood, A. 1999. Best management practices applied to urban runoff quantity and quality control. *Water Science and Technology.* 39 (12): 117 - 121
- Broecker, W. 1987. The Biggest Chill. *Natural History.* 10: 74 – 82
- Campbell, G. 1977. *An introduction to environmental biophysics.* Springer. New York
- Cape Wine Academy. 2002. *Preliminary Wine Course: Introduction to South African Wine.* Cape Wine Academy. Cape Town
- Carpenter, S and Cottingham, K. 1997. Resilience and restoration of lakes. *Conservation Ecology.* 1 (1):
- Chakraborty, S. Murray, G. and Magarey, P. 1998. Potential Impact of Climate Change on Plant Diseases of Economic Significance to Australia. *Australasian Plant Pathology.* 27 (1): 15 – 35
- Chaves, M and Pereira, J. 1992. Water Stress, CO_2 and Climate Change. *Journal of Experimental Botany.* 43: 1131 - 1139
- Chenje, M and Johnson, P. 1996. *Water Resources in Southern Africa.* Maseru/Harare: SADC/IUCN/SARDC
- CMC. 2001. *Draft Water Services Development Plan.* Internal report. Cape Metropolitan Council. Cape Town
- Cracknell, A. 2001. *Remote Sensing and Climate Change: The Role of Earth Observation.* Chichester. Praxis Publishing Ltd.
- Dall, P. 2004. Personal Communication
- Davies, B and Day, J. 1998. *Vanishing Waters.* Cape Town. UCT Press
- Dayhoff, J. 1990. *Neural Network architectures: an introduction.* New York. Van Nostrand Reinhold
- Department of Water Affairs and Forestry, South Africa. 1997. *White Paper on a National Water Policy for South Africa.* DWAF. Pretoria
- Department of Water Affairs and Forestry, South Africa. 2001. *Evaluation of Soil and Climate Suitability for Irrigated Agriculture.* Prepared by J J N Lambrechts, F Ellis and B H A Schloms of

the Department of Soil and Agricultural Water Science, University of Stellenbosch as part of the Breede River Basin Study. DWAF Report No. PH 00/00/1902

- Department of Water Affairs and Forestry (a), South Africa. 2002. *Breede River Basin Study. Hydrology Second Draft.* Prepared by Ninham Shand. DWAF Report No. P H 000/8718
- Department of Water Affairs and Forestry (b), South Africa. 2002. *Breede River Basin Study. Agricultural Water Demand.* Prepared by L Bruwer of Louis Bruwer Inc. DWAF Report No.PH 00/00/1802.
- Department of Water Affairs and Forestry (c), South Africa. 2002. *Proposed First Edition: National Water Resource Strategy.* DWAF. Pretoria
- Department of Water Affairs and Forestry, South Africa. 2003. *Summary Report.* Prepared by H Beuster and M J Shand of Ninham Shand (Pty) Ltd as part of the Breede River Basin Study. DWAF Report No. P H 00/00/3302.
- du Pisani, A and Partridge, T. 1990. Effects of global warming on crop production in South Africa. *South African Journal of Science.* 86: 306 - 310
- Easter, K. 1993. *A World Bank Policy Paper: Water Resources Management.* Washington DC: International Bank for Reconstruction and Development
- Enright, W. "Policy changes and future planning pertaining to water affairs and our fruit industry" presented at the *Cape Pomological Association Technical Symposium.* Stellenbosch. South Africa. 14 September 2004
- Feng, G. 2001. Strategies for Sustainable Water Resources Management in Water Scarce Regions in Developing Countries. In Marino, M and Simonovic, S (eds.) *Integrated Water Resources Management.* Oxfordshire: IAHS Press, 107.
- Gilvear, D, Heal, V and Stephen, A. 2002. Hydrology and the ecological quality of Scottish river ecosystems. *Science of the Total Environment.* 294: 131 - 159
- Harrison, S and Foley, J.1995. General Circulation Models, Climate Change and Ecological Impact Studies. In IUCN *Impacts of Climate Change on Ecosystems and Species: Environmental Context.* Switzerland. SADAG, 9 –27
- Hennessy, K. CSIRO Atmospheric Research Technical Paper no. 37 http://ipcc.ddc.cru.uea.ac.uk/dkrz/dkrz_index.html (accessed 20 July 2002)
- Hewitson, B. and Crane, R. 2002. Self-organizing Maps: applications to synoptic climatology. *Climate Research.* 22: 13 – 26
- Hewitson, B and Crane, R. 2004. Gridded area average precipitation via conditional interpolation. *Journal of Climate.* In Press.
- Hewitson, B. 2004. University of Cape Town. Personal communication.
- Hughes, D. 2001. Providing hydrological information and data analysis tools for the determination of ecological instream flow requirements for South African rivers. *Journal of Hydrology.* 241 (1-2): 140 – 151
- Hughes, D and Hannart, P. 2002. A Desktop model used to provide an initial estimate of the ecological instream flow requirements of rivers in South Africa. *Journal of Hydrology.* 270 (3-4): 167 - 181

- Hulme, M, Jenkins, G, Lu, X, Turnpenny, J, Mitchell, T, Jones, R, Lowe, J, Murphy, J, Hassell, D, Boorman, P, McDonald R and Hill, S. 2002. *Climate Change Scenarios for the United Kingdom: The UKCIP02 Scientific Report.* Tyndall Centre for Climate Change Research, School of Environmental Sciences, University of East Anglia, Norwich, UK. 120pp.
- IPCC, 2001: Climate Change 2001: Synthesis Report. A contribution of Working Groups I, II and III to the Third Assessment Report of the Intergovernmental Panel on Climate Change [Watson, R.T. and the Core Writing Team (eds)]. Cambridge University Press, Cambridge, United Kingdom and New York, NY, USA, 398pp.
- IPCC data distribution centre ECHAM4/OPYC3 description http://cera-www.dkrz.de/IPCC_DDC/IS92a/Max-Planck-Institut/echam4opyc3.html (accessed 11 May 2004)
- IPCC data distribution centre: ECHAM4 http://ipcc-ddc.cru.uea.ac.uk/cru_data/examine/echam4_info.html (accessed 11 May 2004)
- IPCC data distribution centre: HadAM http://ipcc-ddc.cru.uea.ac.uk/dkrz/dkrz_index.html (accessed 11 May 2004)
- Janick, J. 1931. *Horticultural Science 4th Edition.* New York. WH Freeman and Company
- Johnson, I. 2003. *Watermod: Water dynamics, evapotranspiration and crop growth (version 3).* Greenhat Software. Australia
- Johnson, I. 1996. *Watermod: Water dynamics, evapotranspiration and crop growth (version 1).* Greenhat Software. Australia
- Jones, R. 2000. Managing uncertainty in climate change projections - Issues for impact assessment, An Editorial Comment. *Climatic Change.* 45 (3-4): 403 - 419.
- Kohonen, T. Hynninen, J. Kangas, J. and Laaksonen, J. 1996. *SOM_PAK: The Self-Organizing Map Program Package.* Helsinki University of technology
- Kriel, L. "Changes in quality requirements and fruit supply to offshore markets" presented at the *Cape Pomological Association Technical Symposium.* Stellenbosch. South Africa. 14 September 2004
- Le Maitre, D, van Wilgen, B., Chapman, R. and McKelly. D. 1996. Invasive plants and water resources in the Western Cape Province, South Africa: Modelling the consequences of a lack of management. *Journal of Applied Ecology* 33: 161-172.
- List, R.1971. *Smithsonian Meteorological Tables 6th edition.* Smithsonian Institute Press. Washington, DC
- McKnight, D, Brakke, D and Mulholland, P. 1996. Freshwater ecosystems and climate change in North America. *Limnology and Oceanography.* 41(6): 815 - 1149
- Mearns, L, Hulme, M, Carter, T, Leemans, R, Lal, M, Whetton, P. 2001. *Climate Scenario Development.* In: IPCC Climate Change 2001: the Scientific Basis, A contribution of Working Group 1 to the Third Assessment report of the Intergovernmental Panel on Climate Change. Cambridge University Press, Cambridge, United Kingdom, and New York, NY, USA, 881pp.
- Menzel, L. and Bürger, G. 2002. Climate Change Scenarios and Runoff response in the Mulde Catchment (Southern Elbe, Germany). *Journal of Hydrology.* 267 (1-2): 53 - 64

- Morita, T and Robinson, J, 2001. Greenhouse Gas Emission Mitigation Scenarios and Implications. In *Climate Change 2001: Mitigation.* Contribution of Working Group 3 to the IPCC Third Assessment Report.
- Nemec, J. 1988. Implication of a changing atmosphere on water resources. In *WMO/OMM,* 710: 211-225. World Meteorological Organisation. Geneva
- New, M and Hulme, M. 2000. Representing Uncertainty in Climate Change scenarios: a Monte Carlo approach. *Integrated Assessment* 1: 203 - 213
- New, M. 2002. Climate Change and Water Resources in the Southwestern Cape, South Africa. *South African Journal of Science.* 98: 369 – 376
- New, M. 2003. Oxford University. Personal Communication
- Niemczynowicz, J. 1999. Urban Hydrology and Water Management – Present and future Challenges. *Urban Water* 1 (1): 1 – 14.
- Nakic´enovic´, N, Davidson, O, Davis, G, Grübler, A, Kram, T, La Rovere, E, Metz, B, Morita, T, Pepper, W, Pitcher, H, Sankovski, A, Shukla, P, Swart, R, Watson, R, Dadi, Z. 2000. *IPCC Special Report on Emission Scenarios,* Cambridge University Press, Cambridge, United Kingdom and New York, USA, 599pp
- OFWAT. 1998. *Setting Price Limits for Water and Sewerage Services: The Framework and Business Planning Process for the 1999 Periodic Review.* Office of Water Services. Birmingham, United Kingdom
- Pair, C. 1969. *Sprinkler Irrigation.* Washington. Sprinkler Irrigation Association
- Parry, M and Carter, T. 1998. *Climate Impact and Adaptation Assessment.* London. Earthscan Publications Ltd.
- Peixoto, J and Oort, A. 1992. *Physics of Climate.* USA. American Institute of Physics.
- Pittock, A. 1988. *The effects of long-term climate change on water resources.* Paper to National Workshop on Planning and Management of Water Resources. Adelaide. Mimeo, pp 18
- Pope, V, Gallani, M, Rowntree, R and Stratton, R. 2000. The impact of new physical parameterisation in the Hadley Centre climate model HadAM3. *Climate Dynamics.* 16: 123 - 146.
- Popper, K. 1958. *The Logic of Scientific Discovery.* Hutchinson. London
- Pretorius, E and Du Toit De Villiers, G. 2001. Strategies for Sustainable Water Resources Management in Water Scarce Regions in Developing Countries. In Marino, M and Simonovic, S (eds.) *Integrated Water Resources Management.* Oxfordshire: IAHS Press, 107
- Republic of South Africa National Water Act no. 36 of 1998
- Rincon, P. 2005. *Greenhouse Gases 'do warm oceans'.* BBC News http://news.bbc.co.uk/2/hi/science/nature/4275729.stm
- Risien, C. 2002. *Wind-stress Variability over the Benguela Upwelling System.* Thesis (MSc). University of Cape Town
- Roeckner, E, Bengtsson, J, Feichter, J, Lelieveld and Rodhe, H. 1999. Transient climate change simulations with a coupled atmosphere-ocean GCM including the tropospheric sulphur cycle. *Journal of Climate.* 12: 3004 - 3012.

- Sælthun, N. 1996. *The Nordic HBV model. Description and documentation of the model version developed for the project Climate Change and Energy Production*. NVE Publication, 7. Norwegian Water Resources and Energy Administration. Oslo.
- Schulze, R. 1989. *ACRU – Theory, concepts and background*. ACRU Report 35. Department of Agricultural Engineering, University of Natal. Pietermaritzburg
- Schulze, R. 1990. Climate Change and Hydrological Response in Southern Africa: Heading Towards the Future. *South African Journal of Science*. 86: 7 – 10
- Schulze, R. 1995 Hydrology and Agrohydrology: *A Text to Accompany the ACRU 3.00 Agrohydrological Modelling System.* Water Research Commission. Pretoria. Report TT69/95.
- Schulze, R. 1997. *South African Atlas of Agrohydrology and Climatology*. WRC Report No TT 82/96.
- Schulze, R. 2000. Modelling hydrological responses to land use and climate change: a southern African perspective. *Ambio*. 29: 12 – 22
- Schulze, R, Meigh, J and Horan, M. 2001. Present and potential future vulnerability of eastern and southern Africa's hydrology and water resources. *South African Journal of Science*. 97: 150 –160
- Special Report on Emission Scenarios http://ipcc-ddc.cru.uea.ac.uk/asres/sres_home.html (accessed 20 July 2002)
- Starr, C and Taggart, R. 1998. *Biology: The unity and diversity of life (8th edition)*. Wordsworth Publishing Company. California.
- Steynor, A. 2002. *The Impact of Global Climate Change on Apple Farming: A Study of the Overberg*. Thesis (BSc(hons)). University of Cape Town
- Stipp, B. 2004. Personal Communication
- Tennant W, 2003. An Assessment of Intra-seasonal Variability from 13-year GCM Simulations. *Monthly Weather Revue*. 131: 1975-1991
- Tharme, R and King, J. 1998. *Development of the Building Blocks Methodology for Instream Flow Assessments and Supporting Research on the effect of different Magnitude Flows on Riverine Ecosystems – WRC Report No 576/1/98.* Cape town. Water Research Commission
- Thornley, J and Johnson, I. 2000. *Plant and Crop Modelling.* Reprint of 1990 Oxford University Press edition. United Kingdom
- Tompson, R and Parry, A. 1997. *Applied Climatology: Principles and Practice.* London. Routledge.
- Tyson, P and Preston-Whyte, R. 2000. *The Weather and Climate of Southern Africa*. Cape Town. Oxford University Press Southern Africa
- Von Storch, H. 1995. Inconsistencies at the interface of climate impact studies and global climate research. *Meteor. Z*. 4: 72 - 80
- Wand, S and Midgley, G. 2003. "Recent temperature and rainfall trends in the south-western Cape: Implications for the fruit industry" presented at the *Global Change and Regional Sustainability in South Africa National Symposium*. Kirstenbosch. Cape Town. South Africa. 27 – 29 October 2003.

- Watterson, I, O'Farrell, S and Dix M. 1997. Energy transport in climates simulated by a GCM which includes dynamic sea-ice. *Journal of Geophysical Research*. 102(D10): 11027 – 11037.
- Werrity, A. 2002. Living with Uncertainty: Climate Change, River Flows and Water Resource Management in Scotland. *The Science of the Total Environment,* 294 (1-3): 29 – 40
- Wilby, R and Wigley, T. 1997. Downscaling general circulation model output: a review of methods and limitations. *Progress in Physical Geography*. 21: 530 - 548
- Wilson, M, and Henderson-Sellers, A. 1985. A Global Archive of Land Cover and Soils Data for Use in General Circulation Climate Models. *Journal of Climatology*. 5: 119 - 143.
- Yarnal, B. 1984. Relationships between synoptic-scale atmospheric circulation and glacier mass balance in South-Western Canada during the International Hydrological Decade, 1965-74. *Journal of Glaciology*. 30: 188 – 198

Appendix A

Farmer Interviews

Interviews

Farmer A

Crop	Fruit
Place	Worcester
Date of Harvest	Feb - May
Irrigate on soil / canopy	Soil
Irrigate according to soil water status/ plant water status / regular intervals	Regular Intervals
Municipal water / On farm dams	Municipal (Brandvlei water scheme)
Time of day of irrigation	Early or late evening 8pm – 2am
Months of Irrigation	All Year

Farmer B

Crop	Fruit
Place	Robertson
Date of Harvest	Feb – April (apples) June – Aug (citrus)
Irrigate on soil / canopy	Soil
Irrigate according to soil water status/ plant water status / regular intervals	Soil Water status (use neutron probes)
Municipal water / On farm dams	Municipal (Brandvlei water scheme)
Time of day of irrigation	Non-specific
Months of Irrigation	Aug - May

Farmer C

Crop	Apples and Pears
Place	Riviersonderend
Date of Harvest	Jan - Mar
Irrigate on soil / canopy	Soil
Irrigate according to soil water status/ plant water status / regular intervals	Plant status
Municipal water / On farm dams	Municipal (Brandvlei water scheme)
Time of day of irrigation	Early morning (before 11am)
Months of Irrigation	Sept to April

Farmer D

Crop	Grapes
Place	Worcester
Date of Harvest	Feb – April (table grapes towards the end)
Irrigate on soil / canopy	Soil
Irrigate according to soil water status/ plant water status / regular intervals	Regular Intervals
Municipal water / On farm dams	Municipal (Brandvlei water scheme)
Time of day of irrigation	Early or late evening 8pm – 2am
Months of Irrigation	All Year

Farmer E

Crop	C4 crops
Place	Riviersonderend
Date of Harvest	No harvest, dairy
Irrigate on soil / canopy	Soil
Irrigate according to soil water status/ plant water status / regular intervals	Plant Status
Municipal water / On farm dams	Municipal (Brandvlei water scheme)
Time of day of irrigation	Early morning (before 11am)
Months of Irrigation	Sept to June

Farmer F

Crop	C4 crops
Place	Worcester
Date of Harvest	April
Irrigate on soil / canopy	Soil
Irrigate according to soil water status/ plant water status / regular intervals	Regular Intervals
Municipal water / On farm dams	Municipal (Brandvlei water scheme)
Time of day of irrigation	Early or late evening 8pm – 2am
Months of Irrigation	All Year

Appendix B

Summary Watermod3 Output

KEY:

UC = Upper Catchment

MC = Middle Catchment

LC = Lower Catchment

OBSERVED DATA (1979 - 1997)	UC orchards	MC orchards	LC orchards	UC Vineyards	MC vineyards	LC vineyards	UC C4 crops	MC C4 crops	LC C4 crops
Initial soil water	720.33	687.06	688.80	599.67	564.56	566.93	796.01	771.52	765.42
Final soil water	714.44	680.44	679.53	587.06	550.44	550.00	795.28	770.21	765.11
Total rainfall	591.78	324.50	288.80	591.78	324.50	288.80	591.78	324.50	296.44
Total irrigation inputs	591.61	566.56	640.13	570.00	606.06	610.67	1401.56	1633.00	1622.78
Total Crop transpiration	298.33	223.33	256.93	301.78	301.17	309.87	401.17	402.61	394.33
Total canopy evaporation	20.50	17.33	24.40	22.83	18.61	25.27	22.83	22.89	30.06
Total litter evaporation	150.33	141.78	128.80	156.56	134.06	121.80	888.22	767.22	780.22
Total soil evaporation	117.89	90.39	75.53	123.89	92.78	80.13	1083.78	881.50	817.11
Total ET	587.28	472.94	485.80	605.17	546.67	537.20	2395.94	2073.78	2021.06
Total through drainage	131.72	43.11	30.87	203.17	62.00	47.73	956.50	222.00	123.61
Total surface runoff	469.06	379.78	419.47	363.94	333.78	328.20	1006.11	961.50	954.17
Inputs	1183.44	891.11	928.87	1161.94	930.67	899.53	872.09	651.13	621.01
Outputs	1188.06	895.78	936.27	1172.00	942.44	913.07	871.76	651.47	619.81
Change in soil water	-5.83	-6.50	-9.13	-12.56	-14.11	-16.93	-0.67	-1.23	-0.29
Yield	12.03	9.68	10.75	11.78	11.62	11.92	25.39	25.28	25.43
Growing season rain	108.72	76.06	97.80	111.83	78.28	103.80	195.33	138.50	188.33
No of irrigations	11.33	10.94	12.33	10.94	11.67	11.73	27.39	32.00	31.72

ECHAM CONTROL (1979 - 1997)	UC orchards	MC orchards	LC orchards	UC Vineyards	MC vineyards	LC vineyards	UC C4 crops	MC C4 crops	LC C4 crops
Initial soil water	725.67	673.17	666.93	603.00	539.22	531.73	789.51	750.88	743.25
Final soil water	721.67	665.72	657.00	591.39	524.83	512.00	788.90	747.50	739.13
Total rainfall	365.89	177.33	160.93	365.89	177.33	160.93	365.89	177.33	160.93
Total irrigation inputs	761.72	931.39	909.40	675.83	763.83	739.93	1489.28	3218.61	3507.13
Total Crop transpiration	301.89	295.89	295.73	297.78	313.33	317.67	388.72	405.22	404.47
Total canopy evaporation	21.00	14.72	22.73	24.50	17.33	23.53	38.00	26.56	28.27
Total litter evaporation	149.61	125.17	121.00	147.89	117.06	111.33	838.06	752.33	818.93
Total soil evaporation	98.11	65.61	51.13	110.28	69.72	51.93	892.00	969.50	968.33
Total ET	570.33	501.39	490.93	580.39	517.44	504.73	2156.56	2153.56	2219.93
Total through drainage	48.89	7.94	8.40	88.61	16.28	18.53	268.83	9.33	8.07
Total surface runoff	510.00	604.89	577.80	383.28	420.56	394.07	888.22	1944.83	2083.60
Inputs	1127.56	1108.78	1070.00	1041.67	941.17	900.87	663.79	821.08	862.27
Outputs	1129.28	1113.89	1076.73	1052.33	953.94	917.13	662.72	821.81	862.56
Change in soil water	-4.06	-7.39	-9.93	-11.50	-14.28	-19.73	-0.63	-3.32	-4.11
Yield	11.97	11.64	11.79	11.45	11.78	12.05	25.16	25.62	25.66
Growing season rain	60.00	39.11	60.20	75.94	45.56	65.20	233.22	113.00	103.53
No of irrigations	14.61	17.89	17.53	13.00	14.67	14.27	29.17	63.11	68.73

ECHAM FUTURE (2079 - 2099)	UC orchards	MC orchards	LC orchards	UC Vineyards	MC vineyards	LC vineyards	UC C4 crops	MC C4 crops	LC C4 crops
Initial soil water	684.17	664.50	669.20	556.06	526.11	531.33	758.36	743.88	743.43
Final soil water	676.11	656.28	659.67	540.39	509.89	511.40	755.04	740.27	739.36
Total rainfall	197.11	110.11	188.47	197.11	107.61	188.47	197.11	110.11	188.47
Total irrigation inputs	941.17	1043.00	854.53	778.56	838.39	711.00	2657.56	3610.39	3318.33
Total Crop transpiration	318.17	314.00	296.60	315.39	328.00	316.00	419.06	432.11	418.00
Total canopy evaporation	20.00	15.00	37.47	21.50	16.83	39.60	24.72	17.50	35.93
Total litter evaporation	107.83	91.56	110.40	106.33	82.00	105.80	686.89	608.72	870.93
Total soil evaporation	67.28	50.94	47.93	76.56	54.22	52.80	856.50	921.72	947.87
Total ET	513.22	471.56	492.07	520.06	481.22	514.20	1987.50	1979.83	2272.93
Total through drainage	9.94	7.06	8.27	28.44	14.61	18.07	52.33	6.39	7.67
Total surface runoff	620.06	680.39	545.27	440.44	464.56	381.87	1604.83	2176.33	1970.40
Inputs	1138.11	1152.89	1043.00	975.61	945.94	899.47	728.63	832.09	852.17
Outputs	1143.39	1158.56	1045.47	989.17	959.83	913.93	728.90	832.82	850.45
Change in soil water	-8.00	-8.17	-9.53	-15.72	-16.11	-20.00	-3.28	-3.53	-4.07
Yield	10.85	10.62	10.62	10.28	10.52	10.63	25.47	25.85	25.81
Growing season rain	52.22	38.83	104.07	58.72	41.94	109.27	137.39	77.00	133.07
No of irrigations	18.06	20.06	16.40	15.00	16.11	13.67	52.00	70.72	65.00

CSIRO CONTROL (1979 - 1997)	UC orchards	MC orchards	LC orchards	UC Vineyards	MC vineyards	LC vineyards	UC C4 crops	MC C4 crops	LC C4 crops
Initial soil water	691.78	668.61	665.13	564.17	533.39	525.87	773.42	748.61	744.29
Final soil water	685.28	660.56	655.20	549.44	517.33	506.20	771.26	745.26	740.19
Total rainfall	387.56	180.28	158.53	387.56	178.17	158.53	387.56	180.28	158.53
Total irrigation inputs	621.06	911.17	931.93	569.61	751.28	784.80	1891.06	3481.72	3420.40
Total Crop transpiration	294.83	291.44	295.27	305.22	317.44	322.20	400.56	412.11	407.67
Total canopy evaporation	24.33	16.78	20.20	25.06	17.00	22.07	26.11	18.67	26.00
Total litter evaporation	146.67	122.39	124.20	144.72	113.72	118.33	892.94	778.06	806.40
Total soil evaporation	95.39	65.11	53.87	104.00	66.72	57.73	1074.28	1057.72	938.40
Total ET	561.17	495.67	493.60	579.39	515.11	520.27	2393.78	2266.67	2178.60
Total through drainage	31.11	8.06	8.27	68.44	15.56	18.07	290.00	11.89	7.67
Total surface runoff	418.17	592.11	594.33	320.61	412.28	422.07	1145.33	2105.89	2026.80
Inputs	1008.50	1091.22	1090.27	957.22	929.67	943.13	765.79	876.51	842.52
Outputs	1010.28	1095.44	1096.00	968.28	942.50	960.07	765.94	877.07	842.92
Change in soil water	-6.50	-8.06	-10.00	-14.72	-16.11	-19.80	-2.11	-3.40	-4.04
Yield	12.01	11.68	11.79	11.95	12.04	12.17	25.41	25.68	25.69
Growing season rain	112.61	54.94	54.00	114.78	55.94	56.93	163.89	81.11	95.00
No of irrigations	11.94	17.56	17.93	10.94	14.44	15.13	37.06	68.33	67.07

CSIRO FUTURE (2079 - 2099)	UC orchards	MC orchards	LC orchards	UC Vineyards	MC vineyards	LC vineyards	UC C4 crops	MC C4 crops	LC C4 crops
Initial soil water	663.06	661.17	663.80	527.94	527.50	527.33	744.51	741.97	742.28
Final soil water	654.72	653.11	654.00	511.44	511.39	507.33	741.01	738.49	738.19
Total rainfall	166.17	90.61	150.00	166.17	87.89	150.00	166.17	90.61	150.00
Total irrigation inputs	1028.72	1158.33	1082.47	879.44	954.72	880.13	3206.33	4144.11	3856.87
Total Crop transpiration	330.11	325.78	318.80	342.94	348.83	337.53	445.50	456.78	445.33
Total canopy evaporation	13.17	9.06	21.13	14.78	9.67	23.07	14.94	11.56	29.67
Total litter evaporation	99.17	91.50	122.80	97.78	83.28	112.73	613.56	566.72	755.07
Total soil evaporation	63.17	57.83	66.20	75.39	62.83	72.67	954.83	1038.94	1048.40
Total ET	505.67	484.17	528.87	530.94	504.39	546.07	2028.83	2073.78	2278.53
Total through drainage	9.83	7.39	8.27	24.67	15.11	18.07	56.94	7.83	7.67
Total surface runoff	683.56	763.28	701.20	503.00	537.83	483.20	1954.00	2520.22	2313.67
Inputs	1194.83	1248.89	1232.53	1045.44	1042.61	1030.27	807.32	919.50	921.39
Outputs	1199.00	1254.50	1237.93	1058.67	1057.22	1047.07	808.09	920.58	920.17
Change in soil water	-8.44	-8.00	-9.93	-16.44	-16.00	-20.00	-3.47	-3.46	-4.07
Yield	9.45	8.95	8.93	9.04	8.73	8.74	25.36	25.74	25.80
Growing season rain	44.56	24.72	54.07	47.50	26.33	59.47	69.00	44.17	108.67
No of irrigations	19.67	22.28	20.80	16.89	18.33	17.00	62.78	81.22	75.47

HadAM FUTURE (2079 - 2099)	UC orchards	MC orchards	LC orchards	UC Vineyards	MC vineyards	LC vineyards	UC C4 crops	MC C4 crops	LC C4 crops
Initial soil water	689.39	663.89	668.53	562.00	525.50	528.40	769.73	742.09	743.85
Final soil water	682.67	655.61	658.80	547.11	509.06	509.00	767.22	738.61	739.67
Total rainfall	349.89	67.44	70.40	349.89	66.22	70.40	349.89	67.44	70.40
Total irrigation inputs	796.78	1090.00	1003.87	703.00	879.89	840.33	2042.28	4510.06	3681.73
Total Crop transpiration	321.11	319.50	312.93	311.56	338.72	332.47	423.83	444.22	437.67
Total canopy evaporation	14.72	5.50	8.87	15.33	5.17	8.53	19.89	6.94	10.60
Total litter evaporation	141.56	80.11	72.73	143.33	73.72	71.40	787.00	562.00	510.00
Total soil evaporation	98.44	42.17	39.53	115.61	42.67	43.87	1046.28	1096.89	898.13
Total ET	575.83	447.44	434.53	585.83	460.44	456.47	2276.78	2110.67	1856.33
Total through drainage	41.33	7.06	8.27	75.17	14.61	18.07	290.39	6.39	7.67
Total surface runoff	533.17	710.56	640.13	402.39	486.72	455.00	1232.39	2743.33	2184.60
Inputs	1146.61	1157.33	1074.27	1052.94	945.94	910.73	758.36	969.54	806.81
Outputs	1150.22	1164.83	1082.53	1063.28	961.67	929.33	759.92	972.39	810.07
Change in soil water	-6.61	-8.28	-9.80	-14.89	-16.44	-19.40	-2.44	-3.46	-4.15
Yield	10.76	10.47	10.47	10.07	10.51	10.47	25.46	25.98	25.76
Growing season rain	64.28	15.78	23.73	66.17	16.33	25.27	115.39	28.61	44.53
No of irrigations	15.22	20.89	19.27	13.50	16.89	16.07	40.00	88.44	72.13